A Passivity Based Control Methodology for Flexible Joint Robots with Application to a Simplified Shuttle RMS Arm

Pierre Sicard and John T. Wen

NASA Center for Intelligent Robotic Systems for Space Exploration
Rensselaer Polytechnic Institute, Troy, NY 12180-3590, USA

1 Introduction

1.1 Overview

This report summarizes the research effort and results related to the Grant No. NAG 9-462/Basic from the NASA Johnson Space Center (JSC). The overall goal of this research is to develop a general theory for the control of flexible robots, including flexible joint robots, flexible link robots, rigid bodies with flexible appendages, etc. As part of the validation, the theory is applied to the control law development for a test example which consists of three-link arm modeled after the shoulder yaw joint of the space shuttle remote system (RMS). The performance of the closed loop control system is th performance of the existing RMS controller to demonstrate t approach. In this report, we present the theoret the control of flexible robots and demo on the three-link test arm.

Some important ... in this research are noted below. D... ...d and low power consumption, these proper... ...pulators as well.

1. Th... ...in comparison with the motor inertia, even when the joints are hea... ...ed (so the motor inertia seen from the link is multiplied by the square of the gear ratio). This implies large inter-link coupling, especially in the mass matrix.

2. The gearbox model includes a nonlinear spring and hysteresis.

3. The payload is massive compared to the arm (two orders of magnitude larger).

4. Amplifier output, motor torque, joint and Cartesian velocities are limited.

Based on the simulation of the three-link test arm using the existing RMS controller, the following attributes of the current RMS controller performance have been observed:

troller only uses local motor velocity feedback (digital velocity PI loop in plus analog tachometer feedback). This choice has the advantages that link d angular velocities need not be measured and the control law is very simple. wback is that the inter-link coupling and link angular error are not directly sated. Since the links are very massive compared to the motor inertia (even avy gearing), this coupling is quite sizable. As a result, there is a significant of uncommanded motion; for example, if a single joint is commanded to follow y profile, there are large transients at other joints, causing large position errors, the end effector is commanded to follow a Cartesian velocity, large deviations other directions.

trol strategy is to drive the motor velocity (reduced by the gear ratio) to the ink velocity and then let the link oscillation damp out through the link friction. ently, the motor velocity may be adequate but the link velocity performance sh. This problem exists even in the single flexible joint case, the inter-link only compounds the problem.

sting RMS controller appears to be very robust in terms of stability. Load loes not affect stability but the transient performance differs significantly for ed and unloaded cases.

he above observations, we have set out to understand the existing controller n particular, the apparent stability robustness) and to develop a new design to resent shortcomings. The following objectives are formulated for the modified y are also used to compare the closed loop performance between controllers:

he amplitude and duration of oscillations of the link velocity while increasing of response.

the effect of inter-link coupling.

stability and performance robustness with respect to the payload and arm ation.

internal stability, i.e., motor torque and velocity should stabilize.

these objectives, we have focused on a recently developed method which assivity property of flexible robots [1]. Application of this method to flexible nd, in particular, to our test arm, leads to a large family of stabilizing control o justifies the existing RMS control law. A subclass of this family, has proven fective in terms the performance criteria stated above. The structure of this llers basically consists of the kernel of the existing RMS controller augmented riable dependent feedforward. Results in this report mostly pertain to this nalysis and simulation (for performance comparison) of the new controllers, the following assumptions:

state measurement is available, namely, link angles and angular velocities, or angles and angular velocities. In contrast, the existing RMS controller only otor angular velocities and angles (obtained by integrating angular velocities).

1. The co
velocity
angle a
The dra
compen
after he
amount
a veloci
or when
occur in

2. The cor
desired
Conseq
is slugg
coupling

3. The exi
change
the load

Based on
theoretically (
improve the p
controller, the

1. Reduce
rapidity

2. Decreas

3. Maintai
configur

4. Maintai

To achiev
exploits the p
joint robots, a
laws which als
particularly e
class of contro
with a link va
class. In the
we have made

1. The full
and mot
needs m

2. Some controller limits, and hysteresis (unit efficiency for both forward and back drive) are ignored in the analysis. Velocity limit logic has been implemented in simulation. In most of the simulation results, torque limit has also been included.

3. The arm dynamic model is known exactly.

We are in the process to relax all of these assumptions. A nonlinear observer is under investigation for the first case, a saturation-driven command trajectory modifier is considered for the second, and robustness analysis and adaptive control is being studied for the last. These directions of generalization will be discussed more fully in Section 6.

1.2 Introduction to Passivity Approach

Passivity is an input/output property which roughly means that energy can only flow into the system (in other words, the system can never generate energy through the input/output pair). For flexible joint robots, the passive pairs are the motor torque and motor velocity.

The basic structure of our proposed controller is the sum of a model-based feedforward and a model-independent feedback. The procedure of control design for flexible robots involves two steps: feedforward design and feedback stabilization. These steps are explain further below:

- *Feedforward Design*: A feedforward control (possibly dependent on the full state measurements) is chosen to form an error equation so that the system is passive between a particular input/output pair.

- *Feedback Stabilization*: The stabilization procedure involves first finding a static feedback (usually the position proportional feedback) to guarantee observability and maintain passivity and then choosing a strictly passive feedback from the passive output.

The passivity approach described above has the following important features:

- The feedback portion is independent of the model, so the closed loop stability is extremely robust. When the feedforward is inexact or absent altogether, the stability is still maintained, but the steady state error will increase proportional to the model mismatch.

- Only the output (i.e., motor position and velocity) is needed for the stabilization in contrast to the full state in the exact linearization.

- The controller structure is a simple form of stabilizing feedback summed with a feedforward. This clean separation of functionality between the two loops is particularly amenable to adaptive control. In contrast, the two loops are intertwined in the exact linearization approach.

- For the tracking control, the choice of feedforward greatly impacts performance. We have found that it is particularly effective to add a link angle and angular velocity feedback component in the desired link acceleration.

This approach is applicable to both (position) set point stabilization and tracking control. In the set point control case, the feedforward is particularly simple to solve and is usually a constant. In the tracking case, essentially the plant needs to be stably inverted. We will later discuss various approximation that we have used. The rate control used in RMS can be cast as a special case of the tracking problem.

Passivity of mechanical systems has long been recognized as an important property. This property has been used in the feedback stabilization for fully actuated rigid robots [2, 3, 4, 5], satellites [6, 7, 8], and flexible joint robots [9, 10]. Passivity property for flexible jointed robot was recognized in [9] and indeed was used in a proportional-derivative (PD) type controller design. The method requires inherent damping in both joints and motors. Similar results without requiring the inherent damping have recently appeared in [10]. The result on PD stabilization of flexible beams was first shown in [11].

The passivity property of flexible structures with collocated sensors and actuators was noted in [12] when the inherent damping is present. The controller structure, however, is invariably of the simple PD form. As a result of the low damping, the transient performance is typically poor. It was only recently noted that an undamped beam can be stabilized by using PD alone [11, 13]. However, as the open-loop poles and zeros are on the imaginary axis, transient performance is poor. In [14], based on the work in [15] for rigid robots, the PD structure is generalized to a general passive controller for a multiple-flexible-link robot. However, in contrast to [1], intrinsic structural damping in the flexible links is required.

Another prominent approach to the control of flexible joint robots is exact linearization. There has been many published work on this application, for a summary see [16]. In general, this approach requires the exact model information, linear spring assumption, and zero gyroscopic force coupling. Furthermore, the feedforward compensation (for linearization) and the feedback stabilization are intertwined and errors in the feedforward may affect the closed loop stability in an adverse way. The feedforward design in our approach is very similar to the exact linearization approach - both essentially solve an inverse plant problem. But our approach requires much less model information in the set point control case (only the spring characteristics is needed), can be extended to the nonlinear spring case and fully coupled dynamic model, and the additive separation between the feedback and feedforward implies that error in feedforward does not lead to instability. The price to pay is that the closed loop performance cannot be arbitrarily assigned.

1.3 Organization of Report

This report gives a self-contained exposition of the passivity control theory for flexible robots and also presents simulation results for a three-link arm to demonstrate the effectiveness of the scheme. In Section 2, the full model for the three-link test example is presented, including the gearbox characteristics. This material is largely based on the original SPAR report [17] and some additional notes from Richard Theobald at Lockheed [18]. The full model is used in a "truth-model" simulation. We have also used a simplified model (with saturation, hysteresis, and quantization ignored) for controller design and performance comparison between the RMS controller and the proposed controller. The existing RMS controller is explained in Section 3. Again, much of the materials are from [17], some of them are interpreted in a passivity perspective. Several different versions of the modified controller are

presented in Section 4. The performance of the two controllers is compared in Section 5. All of the simulation results are presented here. Proposed future extensions are summarized in Section 6.

The general theory of passive control design methodology for flexible robots is included in the Appendix.

2 Modeling

In this section, we present the dynamical equations for the three–link test arm. The general model is based on the description in [18], [19] and [17]. Additional assumptions are made to obtain models for a high fidelity simulation based in FORTRAN and for a proof–of–concept simulation based in MATLAB. These assumptions are based in part on the classification of critical and non-critical parameters as in [20], and in part on the expected applications.

2.1 General Assumptions

Arm geometry and mass properties parameters are considered as non-critical parameters in the sense that their variations do not affect the arm performance significantly [20]. Crude estimates of the related parameters can thus be used for the study. Among the servo parameters, only the gearbox stiffness, gearbox forward/backdrive efficiencies, motor drive amplifier gain, forward/backdrive current limits, joint and motor friction/stiction, and brake torque are considered as critical parameters [20]. Hence, a precise model of these elements should be used. However, approximations of some of these elements are used for this study in order to simplify the controller design. The controllers will be tested with the precise model at a later date.

2.1.1 Mass and Geometry Properties

The test manipulator is a three–link planar arm (shown in Fig.1). The links are considered to be rigid (i.e., bending stiffness is neglected) uniform homogeneous cylinders. The link parameters are enumerated in table 1 where the inertia of each link is referenced to the center of gravity of the link which is at the geometric center and is expressed in the corresponding joint reference frame. The joint reference frame is rigidly attached to the link at its inboard end.

Table 1: Arm parameters

Variable	Name	Link 1	Link 2	Link 3	Units
length	l_i	7.315289	7.315289	1.828822	m
mass	m_i	175.1825	175.1825	43.79562	Kg
inertia	I_i	781.2183	781.2183	12.2065	$Kg \cdot m^2$

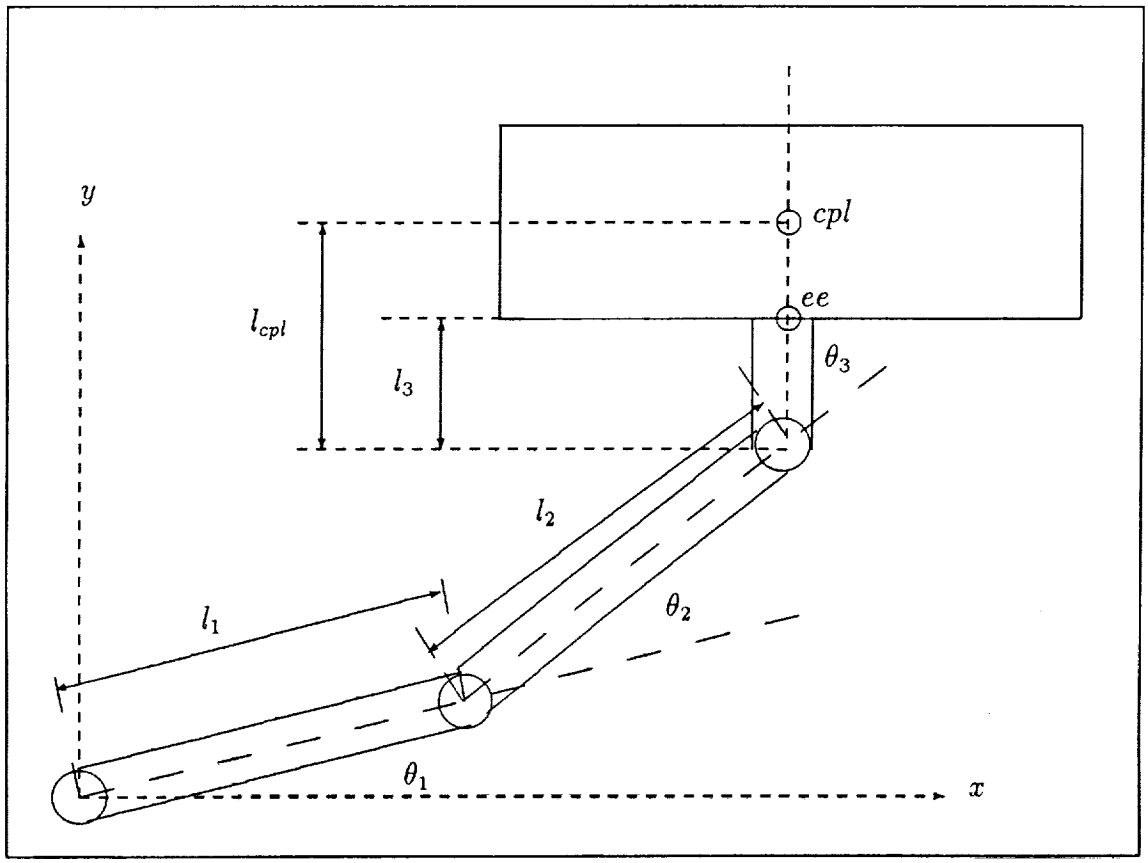

Figure 1: Three-link planar arm and payload

The baseline payload is a homogeneous cylinder and is representative of a typical module to be handled by the RMS. The characteristics of the baseline payload are enumerated in table 2. It is assumed that the payload is grasped by the manipulator by its center such that if the payload is considered as a point mass, the point mass will be in the axis of link three at a distance of half the diameter of the payload from the end effector (see Fig.1).

Table 2: Baseline payload parameters

Variable	Name	Value	Units
mass	m_{pl}	20875.9124	Kg
inertia	I_{pl}	351046.558	$Kg \cdot m^2$
length	le_{pl}	13.71617	m
diameter	l_{pl}	4.267252	m

The manipulator and load dynamics are described by the following equation:

$$\tau_{joint} = M(\theta_\ell)\ddot{\theta}_\ell + C(\theta_\ell, \dot{\theta}_\ell)\dot{\theta}_\ell + \tau_{FL}(\dot{\theta}_\ell) + \tau_{ext} \tag{1}$$

where θ_ℓ represents the link angular positions, τ_{joint} the torque applied at the base of the links (i.e., gear torque), τ_{FL} the stiction/friction link torque and τ_{ext} the effect of external forces applied to the arm. The mass matrix and centrifugal/Coriolis torque are of the following form:

$$M(\theta_\ell) = \begin{bmatrix} 1 & 1 & 1 \\ 0 & 1 & 1 \\ 0 & 0 & 1 \end{bmatrix} \cdot \begin{bmatrix} m_{11} & m_{12} & m_{13} \\ m_{21} & m_{22} & m_{23} \\ m_{31} & m_{32} & m_{33} \end{bmatrix} \cdot \begin{bmatrix} 1 & 0 & 0 \\ 1 & 1 & 0 \\ 1 & 1 & 1 \end{bmatrix} \tag{2}$$

$$C(\theta_\ell, \dot{\theta}_\ell)\dot{\theta}_\ell = \begin{bmatrix} 1 & 1 & 1 \\ 0 & 1 & 1 \\ 0 & 0 & 1 \end{bmatrix} \cdot \begin{bmatrix} 0 & c_{12} & c_{13} \\ c_{21} & 0 & c_{23} \\ c_{31} & c_{32} & 0 \end{bmatrix} \cdot \begin{bmatrix} \left(\dot{\theta}_{\ell_1}\right)^2 \\ \left(\dot{\theta}_{\ell_1} + \dot{\theta}_{\ell_2}\right)^2 \\ \left(\dot{\theta}_{\ell_1} + \dot{\theta}_{\ell_2} + \dot{\theta}_{\ell_3}\right)^2 \end{bmatrix} \tag{3}$$

with :

$$m_{11} = I_1 + l_1^2 \cdot (m_2 + m_3 + m_{pl}) + l_{c1}^2 \cdot m_1 \tag{4}$$
$$m_{12} = l_1 \cdot (l_{c2} \cdot m_2 + l_2 \cdot [m_3 + m_{pl}]) \cdot C2 \tag{5}$$
$$m_{13} = l_1 \cdot [l_{c3} \cdot m_3 + l_{cpl} \cdot m_{pl}] \cdot C23 \tag{6}$$
$$m_{21} = m_{12} \tag{7}$$
$$m_{22} = I_2 + l_{c2}^2 \cdot m_2 + l_2^2 \cdot [m_3 + m_{pl}] \tag{8}$$
$$m_{23} = l_2 \cdot [l_{c3} \cdot m_3 + l_{cpl} \cdot m_{pl}] \cdot C3 \tag{9}$$
$$m_{31} = m_{13} \tag{10}$$
$$m_{32} = m_{23} \tag{11}$$
$$m_{33} = I_3 + I_{pl} + l_{c3}^2 \cdot m_3 + l_{cpl}^2 \cdot m_{pl} \tag{12}$$
$$c_{12} = -l_1 \cdot (l_{c2} \cdot m_2 + l_2 \cdot [m_3 + m_{pl}]) \cdot S2 \tag{13}$$

$$c_{13} = -l_1 \cdot [l_{c3} \cdot m_3 + l_{cpl} \cdot m_{pl}] \cdot S23 \quad (14)$$

$$c_{21} = -c_{12} \quad (15)$$

$$c_{23} = -l_2 \cdot [l_{c3} \cdot m_3 + l_{cpl} \cdot m_{pl}] \cdot S3 \quad (16)$$

$$c_{31} = -c_{13} \quad (17)$$

$$c_{32} = -c_{23} \quad (18)$$

where $l_{ci} = l_i/2$, $l_{cpl} = l_3 + l_{pl}/2$, $I_i = m_i \cdot l_i^2/12$, $C2 = cos\,(\theta_2)$, $C3 = cos\,(\theta_3)$, $C23 = cos\,(\theta_2 + \theta_3)$, $S2 = sin\,(\theta_2)$, $S3 = sin\,(\theta_3)$, $S23 = sin\,(\theta_2 + \theta_3)$.

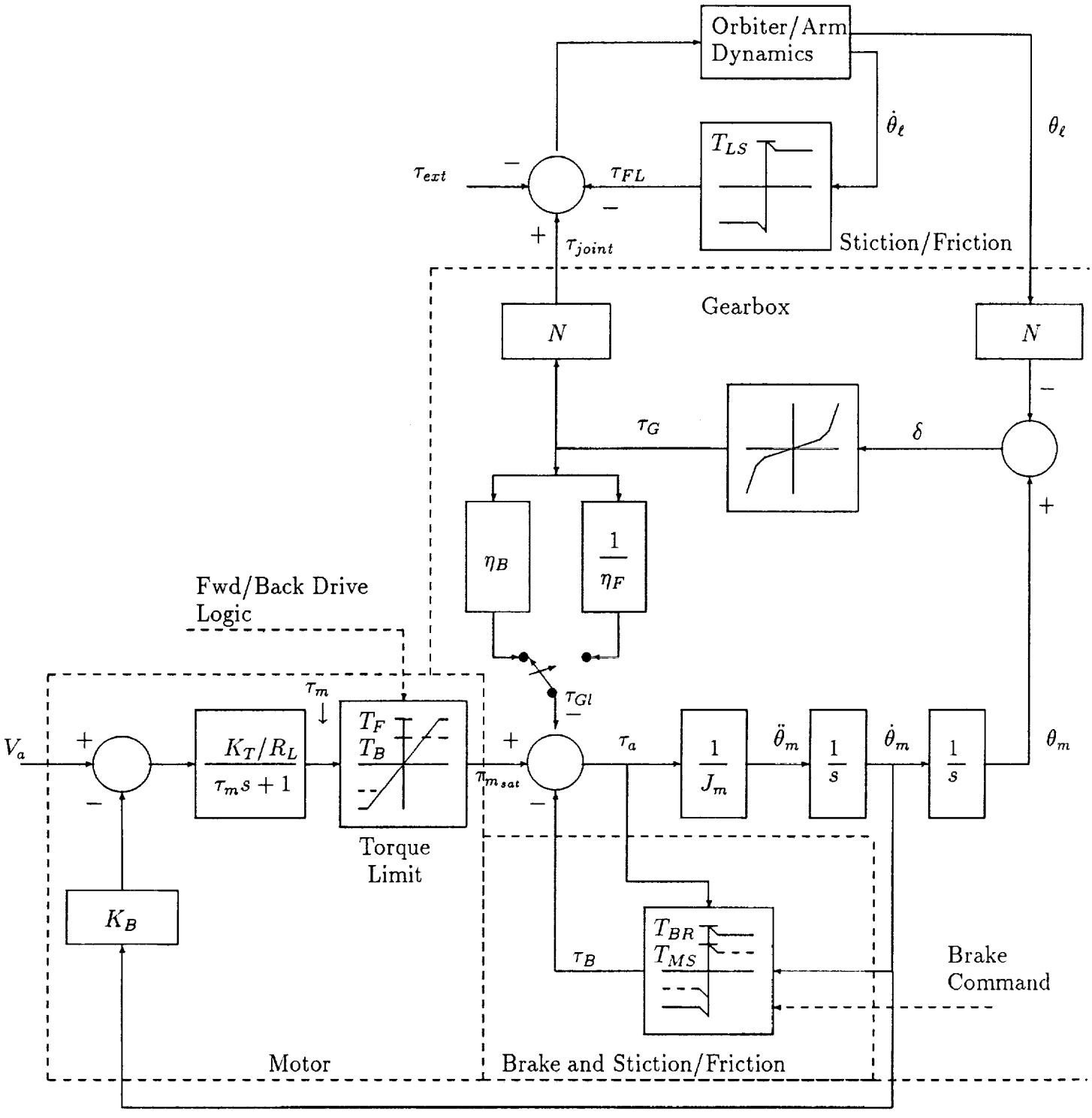

Figure 2: Joint servo model

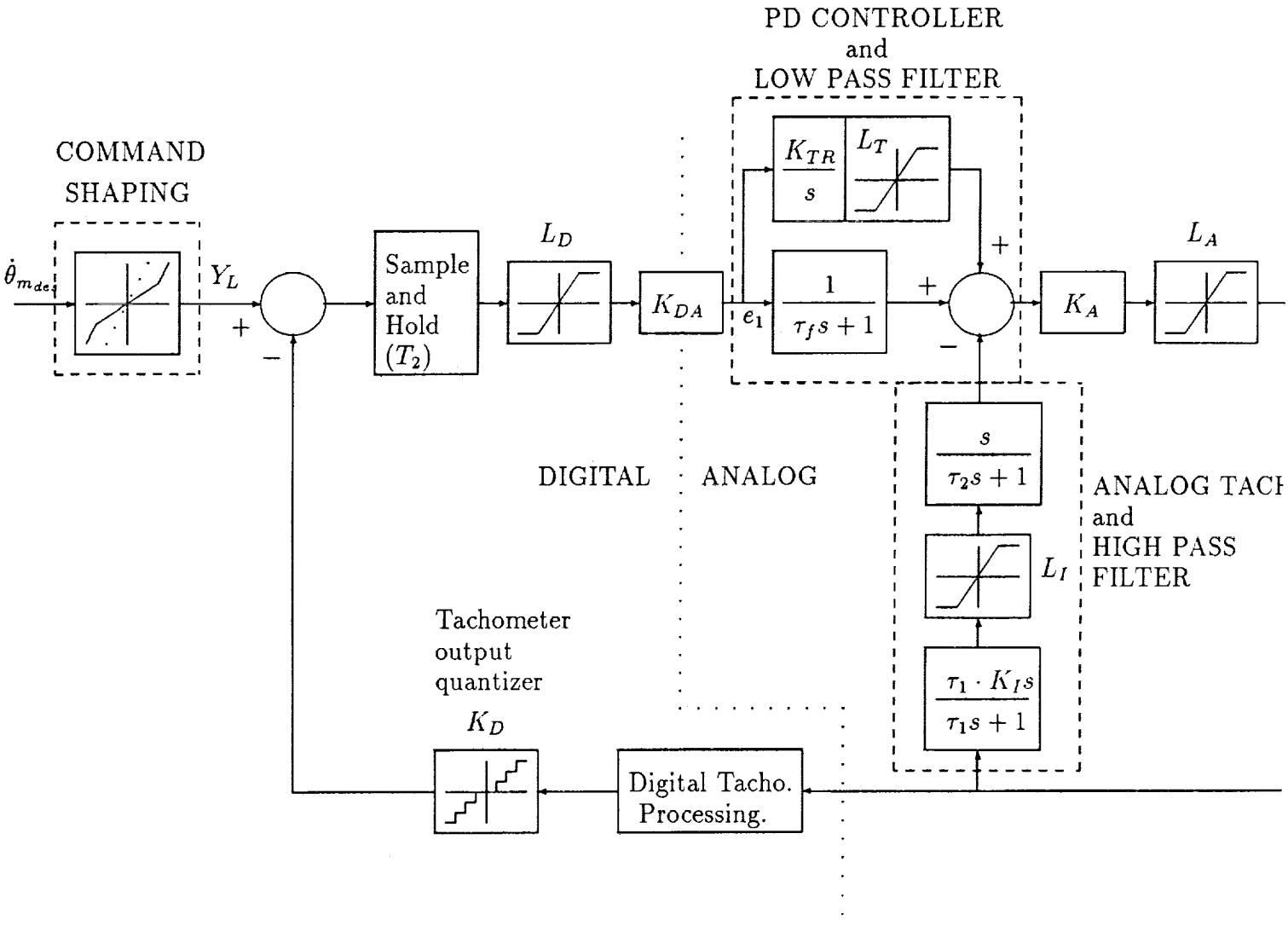

Figure 3: SRMS controller

2.1.2 Joint Servo Model Description

The joint servo model for each joint is shown in Fig. 2 and the existing RMS controller is shown in Fig. 3. The three joints in the manipulator model for this study are identical and the parameters are listed in table 3. The motor drive amplifier is modeled as a constant gain K_A. The motor time constant τ_m is ignored. The motor shaft and the gearbox input shaft are one and the same so that the moment of inertia for all the component rigidly attached to that shaft are included in the gearbox input moment of inertia J_m. The motor brake and stiction/friction functions are modeled by a single nonlinear function as shown in Fig. 4 where

$$f\left(\dot{\theta}_m\right) = \left[(T_{B0} - T_C) \cdot e^{-\frac{|\dot{\theta}_m|}{\nu}} + T_C \right] \cdot \text{sgn}\left(\dot{\theta}_m\right) \tag{19}$$

where ν represents the rate of transition from stiction to friction. Application of the brake increases the stiction/friction level to the sum of the motor stiction/friction plus that of the brake.

Table 3: Joint parameters

Variable	Name	Value	Units
Motor inertia	J_m	3.6755E-4	$Kg \cdot m^2$
Motor constant	K_T/R_L	0.081345	$N \cdot m/V$
Back Emf	K_B	0.235	$V/rad/s$
Motor friction	T_{mf}	0.02819957	$N \cdot m$
Motor friction (brake on)	T_{BR}	0.4430586	$N \cdot m$
Torque limit (fwd)	T_F	0.9057755	$N \cdot m$
Torque limit (bkd)	T_B	0.5139642	$N \cdot m$
Motor drive gain	K_A	1.92	V/V
Motor drive output limit	L_A	20.0	V
Output friction	T_{of}	54.9485	$N \cdot m$
Gear ratio	N	1841.95	
Gearbox stiffness	K_G	0.47153	$N \cdot m/rad/s$
Backlash angle	Δ	1.6872	rad
Torque at Δ	T_Δ	0.23	$N \cdot m$
Efficiency (fwd)	η_F	0.78	
Efficiency (bkd)	η_B	0.845	
D/A gain	K_{DA}	0.1615	V/cnt
D/A input limit	L_D	63	cnt
Digital tach. gain	K_D	11.378	$cnts/rad/s$

The effect of the motor drive amplifier current limit is included as a torque limit in the motor model. This torque limit depends on the motor mode of operation, i.e. forward

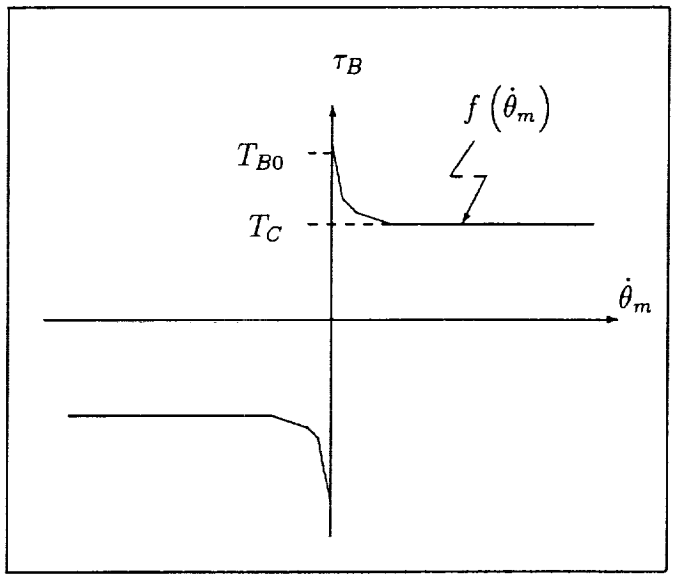

Figure 4: Motor brake and stiction/friction functions

drive or backdrive mode. Motor forward drive mode corresponds to the case when the gearbox is forward driven by the motor and similarly for the backdrive mode. The motor forward/backdrive logic is as follows :

Motor forward/backdrive logic

IF $\mathbf{sgn}(\tau_m) \cdot \dot{\theta}_m > 0.17580 rad/s$ **THEN torque limit** $= T_F$

IF $\mathbf{sgn}(\tau_m) \cdot \dot{\theta}_m \leq 0.17580 rad/s$ **THEN torque limit** $= T_B$

where the motor torque τ_m is defined as (Fig. 2) :

$$\tau_m = (V_a - K_B \cdot \dot{\theta}_m) \cdot K_T / R_L \tag{20}$$

The servo drive amplifier output is saturated at L_A. The link stiction/friction characteristic is the same as that of the motor-brake stiction/friction.

The gearbox is represented by a single stage model where the backlash of all the gear meshes is concentrated in a single mesh and is modeled as a nonlinear spring function where the function represents the gradual increase in stiffness as more and more of the planetary gears of the gearbox mesh. The nonlinear spring function is shown in Fig. 5 where

$$\tau_G = \begin{cases} T_\Delta \cdot (\delta/\Delta)^2 \cdot \mathrm{sgn}(\delta) & if \quad \mid \delta \mid \leq \Delta \\ K_G \cdot \delta + (T_\Delta - K_G \cdot \Delta) \cdot \mathrm{sgn}(\delta) & if \quad \mid \delta \mid > \Delta \end{cases} \tag{21}$$

The gearbox efficiency depends on the gearbox mode of operation, i.e. forward drive or backdrive mode. The gearbox forward/backdrive logic is as follows :

Gearbox forward/backdrive logic

IF $\dot{\theta}_m \cdot \delta > 0$ **THEN** η_F **(forward drive)**

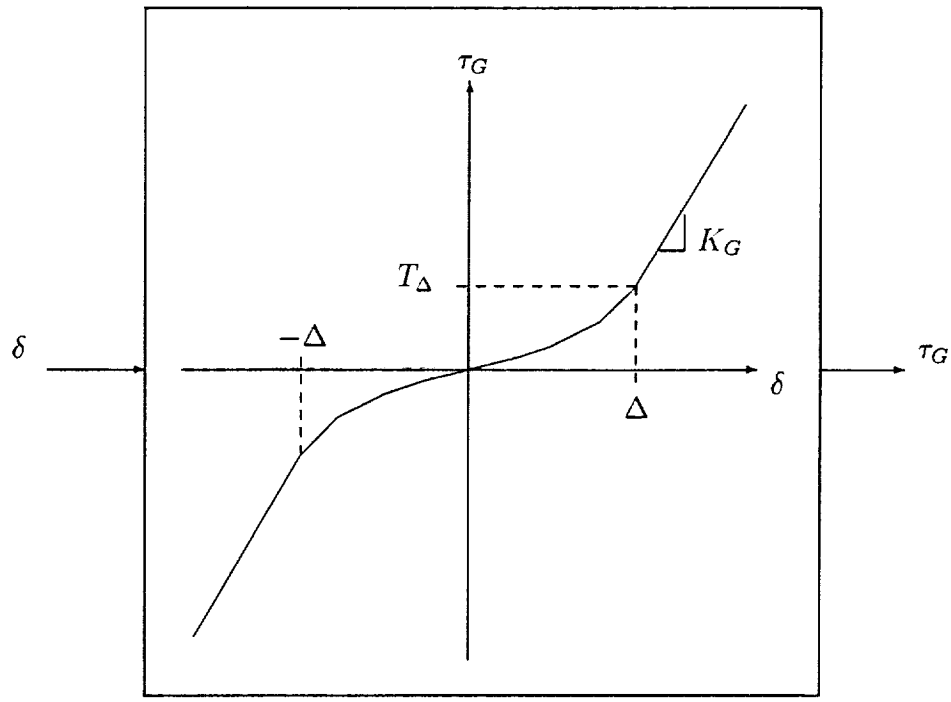

Figure 5: Nonlinear spring backlash model

IF $\dot{\theta}_m \cdot \delta \leq 0$ **THEN** η_B **(backdrive)**

Note that η_F, $\eta_B < 1$.

Finally, the orbiter dynamics and attitude control system are ignored. Also, we assume that no external force is exerted on the manipulator.

To summarize, the complete equations of motion (with voltage input V_a) are given by:

$$\tau_m = \left[\text{sat}\left(V_a \cdot K_A, L_A\right) - K_B \cdot \dot{\theta}_m\right] \cdot K_T / R_L \tag{22}$$

$$\ddot{\theta}_m = J_m^{-1} \cdot \left[\text{sat}\left(\tau_m, (T_F, T_B)\right) - \tau_B(\dot{\theta}_m) - \tau_G \cdot (\eta_B, 1/\eta_F)\right] \tag{23}$$

$$\delta = \theta_m - N \cdot \theta \tag{24}$$

$$\tau_G = \begin{cases} T_\Delta \cdot (\delta/\Delta)^2 \cdot \text{sgn}(\delta) & IF \quad |\,\delta\,| \leq \Delta \\ K_G \cdot \delta + (T_\Delta - K_G \cdot \Delta) \cdot \text{sgn}(\delta) & IF \quad |\,\delta\,| > \Delta \end{cases} \tag{25}$$

$$N \cdot \tau_G - \tau_{FL}(\dot{\theta}_\ell) = M(\theta_\ell)\ddot{\theta}_\ell + C(\theta_\ell, \dot{\theta}_\ell)\dot{\theta}_\ell \tag{26}$$

2.2 Baseline Control Mode

2.2.1 Resolved Rate

The resolved rate mode of control is the baseline mode for the system. The joint rate commands are computed from the inverse Jacobian:

$$\dot{\theta}_{\ell_{des}} = J^{-1} \cdot V_{des} \tag{27}$$

where $V_{des} = \left[\dot{\theta}_{des}, \dot{x}_{des}, \dot{y}_{des}\right]^T$ is the command velocity of the point of resolution (POR). For this study, the **end effector** is used as the POR. The Jacobian matrix in a coordinate

system fixed at the shoulder joint and aligned with the base (Fig. 1) is given by:

$$J = \begin{bmatrix} 1 & 1 & 1 \\ (-l_1 \cdot S1 - l_2 \cdot S12 - l_3 \cdot S123) & (-l_2 \cdot S12 - l_3 \cdot S123) & (-l_3 \cdot S123) \\ (l_1 \cdot C1 + l_2 \cdot C12 + l_3 \cdot C123) & (l_2 \cdot C12 + l_3 \cdot C123) & (l_3 \cdot C123) \end{bmatrix} \quad (28)$$

where $C1 = cos(\theta_1)$, $C12 = cos(\theta_1 + \theta_2)$, $C123 = cos(\theta_1 + \theta_2 + \theta_3)$, $S1 = sin(\theta_1)$, $S12 = sin(\theta_1 + \theta_2)$, $S123 = sin(\theta_1 + \theta_2 + \theta_3)$.

2.2.2 Rate Limits

In addition to using the resolved rate mode of operation, the manipulator is also a velocity limited device. The RMS is velocity limited at the joints and the end effector. In this study, a single joint rate limit is considered since all the joints are identical. Also, rotation and translation velocity limits are assumed decoupled. The end effector limits and joint rate limits for the unloaded manipulator and the manipulator with the baseline payload attached are given in table 4 where

$$V_{\max} = \sqrt{\dot{x}_{\max}^2 + \dot{y}_{\max}^2} \quad (29)$$

Table 4: Rate limits

Variable	Payload		Units
	Unloaded	Baseline	
$\dot{x}_{\max}$	0.36576	0.03048	m/s
$\dot{y}_{\max}$	0.36576	0.03048	m/s
$V_{\max}$	0.36576	0.03048	m/s
$\dot{\theta}_{\max}$	0.04	0.003	rad/s
$\dot{\theta}_{\ell_{\max}}$	0.04	0.003	rad/s

The rate limiting algorithm is such that all the rates are scaled down if a cartesian velocity limit or a joint rate limit is exceeded. Hence, the same path is followed but at a lower rate. The logic is the following :

1. **IF** command given in joint space
   (a) $V_{des} = J \cdot \dot{\theta}_{\ell_{des}}$
2. **END**
3. **Saturate the cartesian velocity**
   (a) $r_1 = |\dot{x}_{des}|/\dot{x}_{\max}$
   (b) $r_2 = |\dot{y}_{des}|/\dot{y}_{\max}$
   (c) $r_3 = |\sqrt{\dot{x}_{des}{}^2 + \dot{y}_{des}}|/V_{\max}$

(d) $r_4 = |\dot{\theta}_{des}|/\dot{\theta}_{\max}$

(e) $r = max\,(1, r_1, r_2, r_3, r_4)$

(f) $V_{des} = V_{des}/r$

4. $\dot{\theta}_{\ell_{des}} = J^{-1} \cdot V_{des}$

5. **Saturate the joint rates**

   (a) **FOR** each joint, compute : $s_j = |\dot{\theta}_{\ell_j}|/\dot{\theta}_{\ell_{max}}$

   (b) $s = max\,(1, s_j)$

   (c) $\dot{\theta}_{\ell_{des}} = \dot{\theta}_{\ell_{des}}/s$

2.3 Fortran Program Assumptions

This program is used as a high fidelity simulation. It includes the complete model of the system as described in section 2.1, except for the electrical time constant, feedback quantization, and digital tachometer processing.

The logic for the implementation of the motor brake and stiction/friction is described by the flowchart in figure 6 (see Figures 2 and 4 for the variables definition). The logic in the flow chart allows the motor to come to a rest even though a discontinuous feedback function is used.

A similar logic cannot be easily implemented on the link side due to the inter-link coupling torques. However, since the link inertia is relatively large when the baseline payload is carried, only insignificant numerical oscillations can occur due to the discontinuous feedback function. Therefore, the friction function without the logic is used for the links.

The following is a list of features that are supported by the Fortran program:

- All nonlinearities are included, such as

  (i) gearbox nonlinearity and hysteresis: nonlinear spring, variable efficiency.

  (ii) centrifugal/Coriolis torque.

  (iii) limits for torque, voltage command, integrator, measurement, velocities (link and Cartesian space).

  (iv) friction for links and motors.

- Sample and hold circuit is included.

- Simulation is performed with an efficient ODE solver which allows control of both relative and the absolute errors.

- States are scaled in order to take advantage of the ODE solver error controls.

- Parameters for simulations are initialized by data files which allows easy modification of the operating condition and system parameters.

- Velocity reference signal can be defined in Cartesian space and in link angle space.

2.4 Matlab Program Assumptions

To quickly experiment with different structures and parameters for the controller, we have also developed a simplified simulation program within the interpretive MATLAB environment. The assumptions posed in addition to those in the FORTRAN program are listed below:

1. The brake stiction/friction is replaced by the motor friction T_{mf}, i.e. they are considered as having the same value. Also, the link stiction/friction is replaced by the joint friction. The logic for the implementation of the motor brake and stiction/friction is described by the flowchart in Fig. 7 where ϵ is a small positive number (see figures 2 and 4 for the variables definition).

2. The gearbox is assumed to have unit efficiency.

3. Only the motor torque limit and the velocity limits are considered, i.e., the servo drive amplifier output voltage limit and the electronic circuit limits are not considered. The motor torque limit is assumed unique, i.e. does not depend on the motor driving mode (the forward mode limit level is used).

Except for those assumptions mentioned above, this program shares all other features of the Fortran program described in section 2.3.

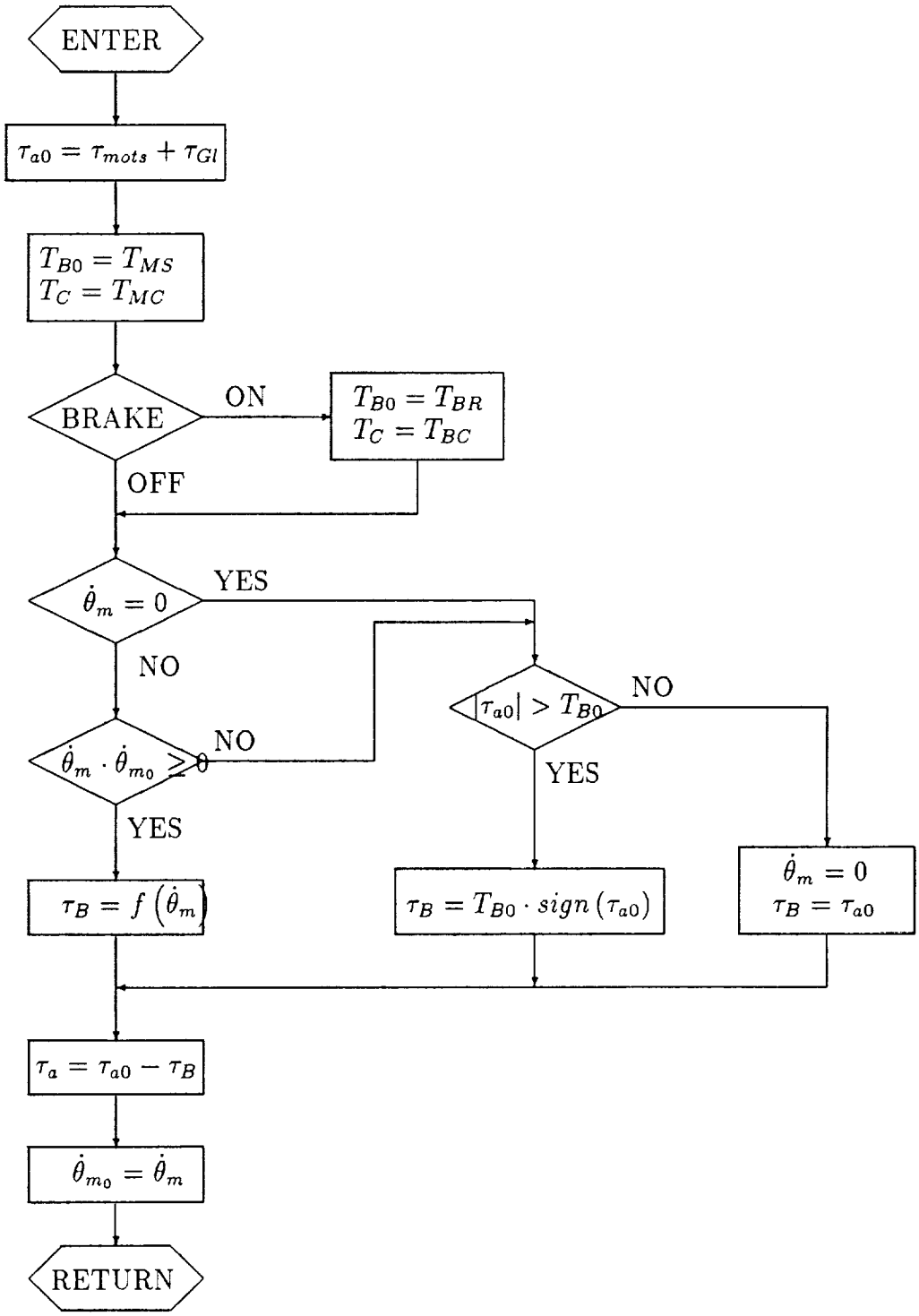

Figure 6: Stiction/friction and brake model flow chart

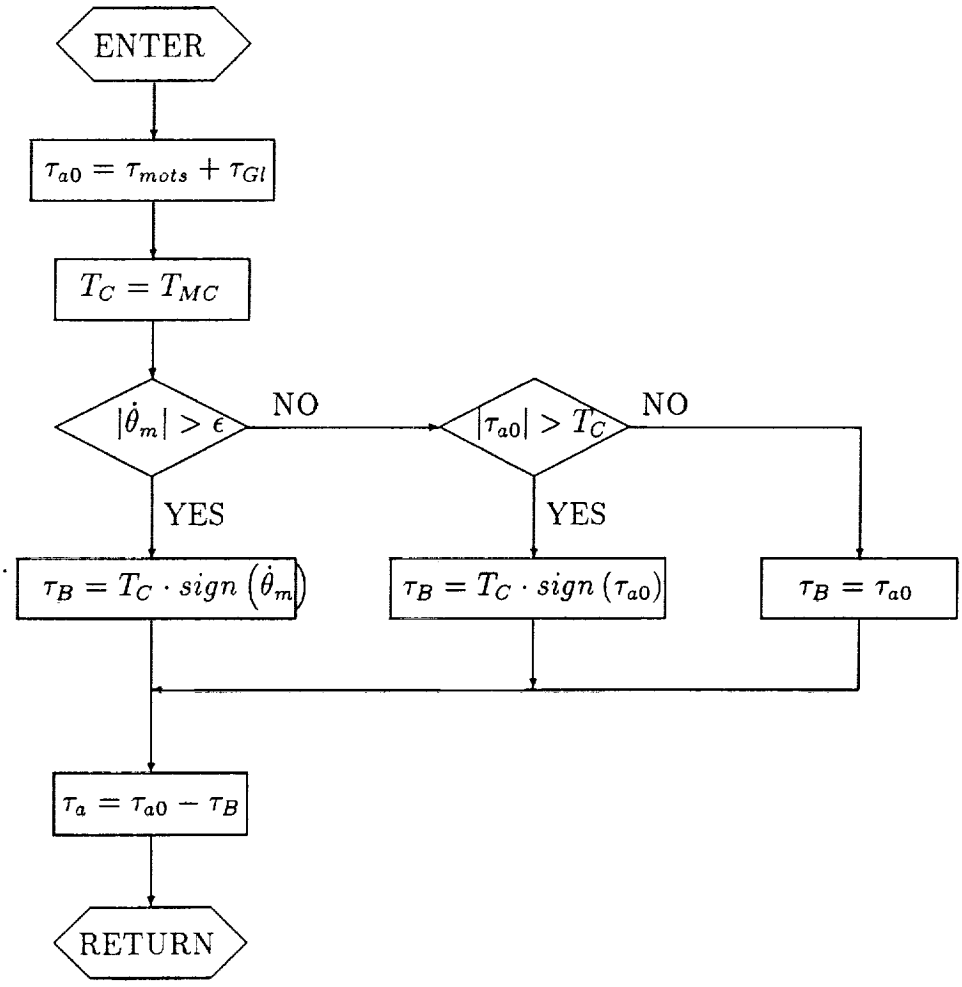

Figure 7: Motor friction model flow chart

3 RMS controller

In this section, the existing RMS controller is described and briefly analyzed.

3.1 Description of RMS Controller

The main idea behind the RMS controller (shown in Fig. 3 and table 5) is to rotate the motors at the desired link velocities (scaled by the gear ratio), and because of friction and joint spring, the links will eventually also stabilize at the desired velocities. Hence, only the motor velocities are controlled.

The controller is composed of the following elements (some of the terminology is different than that in [17], for example, proportional and integral feedback in [17] means velocity and position, since velocity feedback is considered as the primary loop; here we use the convention based on position feedback, so proportional and derivative feedback means position and velocity feedback):

1. **Proportional–Derivative (PD) controller with low pass filter.** The purpose of the proportional feedback is to provide a high gain at low frequencies to break motor and drive train stiction and eliminate small errors. The amount of proportional feedback is limited at $\pm L_T$. Position error is obtained via integration of the velocity error. Integration stops when the limit is reached; it resumes when the input of the integrator changes sign. This controller has the following input/output transfer function :

   - Not in limit mode :

   $$V_{c1} = \frac{\left[(K_{TR}+1) + \frac{K_{TR}}{s}\right]}{[\tau_f s + 1]}\, e_1 \tag{30}$$

   - In limit mode :

   $$V_{c1} = \pm L_T + \frac{e_1}{[\tau_f s + 1]} \tag{31}$$

2. **Analog tachometer and high pass filter.** This element is used to improve the transient performance of the controller (it slows down the motor response, resulting in smoother transients). The high pass filter is composed of two stages with a limiter (figure 3) and has the following transfer function when it is not in limit mode :

   $$V_{c2} = \frac{[\tau_1 \cdot K_I \cdot s^2]}{[\tau_1 s + 1] \cdot [\tau_2 s + 1]}\, \dot{\theta}_m \tag{32}$$

3. **Command shaping.** This module is used in order to maintain accurate steady-state response in presence of limiting of the integral term of the velocity error. The command shaping is described by the following equation (figure 8):

   $$Y_L = \begin{cases} K_D \cdot \dot{\theta}_{m_{des}} & IF \quad |\dot{\theta}_{m_{des}}| \le L \\ K_1 \cdot \dot{\theta}_{m_{des}} - K_2 & IF \quad |\dot{\theta}_{m_{des}}| > L \end{cases} \tag{33}$$

where

$$\dot{\theta}_{m_{des}} = N \cdot \dot{\theta}_{\ell_{des}} \tag{34}$$

$$L = L_T \cdot K_A / K_B \tag{35}$$

$$K_1 = K_D + \frac{K_B}{K_{DA} \cdot K_A} \tag{36}$$

$$K_2 = \frac{L_T}{K_{DA}} \mathrm{sgn}\left(\dot{\theta}_{m_{des}}\right) \tag{37}$$

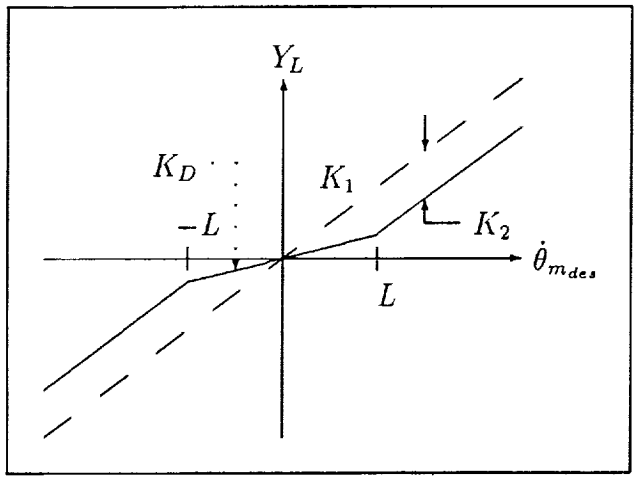

Figure 8: Command shaping

We note that the scaling depends on whether the velocity integral term (i.e., proportional feedback) is sufficient to compensate for the back emf due to the commanded joint velocity scaled by the gear ratio. If it is sufficient, the commanded motor velocity is the commanded joint velocity scaled by the gear ratio and by the tachometer gain. Otherwise, a term is added to compensate for the back emf and another one to subtract the velocity integral term. We note that the back emf is compensated in steady state. However, there is no compensation for stiction/friction and for the loading effect of the gearbox which will lead to a steady state error.

NOTE : The values listed for L, K_1 and K_2 in table 5 do not correspond to the values obtained by applying (35), (36) and (37). Values in the table were obtained from [18] and are also listed in [20] where no explanation is provided to explain the change of values. These changes may modify the above comments regarding which effects are or are not compensated if the integrator saturates but does **not** affect the results presented in this report since the velocity integral limit is not used.

The complete controller has been implemented in the Fortran program while not all the limits are used in the Matlab version. In particular, the limit on the velocity integral L_T, the limit on the high pass filter L_I, the limit on the D/A converter input L_D and the voltage limit at the output of the motor drive amplifier L_A are not implemented in the Matlab program.

Table 5: RMS controller parameters

Variable	Name	Value	Units
Integral trim limit	L_T	1.5	V
Integral trim gain	K_{tr}	0.05	s^{-1}
PD contr. filter time constant	τ_f	0.1	s
Analog tach processing gain	K_I	0.12	$V/rad/s$
Analog tach pro. time constant	τ_1	0.1	s
Analog tach pro. time constant	τ_2	0.1	s
Analog tach pro. output limit	L_I	13.0	V
Command shaping	K_1	11.378	$cnts/rad/s$
Command shaping	K_2	6.757	$cnts$
Command shaping	L	8.86	rad/s

3.2 Analysis of RMS Controller

The main characteristics of the controller are :

- Controller uses only motor velocities (motor PD control + analog tachometer feedback).
- Motor velocity is brought to the desired link velocity and link oscillation damp out due to link friction.
- No corrective action is taken by the RMS controller if the motor torque saturates or if any other limit is exceeded except for the velocity integral limit (by the use of command shaping). Also, steady state correction for the velocity integral limit is not exact in the sense that it does not consider the loading effect of the gearbox and the motor friction. This may lead to a steady state error.
- Joints are assumed decoupled.
- Stability is maintained in presence of load changes.

Some problems were observed :

1. Coupling between the joints causes uncontrolled motions. For example, given a velocity command in the x-direction, the orientation and the y-position both vary during the motion and deviations are not corrected by the controller.
2. Link velocity oscillations damp out slowly.
3. Link errors are corrected slowly; the controller must wait for the motors to be affected before any corrective action is initiated.
4. Small proportional feedback gain (i.e., the velocity integral gain) leads to large link position error.

5. Larger errors are observed when limits are reached.

These problems are caused mainly by the lack of link angle feedback, the large coupling between the links, the nonlinear spring characteristic of the gearbox, the small inertia of link 3 (higher frequency natural mode) and the inexact or nonexistent compensation for the limiters.

4 Modified Controller

As described in section 3, the RMS controller consists of two loops. There is a digital joint feedback loop that is closed at 8.75ms:

$$u_{m_1} = -K_{p_m}(\theta_m - \theta_{m_{des}}) - K_{v_m} z \tag{38}$$

where z is the low pass filtered version of the motor velocity error $\dot{\theta}_m - \dot{\theta}_{m_{des}}$. An analog high pass motor feedback is added to the output of the digital loop:

$$u_{m_2} = H(s)\dot{\theta}_m. \tag{39}$$

For the RMS controller, $H(s)$ is given by

$$H(s) = \frac{\tau_I K_I s^2}{(\tau_I s + 1)^2} \tag{40}$$

where $\tau_I = \tau_1 = \tau_2$ in Table 5. The overall motor voltage control signal is given by

$$u_m = u_{m_1} + u_{m_2}.$$

The proposed controller builds on top of the RMS controller. The following modifications have been tried, to varying degrees of effectiveness:

1. A feedforward term is added, so the motor voltage is now:

$$u_m = u_{m_1} + u_{m_2} + u_{m_{ff}}.$$

   The structure of the many possible feedforward signals will be discussed below.

2. Several different alternate filters are tried in place of the high pass filter.

3. Smoothed desired rate trajectories are tried in place of the step.

The rest of this section describes these modifications in detail.

Feedforward Design

As described in Section A.6 of the Appendix, the basic idea behind the feedforward design is that given the desired output trajectory, $\theta_{\ell_{des}}(t)$, $t \geq 0$, in the flexible joint robot case, find the desired state (i.e., $\theta_{m_{des}}(t)$, since $\theta_{\ell_{des}}(t)$ is given) and the feedforward control which can produce this output. The intuitive idea for the feedforward control in flexible joint robot control is that the joint spring is wound up in anticipation to the desired *link* motion rather than the desired motor motion.

The feedforward design essentially involves an inverse plant problem. Consider the following simplified model for a flexible joint robot:

$$M(\theta_\ell)\ddot{\theta}_\ell + C(\theta_\ell, \dot{\theta}_\ell)\dot{\theta}_\ell + Nk(N\theta_\ell - \theta_m) + T_\ell(\dot{\theta}_\ell) = 0 \tag{41}$$

$$J_m\ddot{\theta}_m + D_m\dot{\theta}_m - k(N\theta_\ell - \theta_m) + T_m(\dot{\theta}_m) = \tau. \tag{42}$$

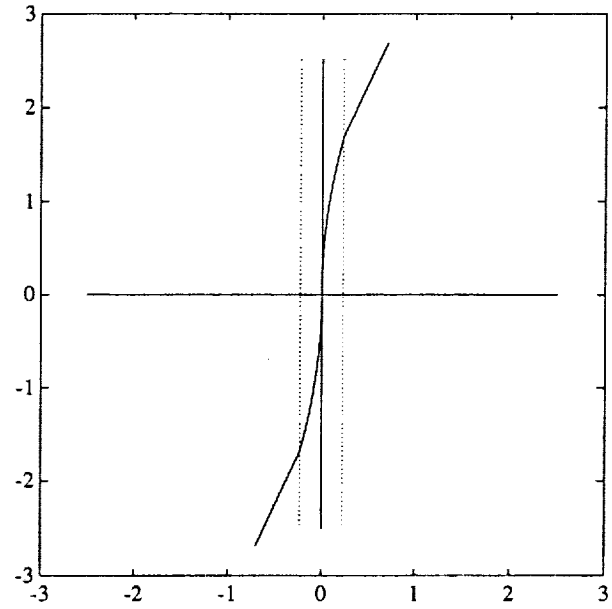

Figure 9: Inverse Joint Spring Function

Given the desired $\theta_{\ell_{des}}(t)$ (which means all of its higher derivatives can be calculated), the desired $\theta_{m_{des}}$ can be solved from (41)

$$\theta_{m_{des}} = \frac{1}{N}k^{-1}(M(\theta_\ell)\ddot{\theta}_{\ell_{des}} + C(\theta_\ell, \dot{\theta}_\ell)\dot{\theta}_{\ell_{des}} + T_\ell(\dot{\theta}_\ell)) + N\theta_{\ell_{des}} \tag{43}$$

where k^{-1} is the inverse function of the nonlinear joint spring (see Fig. 9):

$$k_i^{-1}(x_i) = \begin{cases} (x_i - (T_\Delta - K_G\Delta)\text{sgn}(x_i))K_G{}^{-1} & |x_i| \geq T_\Delta \\ \Delta\sqrt{\frac{x_i}{T_\Delta}}\text{sgn}(x_i) & |x_i| < T_\Delta \end{cases}.$$

Higher derivatives of the desired motor angle, $\theta_{m_{des}}$, can be obtained by directly differentiating (43). The feedforward control is then

$$\tau_{ff} = J_m\ddot{\theta}_{m_{des}} + D_m\dot{\theta}_{m_{des}} - k(N\theta_{\ell_{des}} - \theta_{m_{des}}) + T_m(\dot{\theta}_m). \tag{44}$$

The calculation of $\ddot{\theta}_{m_{des}}$ and $\dot{\theta}_{m_{des}}$ requires higher derivatives of θ_ℓ and $\theta_{\ell_{des}}$ which in turn depend on higher derivatives of Coulomb friction and k^{-1} which are unbounded functions. Since the arm is anticipated to move very slowly, a reasonable approximation can be made by dropping higher order terms in $\dot{\theta}_\ell$ and $\dot{\theta}_{\ell_{des}}$ (and higher derivatives). This then leads to a simplified expression for the desired motor angle:

$$\theta_{m_{des}} = \frac{1}{N}k^{-1}(M(\theta_\ell)\ddot{\theta}_{\ell_{des}} + T_\ell(\dot{\theta}_\ell)) + N\theta_{\ell_{des}} \tag{45}$$

This still leads to complicated expressions for higher derivatives of $\theta_{m_{des}}$ which are required in the feedforward control. We make a further approximation for $\dot{\theta}_{m_{des}}$ by dropping the gear contribution in the derivative of $\theta_{m_{des}}$. This approximation is plausible since the second term

in (45) usually dominates the first term, but it does not have a firm theoretical justification at the present (it is a major part of the future work):

$$\dot{\theta}_{m_{des}} = N\dot{\theta}_{\ell_{des}}. \tag{46}$$

The feedforward control then becomes

$$\tau_{ff} = J_m N\ddot{\theta}_{\ell_{des}} + D_m N\dot{\theta}_{\ell_{des}} - k(N\theta_{\ell_{des}} - \theta_{m_{des}}) + T_m(\dot{\theta}_m). \tag{47}$$

where $\theta_{m_{des}}$ is given by (45). This feedforward is reasonable to implement in real time since no higher derivatives of $\theta_{m_{des}}$ is used.

So far, direct link coordinate measurements have not been used. To further enhance the performance of link responses, an additional modification of the feedforward control, motivated by [21], is made. The open loop desired link angular response $\ddot{\theta}_{\ell_{des}}$ is replaced by a desired feedback control for the robot links, i.e., define the desired closed loop link angular acceleration by

$$a_{l_{des}} = \ddot{\theta}_{\ell_{des}} - K_{p_\ell}(\theta_\ell - \theta_{\ell_{des}}) - K_{v_\ell}(\dot{\theta}_\ell - \dot{\theta}_{\ell_{des}}). \tag{48}$$

Then the expression for $\theta_{m_{des}}$ becomes

$$\theta_{m_{des}} = \frac{1}{N}k^{-1}(M(\theta_\ell)a_{l_{des}} + T_\ell(\dot{\theta}_\ell)) + N\theta_{\ell_{des}} \tag{49}$$

The same approximation of the higher derivatives of $\theta_{m_{des}}$ is used as in (46), so the feedforward torque is still given by (47) (using $\theta_{m_{des}}$ from (49). In all the simulation results in the next section, $M(\theta_\ell)$ in (45) is further approximated by $M(\theta_{\ell_{des}})$ which is easier to implement in real time (perhaps by table lookup and interpolation). The PD type of feedback for the link in (48) can be replaced by higher order positive real filters. This possibility has not been explored yet.

The above scheme for computing the feedforward also affects the feedback servo loop since $\theta_{m_{des}}$ and $\dot{\theta}_{m_{des}}$ are used in the feedback control law. In contrast, in the RMS controller, $\theta_{m_{des}}$ is given by $\theta_{m_{des}} = N\theta_{\ell_{des}}$. Consequently, the motor response may be satisfactory but the link response is not. In effect, the modified scheme we have presented allows the joint spring to be wound up just right so spring torque emulates a link feedback control law (i.e., as if the link is feedback controlled by the spring torque). Furthermore, since the mass matrix is incorporated in the link feedback control law in (49), the interlink coupling is compensated, and the gains K_{p_ℓ} and K_{v_ℓ} can be tuned for each individual link.

High Frequency filter

Several high frequency filters have been tried beside the RMS high pass filter in (40). The first is also a high pass filter (the one used in the original SPAR report [17]) and it is positive real (i.e., passive):

$$H_1(s) = \frac{K_I s}{\tau_I s + 1}.$$

The second is a bandpass filter which is also positive real:

$$H_2(s) = k\frac{b(s)}{a(s)}$$

where $k = 10E5$ is the high frequency gain, b and a are both monic polynomials with roots of b at $(0.5, 70, 125)$ and roots of a at $(50, 100, 200, 300)$. Simulation results of using different filters are not included in this report. However, we have observed that different filters lead to very different transient responses, especially in terms of the amplitude of oscillations. A systematic tuning procedure, perhaps based on some performance optimization criterion, will be investigated as part of the future work.

Command Trajectory Smoothing

Beside the step rate command, several other smoothed rate command trajectories have been used, including ramped velocity, exponential, and ramped acceleration. The conclusions drawn about the performance is similar for these three cases, and only the ramped velocity result is included in this report. The desired link angle, angular velocity, and angular acceleration for the ramped link velocity case are given below (the Cartesian case is identical):

$$\theta_{\ell_{des}}(t) = \begin{cases} \frac{\dot{\theta}_{\ell_f}}{T}\frac{t^2}{2} + \theta_\ell(0) & t < T \\ \dot{\theta}_{\ell_f}(t-T) + \theta_\ell(0) + \dot{\theta}_{\ell_f}\frac{T}{2} & t \geq T \end{cases} \tag{50}$$

$$\dot{\theta}_{\ell_{des}}(t) = \begin{cases} \dot{\theta}_{\ell_f}\frac{t}{T} & t < T \\ \dot{\theta}_{\ell_f} & t \geq T \end{cases} \tag{51}$$

$$\ddot{\theta}_{\ell_{des}}(t) = \begin{cases} \frac{\dot{\theta}_{\ell_f}}{T} & t < T \\ 0 & t \geq T. \end{cases} \tag{52}$$

We shall see in the next section that, not surprisingly, the ramped velocity profile produces much less uncommanded motion and oscillation, and improves the settling time at the same time. This is true for both the existing controller and the modified controller, but the modified controller tracks much more closely. The contrast between the performances of the two controllers is most evident during the initial stage where the motor torque needs to overcome stiction to cause link motion. If only motor feedback is used, there is an initial delay where enough motor error needs to accumulate before the control torque becomes greater than the stiction. With the feedforward, link error causes the joint spring to wind up faster, leading to a much reduced delay.

5 Comparison of Controllers

In this section, we will compare the performance of the RMS controller versus our proposed controller for the following cases:

1. End effector step response for the unloaded and loaded cases. The command is a rate step along one of the coordinate directions (x, y, and θ) at the following rate limits:

Variable	Unloaded	Baseline payload
$\dot{x}$ rate (m/sec)	0.36576	0.03048
$\dot{y}$ rate (m/sec)	0.36576	0.03048
$\dot{\theta}$ (rad/sec)	0.040	0.003

Due to the velocity limiting logic, the rate command may be modified.

2. End effector response in loaded and unloaded cases for a ramp rate command.

We will compare the response in terms of the following measures:

1. Uncommanded motion. This is measured in terms of the peak and steady state position and velocity deviation in the uncommanded variables, which in the joint case are the uncommanded joints and in the end effector response case, they are the uncommanded coordinate directions.

2. Transient response. This is measured in terms of the settling time and overshoot of the commanded variable.

3. Steady state response. This is measured in terms of the steady state velocity and position tracking error for the commanded variables.

Additional considerations that should be taken into account in the performance comparison include:

1. The torque limit is removed in some runs to indicate the effect of saturation. In most cases, the performance degrades only slightly. However, a systematic method to avoid saturation is an important topic that will be investigated in the future.

2. The closed loop performance depends heavily on the choice of gains. At the present, no extensive tuning has been performed.

3. In simulating the proposed controller, the feedforward is approximated to somewhat address the robustness and implementation issues. A rigorous investigation of the robustness issue needs to performed in the future.

4. In the simulations for comparing the two controllers, we have removed the hysteresis effect (i.e., dependence of torque limits and motor efficiencies on velocity) to obtain a baseline comparison (so there will not be too many variables to cloud the interpretation of results). Simulation using the full nonlinear model is currently underway.

Loaded Case

We first compare the step end effector velocity responses. The arm is initially in the following configuration:

$$\theta_\ell(0) = [-0.6242,\ 1.3002,\ -0.6260]^T \text{rad} \tag{53}$$

with $\theta_m(0) = \theta_\ell(0) * N$ (N is the gear ratio). This configuration corresponds to the end effector location

$$x(0) = 13.469\text{m},\ y(0) = 0.39\text{m},\ \theta(0) = 0.05\text{rad}. \tag{54}$$

The configuration is shown in Fig.10. The nominal command is a step of 3E-3rad/sec in $\dot{\theta}$ for 10sec and drops to zero after 10sec. Due to joint velocity saturation and velocity limiting logic, the actual commanded rate is slower. Fig.11 shows the arm response with the RMS

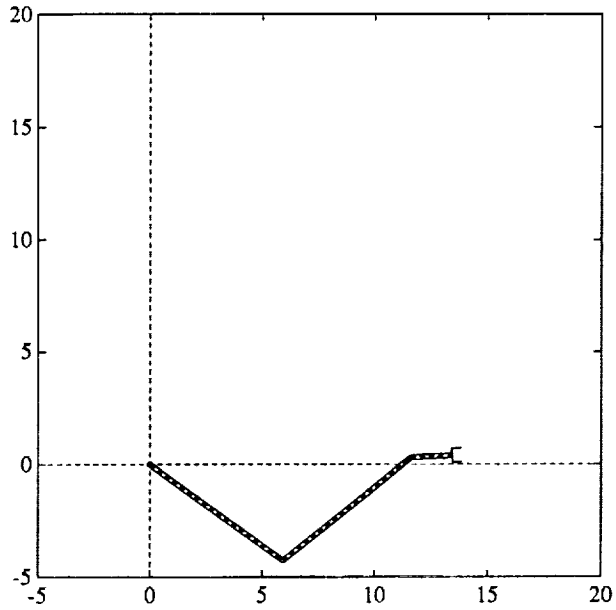

Figure 10: Initial Configuration

controller and Fig.12 and Fig.13 show the responses under the modified controller with two different sets of gains. The first set uses the existing RMS motor feedback gains and low link feedback gains (for all joints):

$$\text{Gain 1:} \qquad K_{p_\ell} = 1 \quad K_{v_\ell} = 2 \quad k_p = .1764 \quad k_v = 3.53, \tag{55}$$

The second set uses higher motor proportional gain and lower derivative gain, and higher link feedback gains:

$$\text{Gain 2:} \qquad K_{p_\ell} = 5 \quad K_{v_\ell} = 4.5 \quad k_p = 4 \quad k_v = .1. \tag{56}$$

As seen clearly from these plots, the modified controllers exhibit all around superior performance (in terms of the stated measures) over the RMS controller. Within the modified controller, the higher gain case performs much better. It should be emphasized that high gain is not the reason that the modified controller outperforms the RMS controller, the key is in its ability to wind up the joint spring based on the link angular error. In fact, when gains in the RMS controller are increased, the performance actually degrades. It is perhaps not surprising that modified controller demands much more command torque than the RMS controller. The large torque, however, only last over a small period of time since the error is reduced very quickly. When torque saturation is imposed, the response (shown in Fig. 14) is still quite good. There is slightly more rotational velocity oscillation during the initial step command, but the uncommanded motion and steady state error are much improved over the RMS controller case. Simply clamping the input at the saturation level clearly is not the best solution; for example, it may be advisable to reduce the commanded velocity when input saturation occurs. When saturation level is exceeded by a large amount or for an extended period of time, then direct clamping may lead to instability, for example, see the commanded $\dot{y}$ case in Fig.23. A systematic solution to the saturation issue is a key item for our future research.

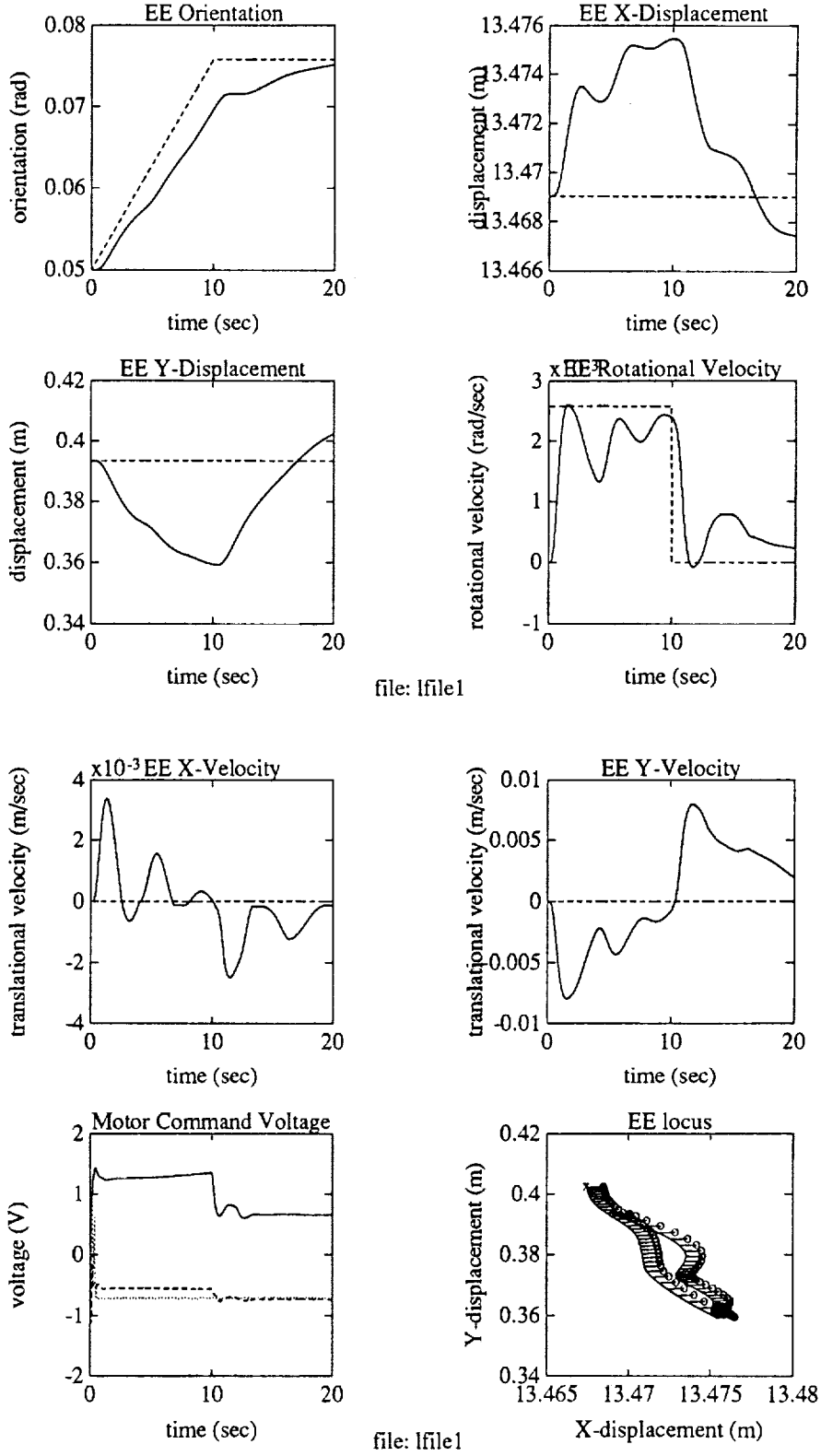

Figure 11: Step θ Velocity with RMS Controller

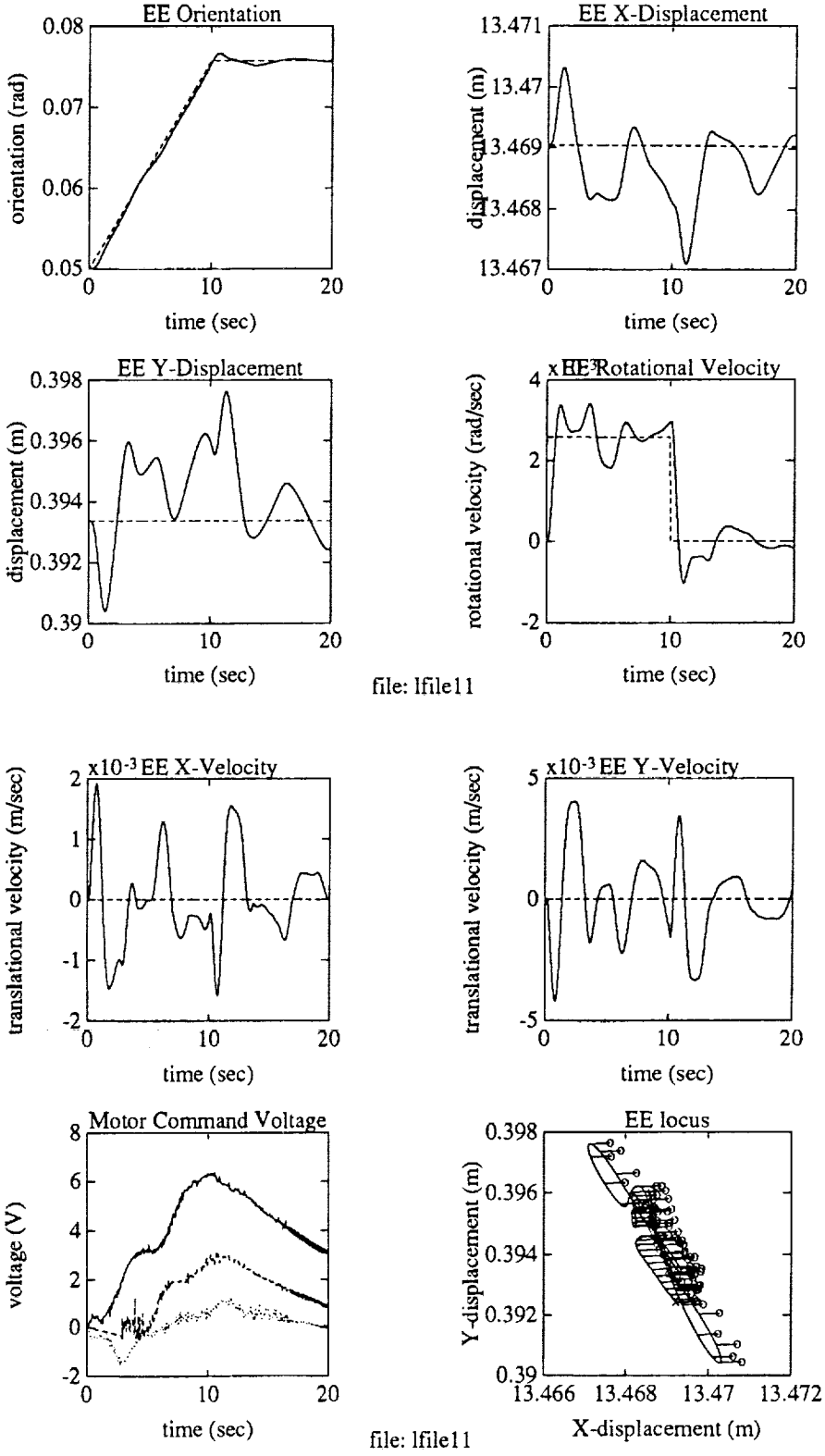

Figure 12: Step θ Velocity with Modified Controller (Gain 1)

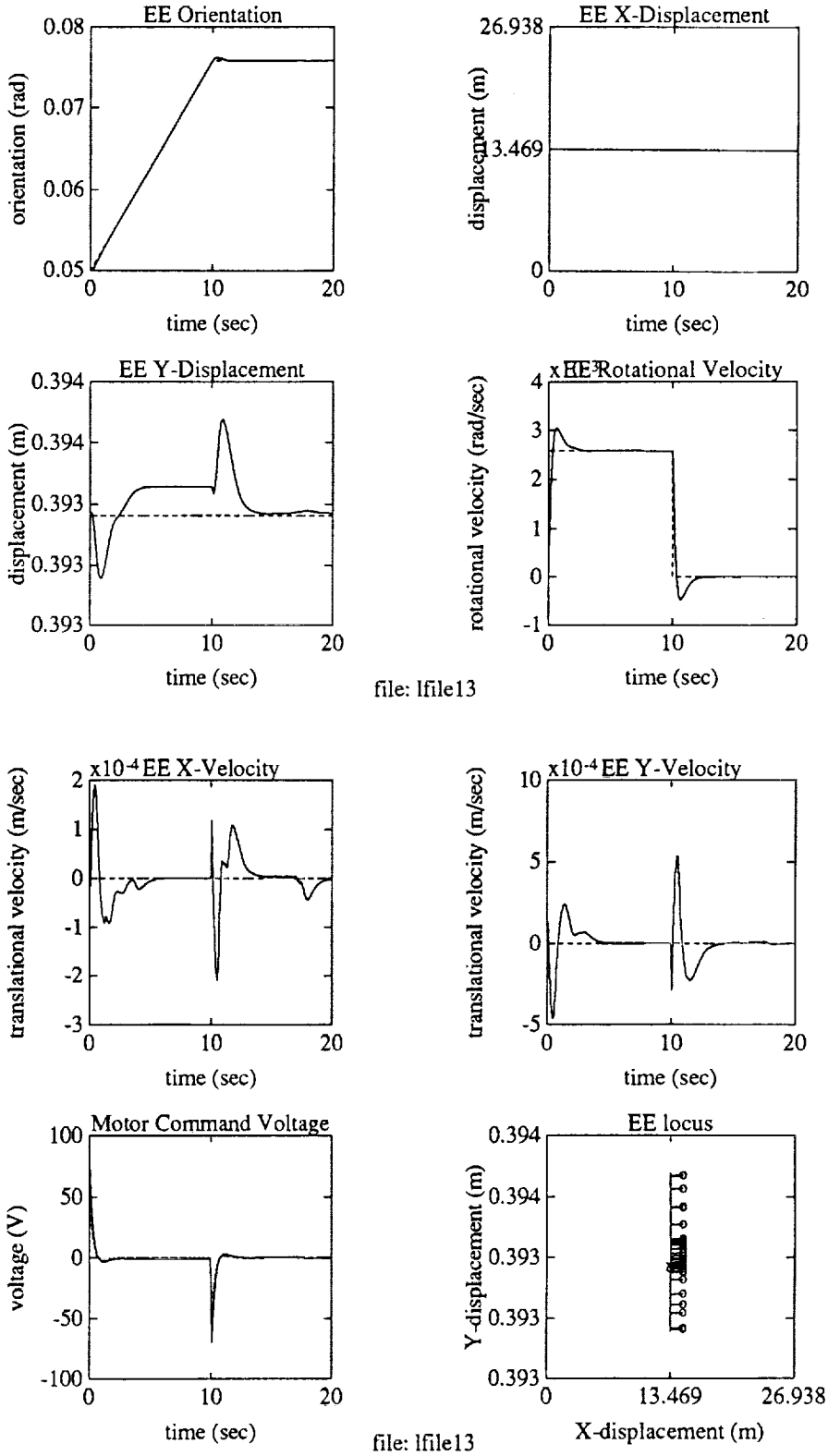

Figure 13: Step θ Velocity with Modified Controller (Gain 2)

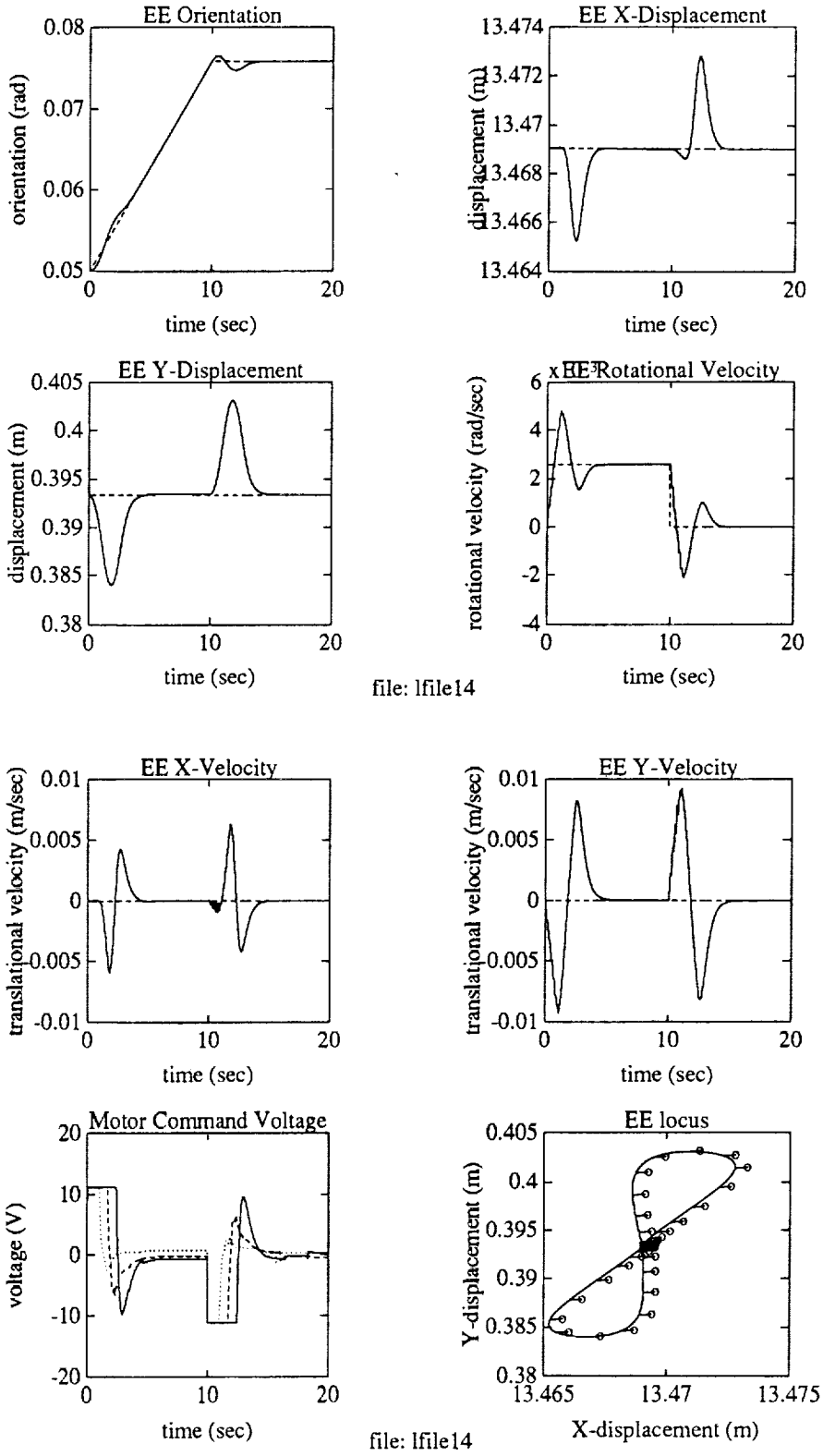

Figure 14: Step θ Velocity with modified controller (Gain 2) and Torque Saturation

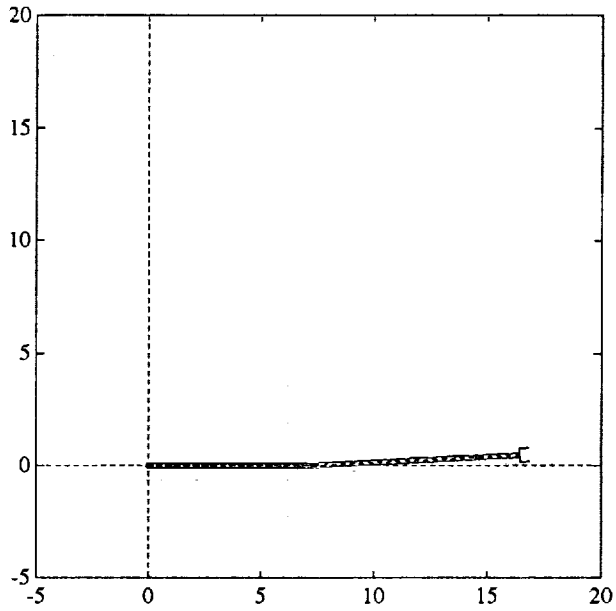

Figure 15: Initial Configuration

Comparison between the performances of the RMS controller and the modified controller is even more striking with another initial condition:

$$\theta_\ell(0) = [0,\ 0.05,\ 0]^T \text{rad} \tag{57}$$

This configuration is shown in Fig.15. The response of the RMS controller is shown in Fig.16, and the response of the modified controller is shown in Fig.17. The gains used in the modified controller is relatively low:

$$\text{Gain 3:} \qquad K_{p_\ell} = .25 \quad K_{v_\ell} = 1 \quad k_p = 1 \quad k_v = .1. \tag{58}$$

Figures 18, 19, 20 show responses of the arm with an x direction rate command, under the RMS controller and the modified controller with gains as in (56), with and without saturation. Figures 21, 22, 23 show responses of the arm with an y direction rate command. The initial condition for all cases is (53). With the modified controller, the uncommanded motion and steady state error are virtually eliminated, and the transient response (in the unsaturated case) is also better. Even with saturation, the commanded rate overshoot is slightly larger than the RMS case, but the position error is much smaller. The only exception is for the step commanded in $\dot{y}$. In Fig.22, the saturation level is exceeded by a large amount, and direct saturation of the control signal leads to major degradation of performance in Fig.23.

To demonstrate the impact of trajectory shaping, we consider a ramp velocity profile instead of a step. The ramp up takes the first 10sec, beyond which the velocity stays at a steady state value (at the same level as the step cases). The responses for the RMS arm versus the modified arm (with gains (56)) for θ, x, and y rate commands are shown in Figures 24–29. As expected, for both controllers, the responses improve over the step command cases.

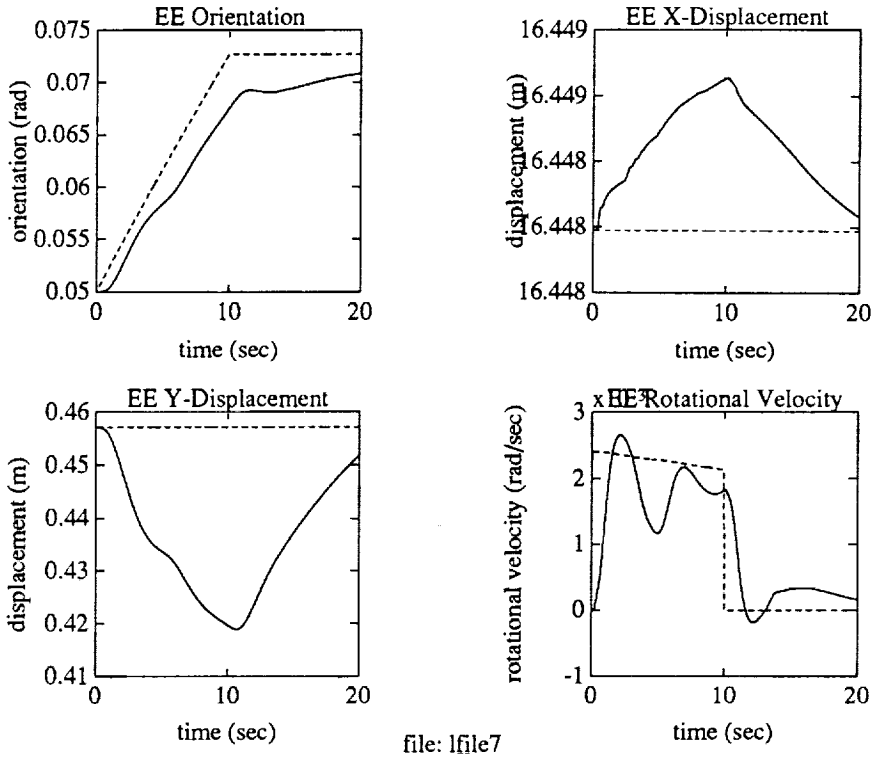

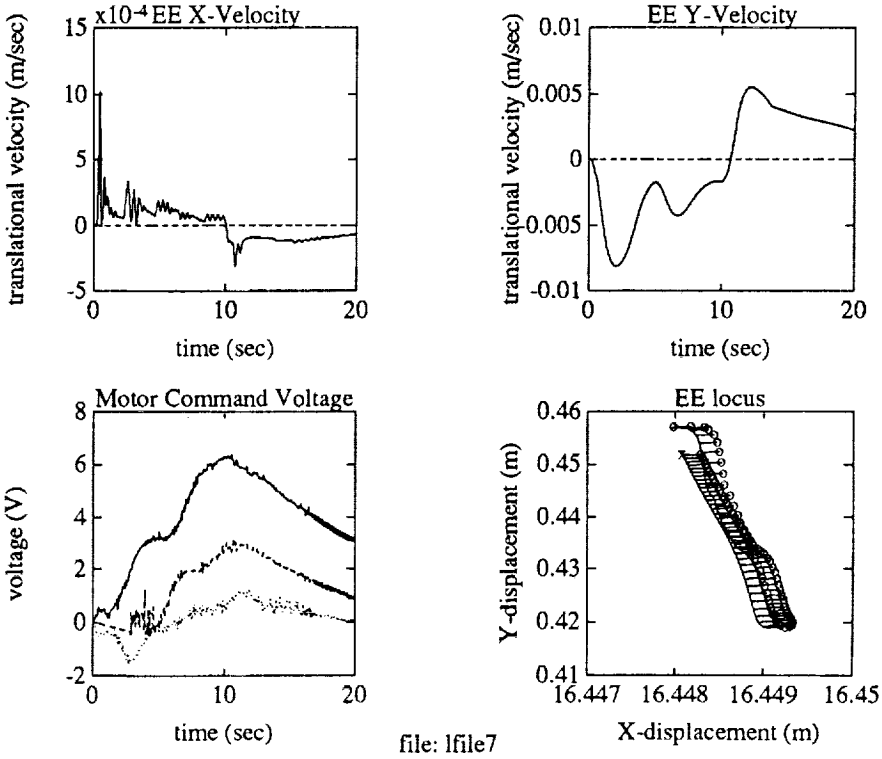

Figure 16: Step θ Velocity with RMS Controller

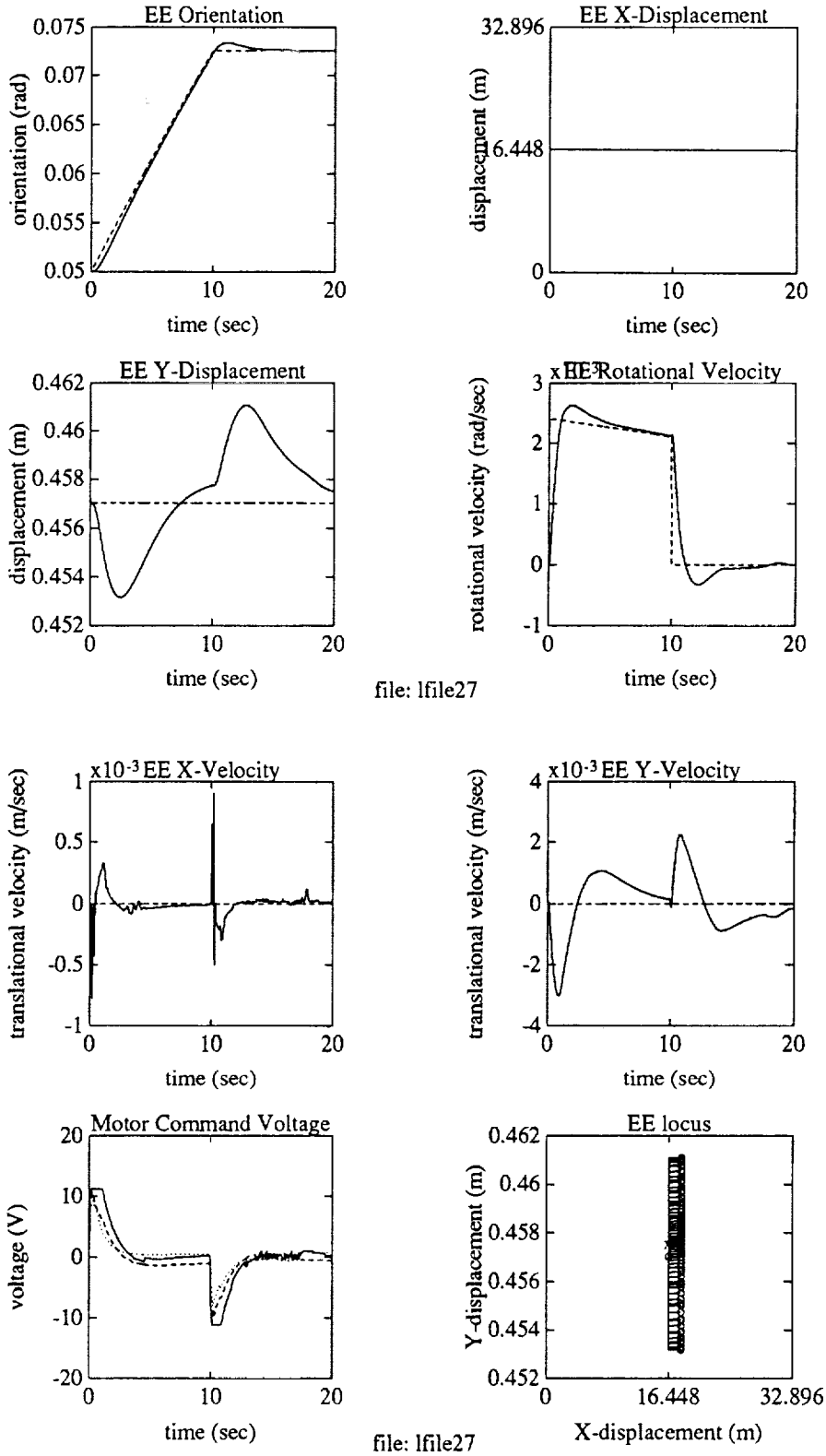

Figure 17: Step θ Velocity with Modified Controller (Gain 3) and Torque Saturation

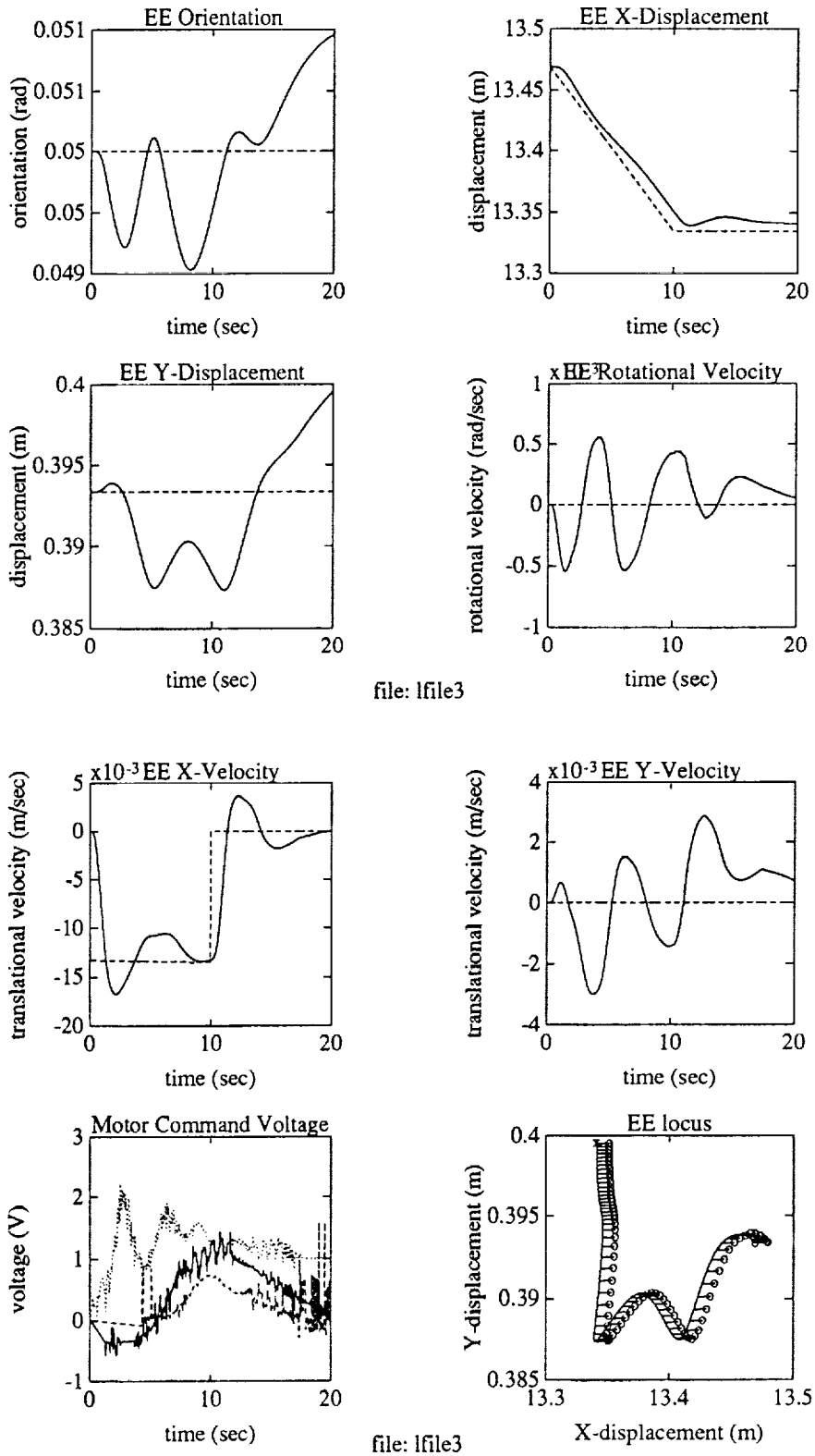

Figure 18: Step x Velocity with RMS Controller

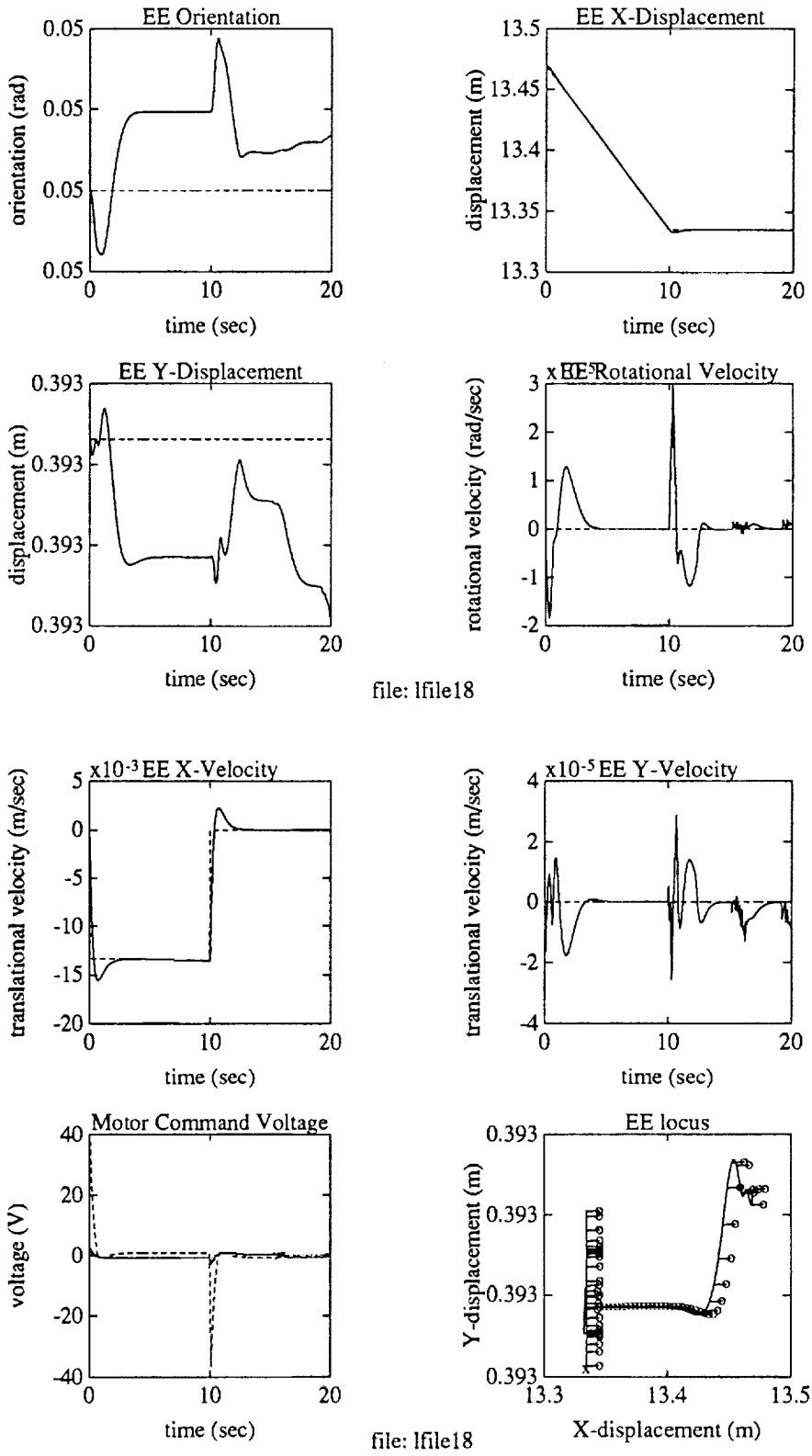

Figure 19: Step x Velocity with Modified Controller (Gain 2) and without Torque Saturation

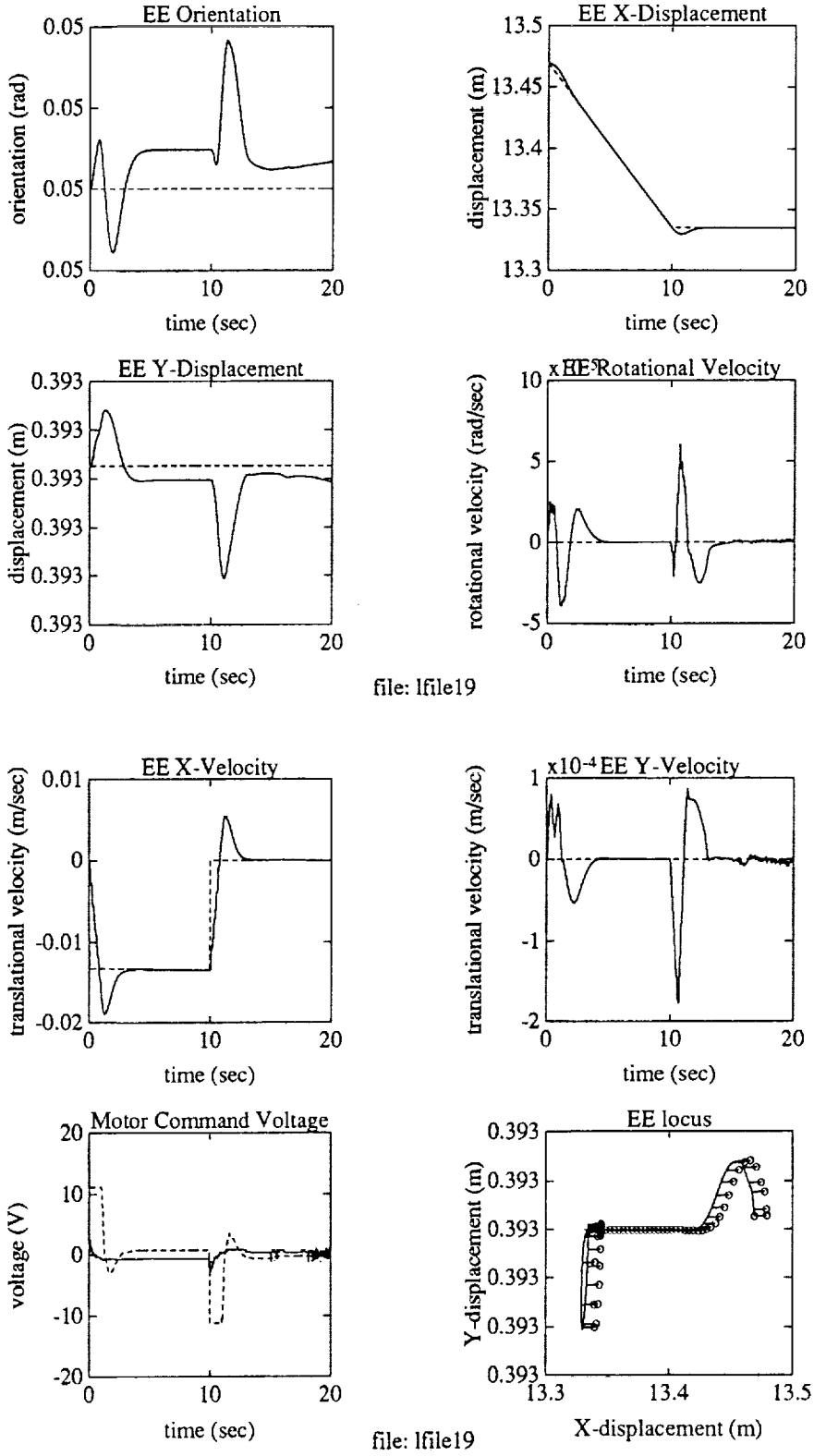

Figure 20: Step x Velocity with Modified Controller (Gain 2) and with Torque Saturation

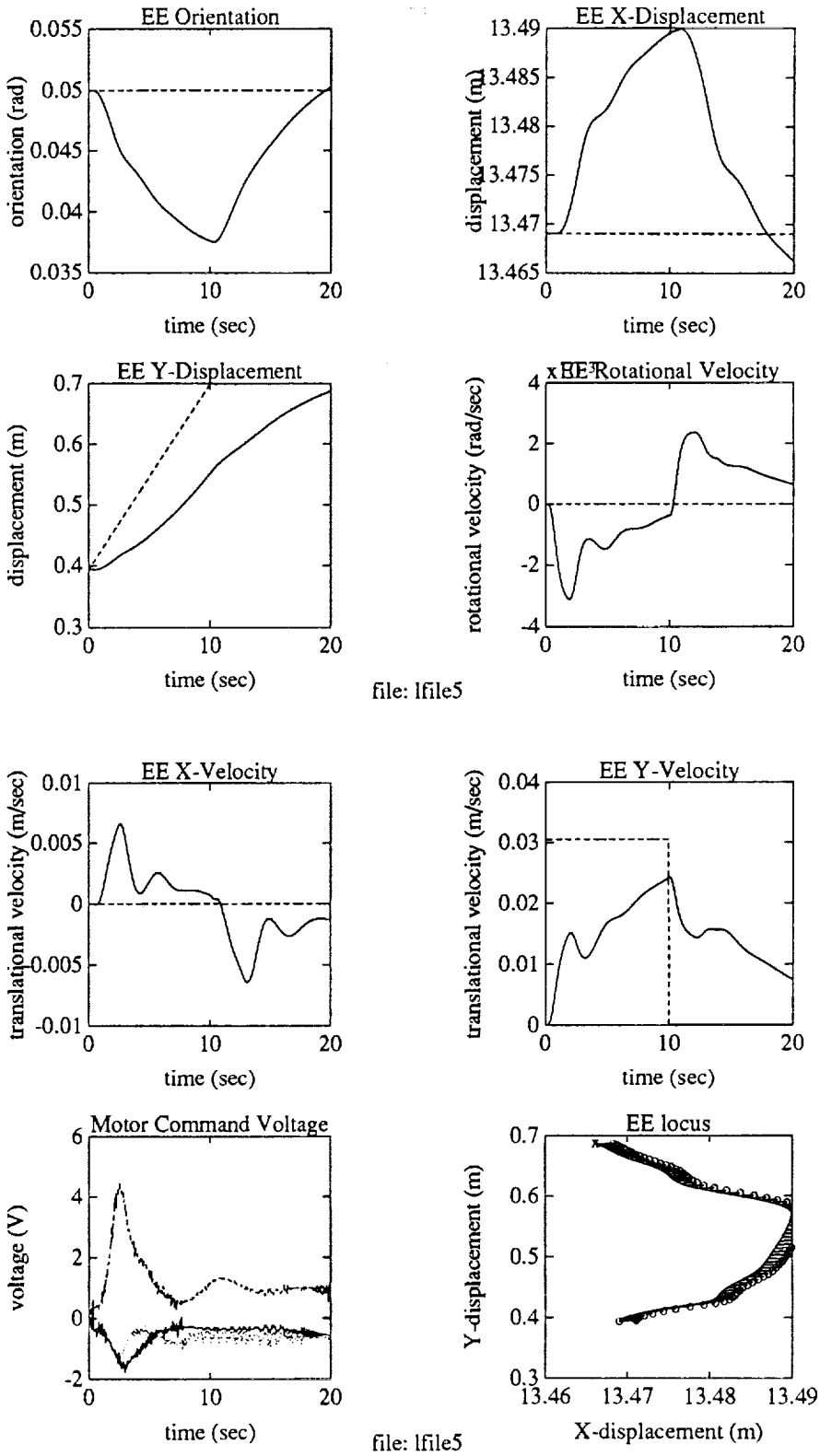

Figure 21: Step y Velocity with RMS Controller

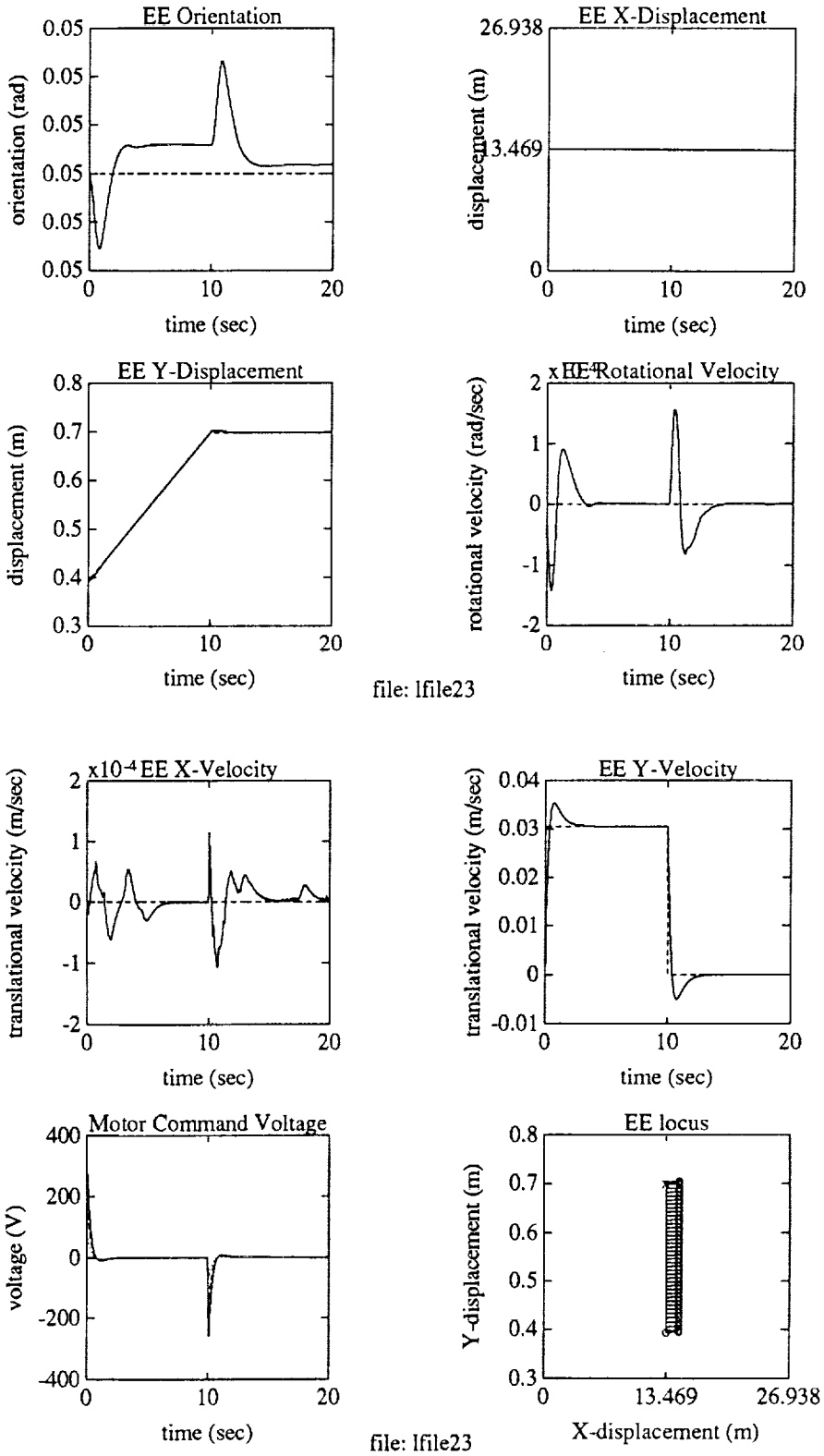

Figure 22: Step y Velocity with Modified Controller (Gain 2) and without Torque Saturation

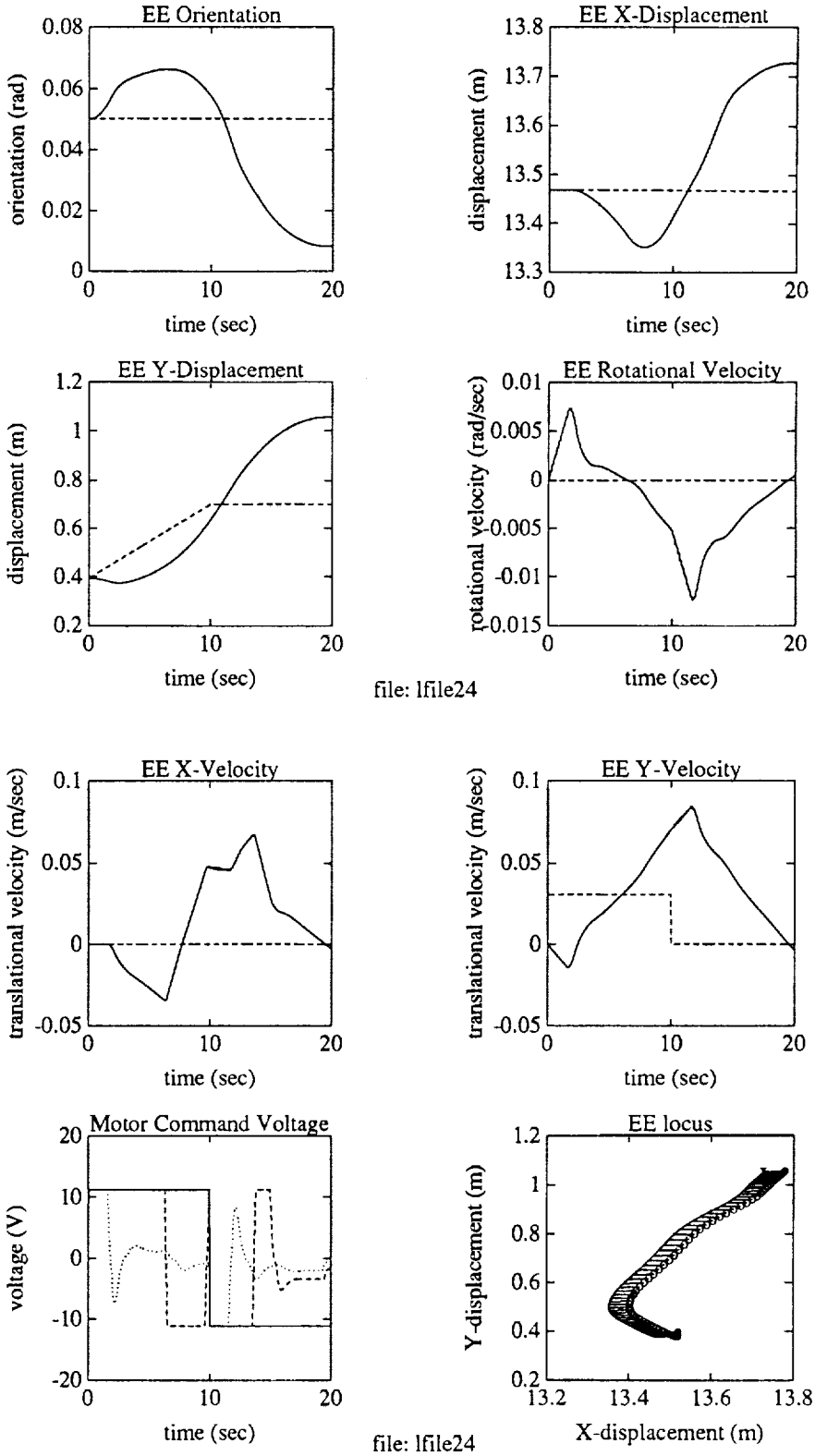

Figure 23: Step y Velocity with Modified Controller (Gain 2) and with Torque Saturation

The modified controller again outperforms the RMS controller by all measures. Furthermore, the input is no longer saturated. This demonstrates a promising direction to pursue for the saturation problem: filter the input command (i.e., slow down the commanded trajectory) until the input is out of saturation. This will be described further in the next section.

Unloaded Case

When the arm is unloaded, the inertia of the last link is two orders of magnitude smaller than the first two links. As a result, the response tends to be more oscillatory (especially in end effector orientation). The oscillation is usually very noticeable in $\dot{\theta}$, but because of the link inertia, the effect is small on the orientation θ (especially for high frequency oscillations). We will first show the arm responses with the RMS controller and the modified controller with step $\dot{\theta}$, $\dot{x}$, $\dot{y}$, responses, respectively. The plots are shown in Figures 30–35. The initial condition is chosen to be (53) and the gain for the modified controller is given by (56), which is the same as the loaded case (gain adaptation based on payload is not considered here). Input saturation is imposed in all cases. By all performance measures, the modified controller clearly outperforms the RMS controller.

Arm response for a ramp command velocity input is shown in figures 36–41. The contrast between the two controllers is even more pronounced. The modified controller exhibits a high frequency oscillation in $\dot{\theta}$ which is almost undetectable in θ due to the link inertia. This oscillation is likely caused by the feedback gains which are tuned for the loaded case. A systematic method for selecting the gains, k_p, k_v, K_{p_ℓ}, and K_{v_ℓ}, will be developed in the future.

General Observations

Based on voluminous simulation data (only a small portion of which is shown here), we can make the following general observations on the comparison between the RMS controller and the modified controller:

1. The RMS controller is simpler in structure. The modified controller requires more model information (mass matrix, friction, and joint spring characteristics) and more on–line measurement information (link angle and angular velocity).

2. For the RMS controller, commanded velocity tends to undershoot its set point due to its relatively low gain. As a result, the link position almost always lag way behind the commanded trajectory. For the modified controller, since the proportional gain (for both link and motor) is higher, there tends to be more velocity overshoot. However, the positional response is in general much better than the RMS controller case.

3. Almost in all cases involving the modified controller, link velocities overshoot their set points. This is due to the fact that in order for the link angle to catch up with the desired trajectory, link velocity has to exceed its set point to compensate for the initial lag (due to friction). An important consideration in choosing the feedback gains is in deciding which one of the responses, link angular velocity or angular position, is more important to the operator. The gains should then be selected accordingly to emphasize that variable.

4. If the input torque is not explicitly clamped at the saturation level, the modified controller tends to require very large input over a short period of time during the step response (when the error is large). With saturation, the performance degrades somewhat, but is usually still quite satisfactory. Even though the saturation does not seriously affect performance in most cases, it is desirable to have a safety mechanism to guard against saturation. We are developing a command trajectory modification algorithm to explicitly address this issue. As a preliminary check of this idea, when the commanded velocity step is slowed to a ramp, saturation no longer occurs.

5. The same set of gains (56) has been shown effective for both loaded and unloaded case. A systematic tuning of gain should be developed in the future.

6. We have noted that to improve the performance for the modified controller, motor feedback gains have to be increased together with the link feedback gains. This is due to the fact that a tight motor loop is required so that the spring torque can closely emulate the desired link feedback control law.

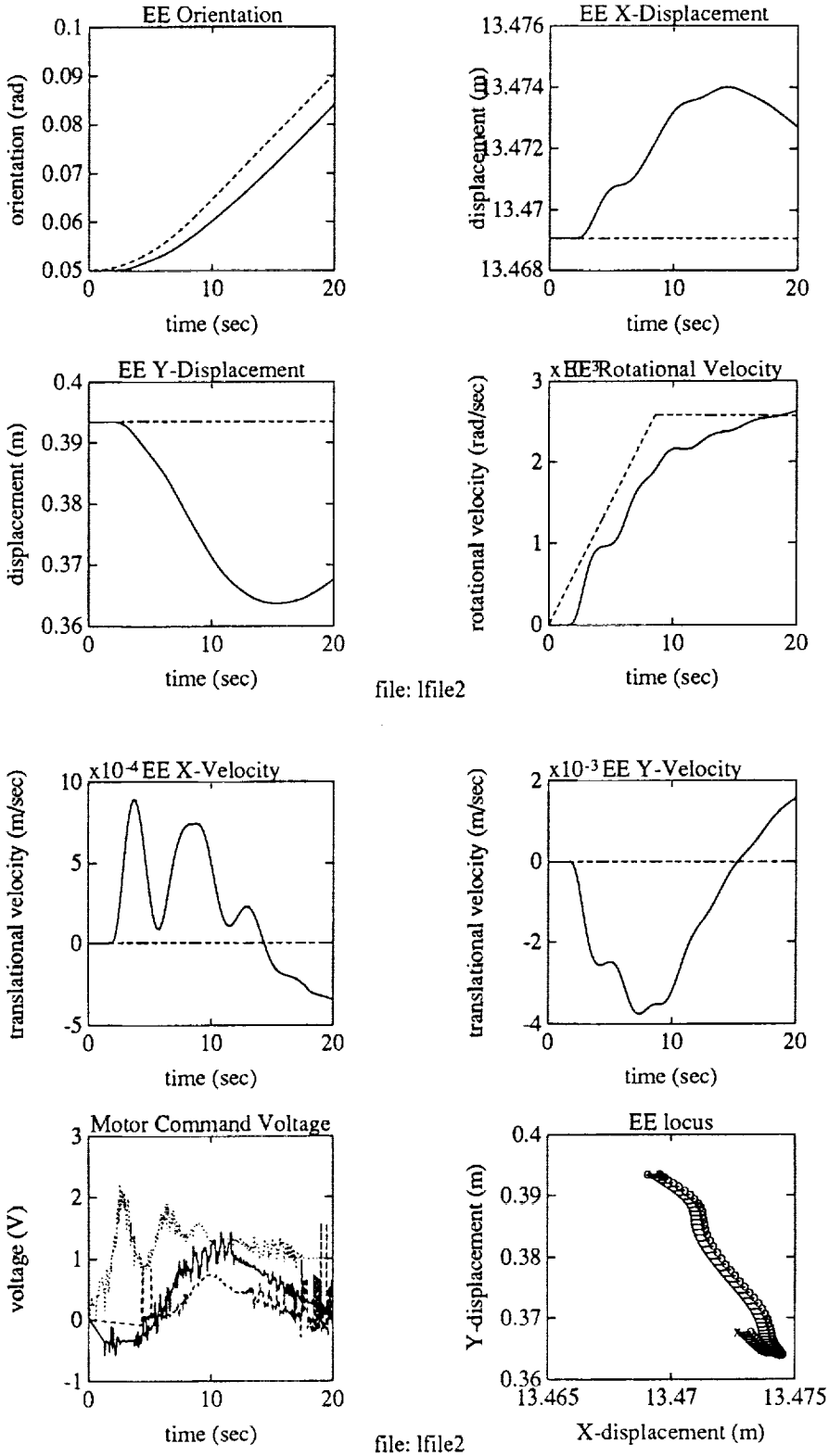

Figure 24: Ramp θ Velocity with RMS Controller

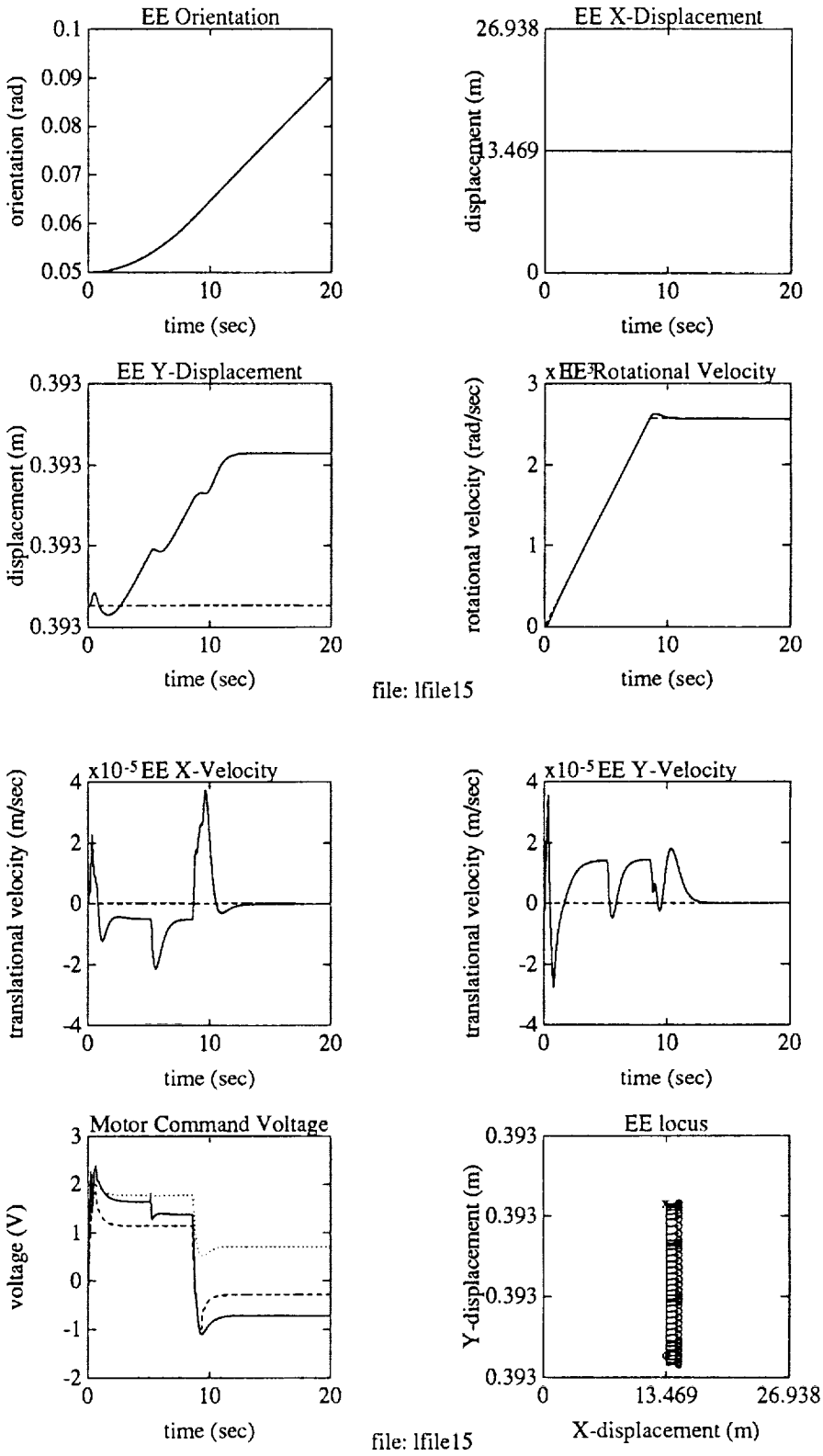

Figure 25: Ramp θ Velocity with Modified Controller (Gain 2) and with Torque Saturation

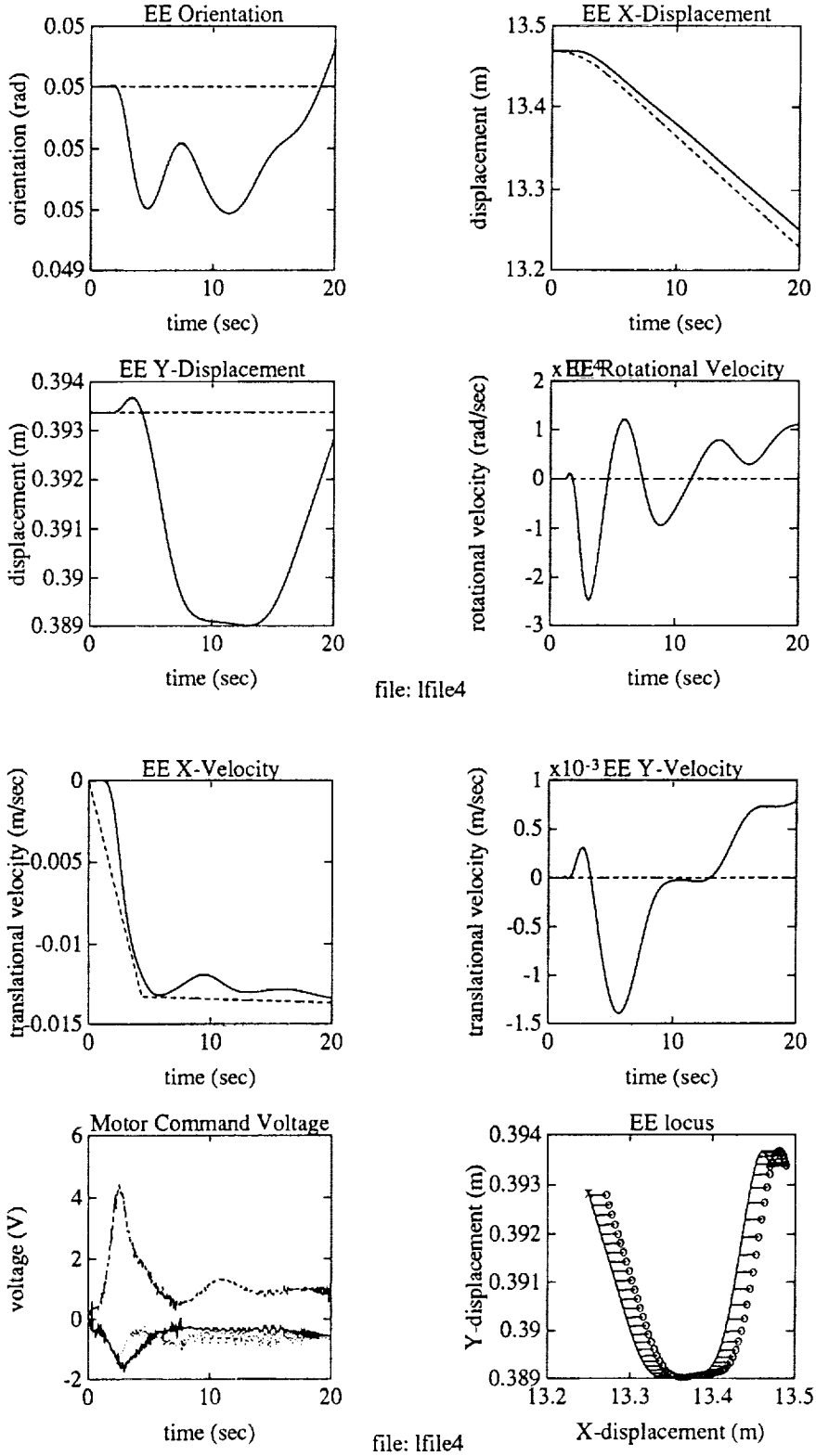

Figure 26: Ramp x Velocity with RMS Controller

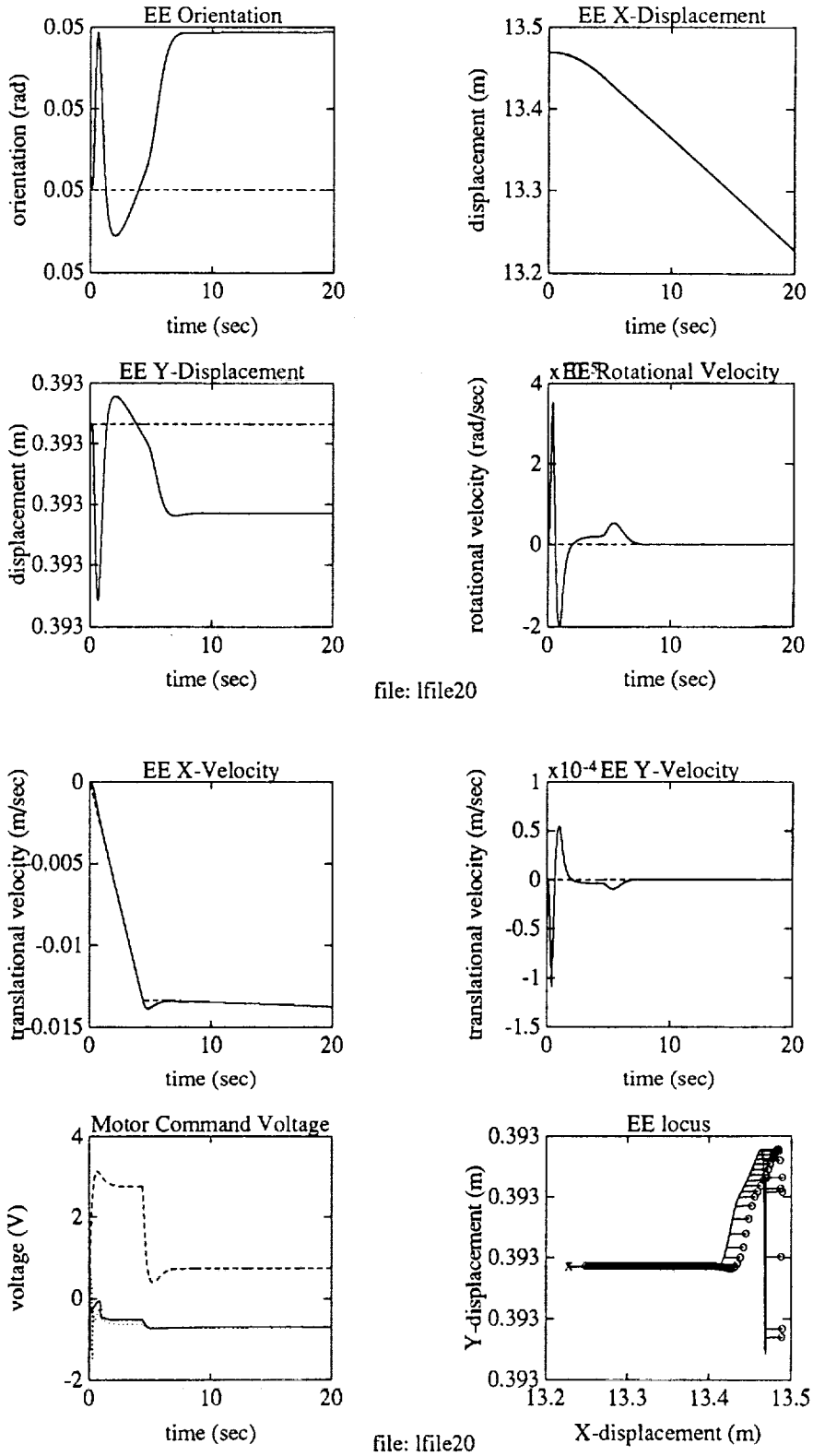

Figure 27: Ramp x Velocity with Modified Controller (Gain 2) and with Torque Saturation

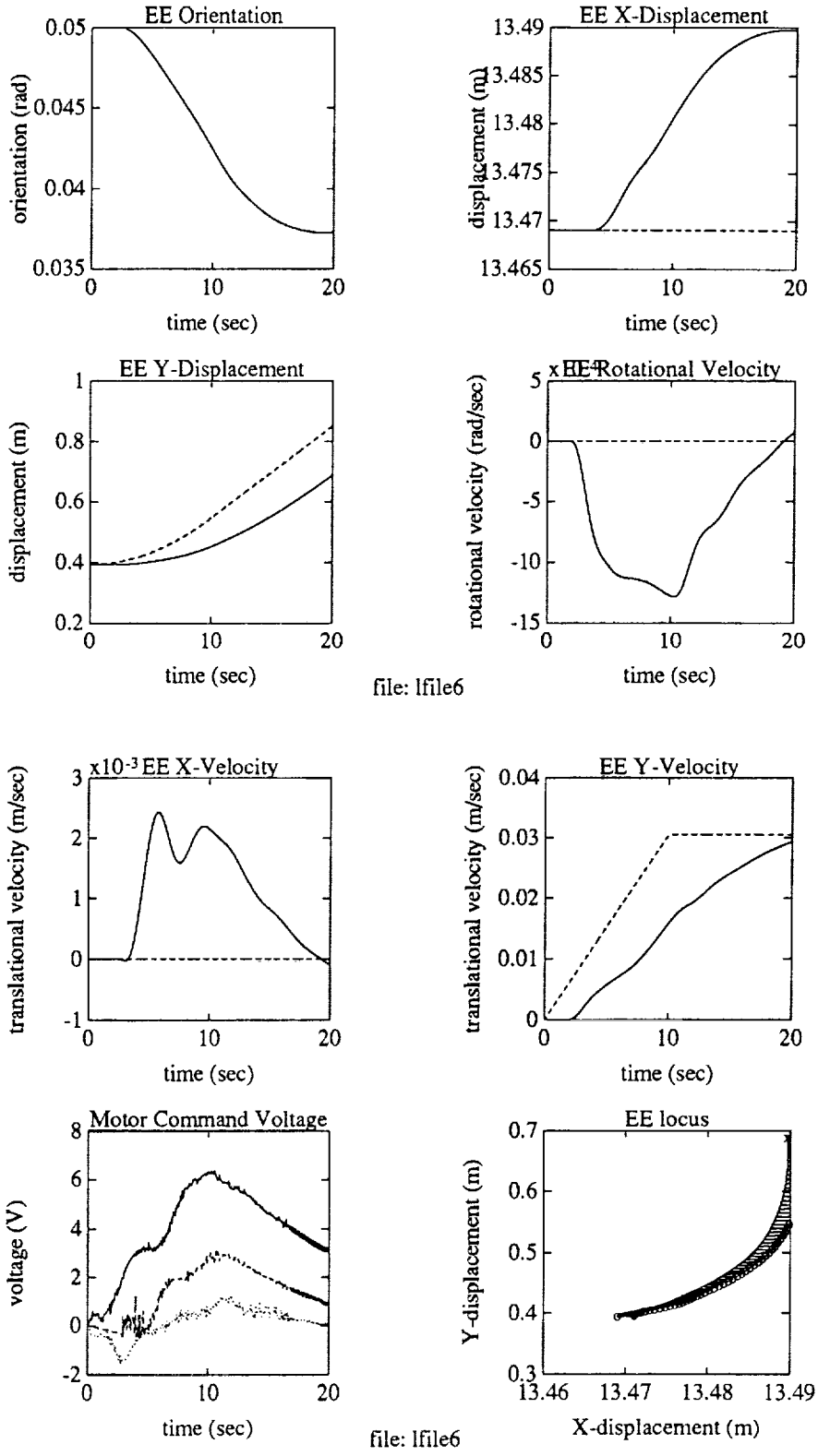

Figure 28: Ramp y Velocity with RMS Controller

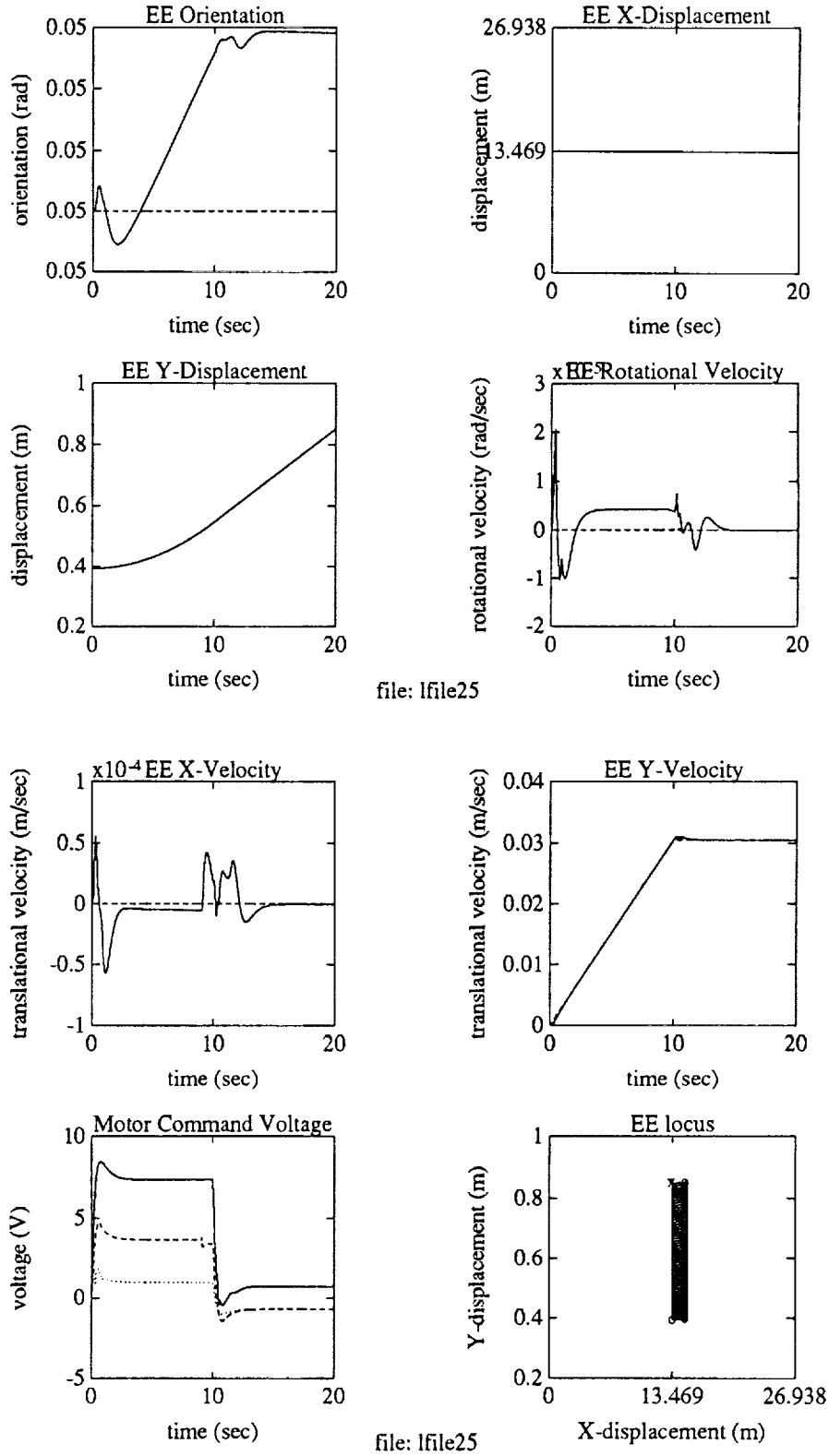

Figure 29: Ramp y Velocity with Modified Controller (Gain 2) and with Torque Saturation

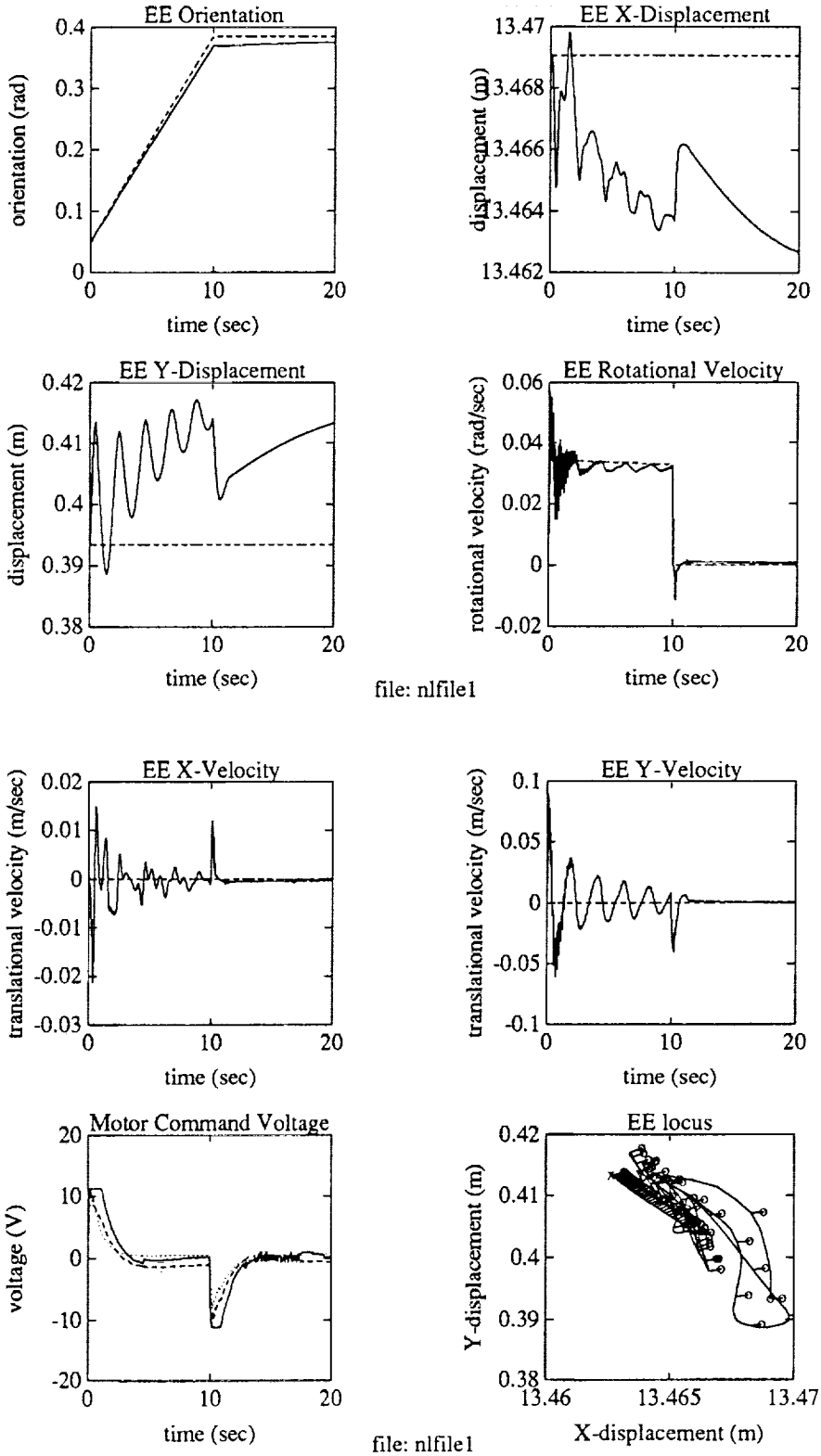

Figure 30: Step θ Velocity with RMS Controller

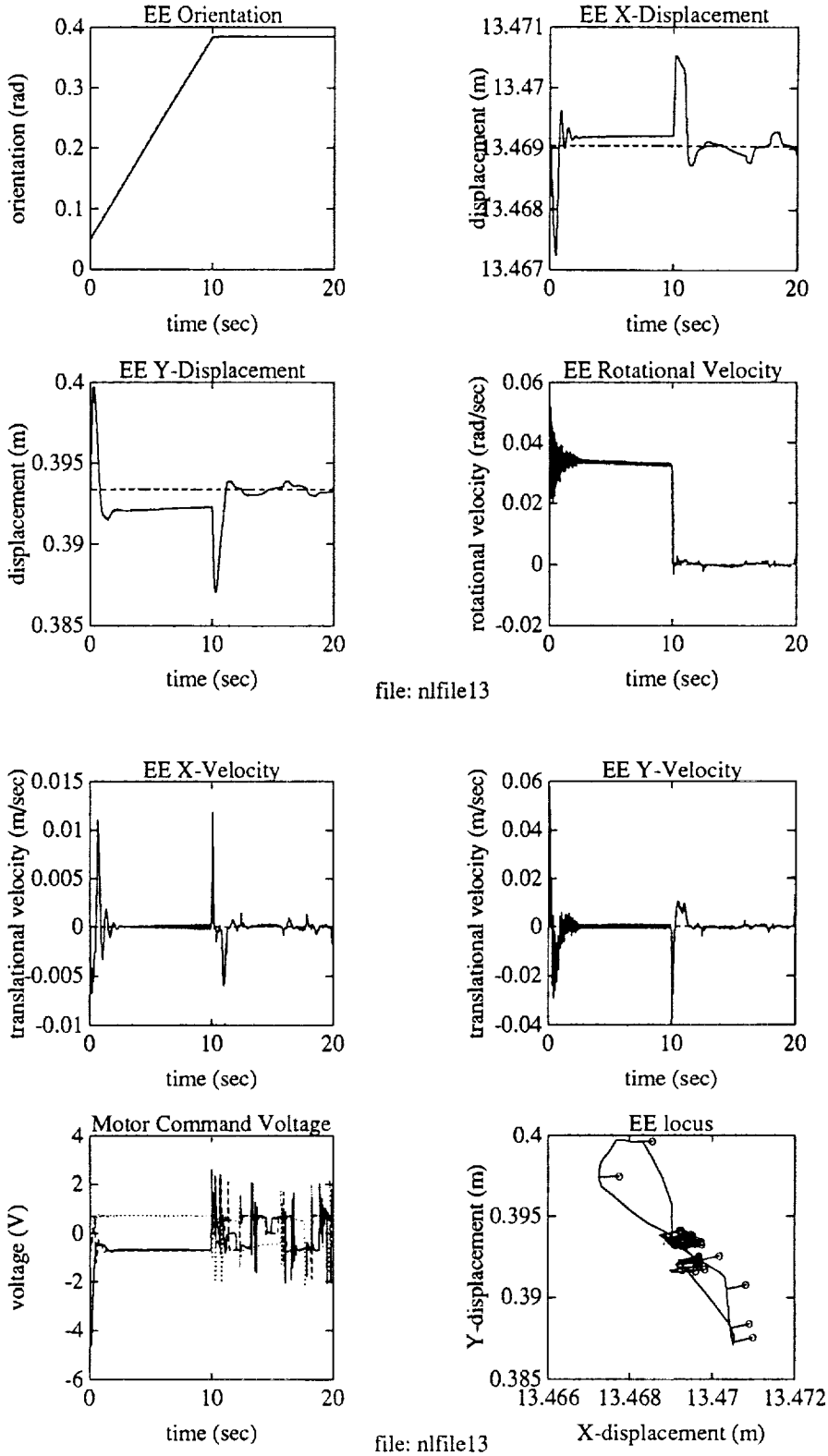

Figure 31: Step θ Velocity with Modified Controller (Gain 2) and with Torque Saturation

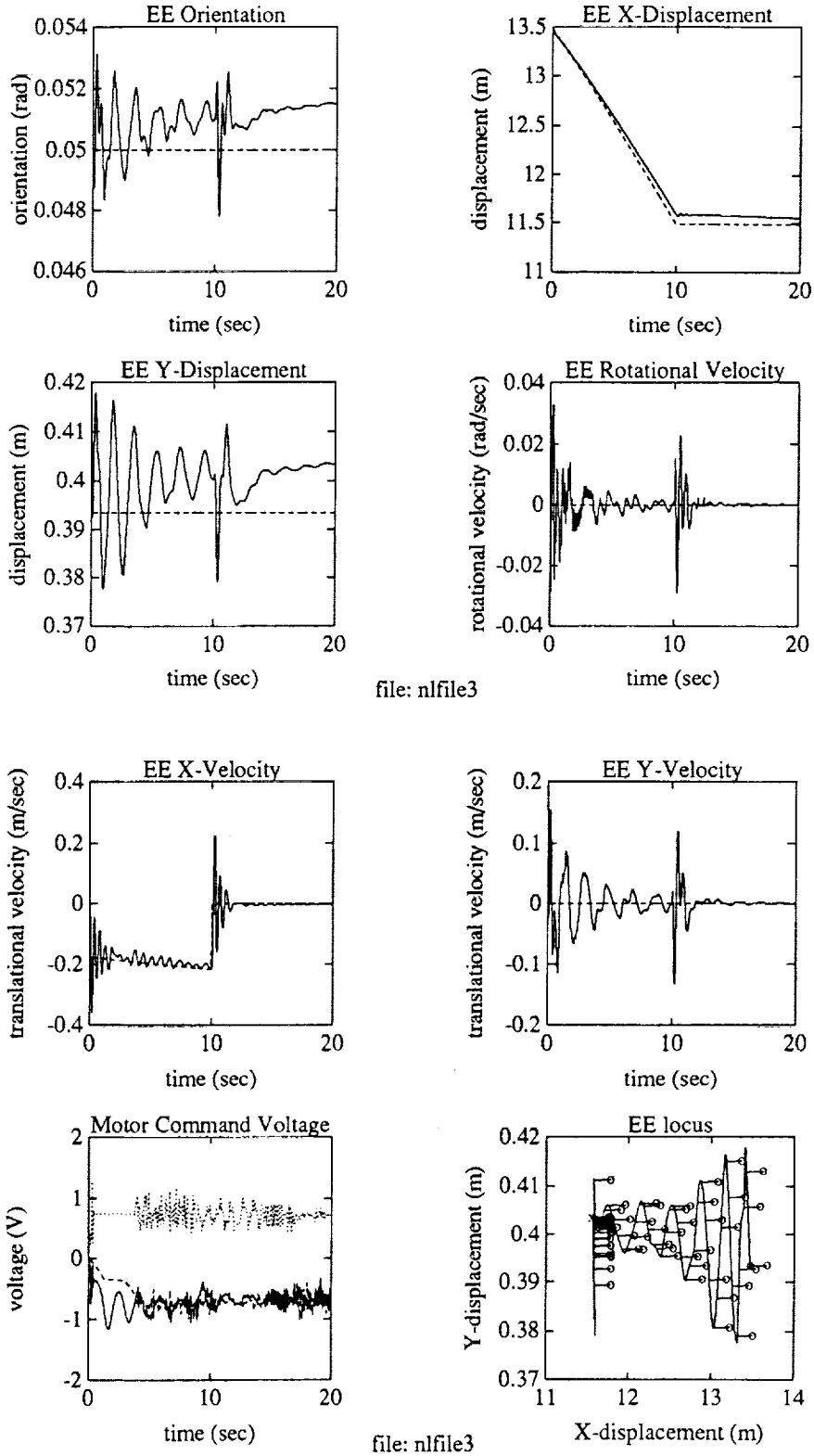

Figure 32: Step x Velocity with RMS Controller

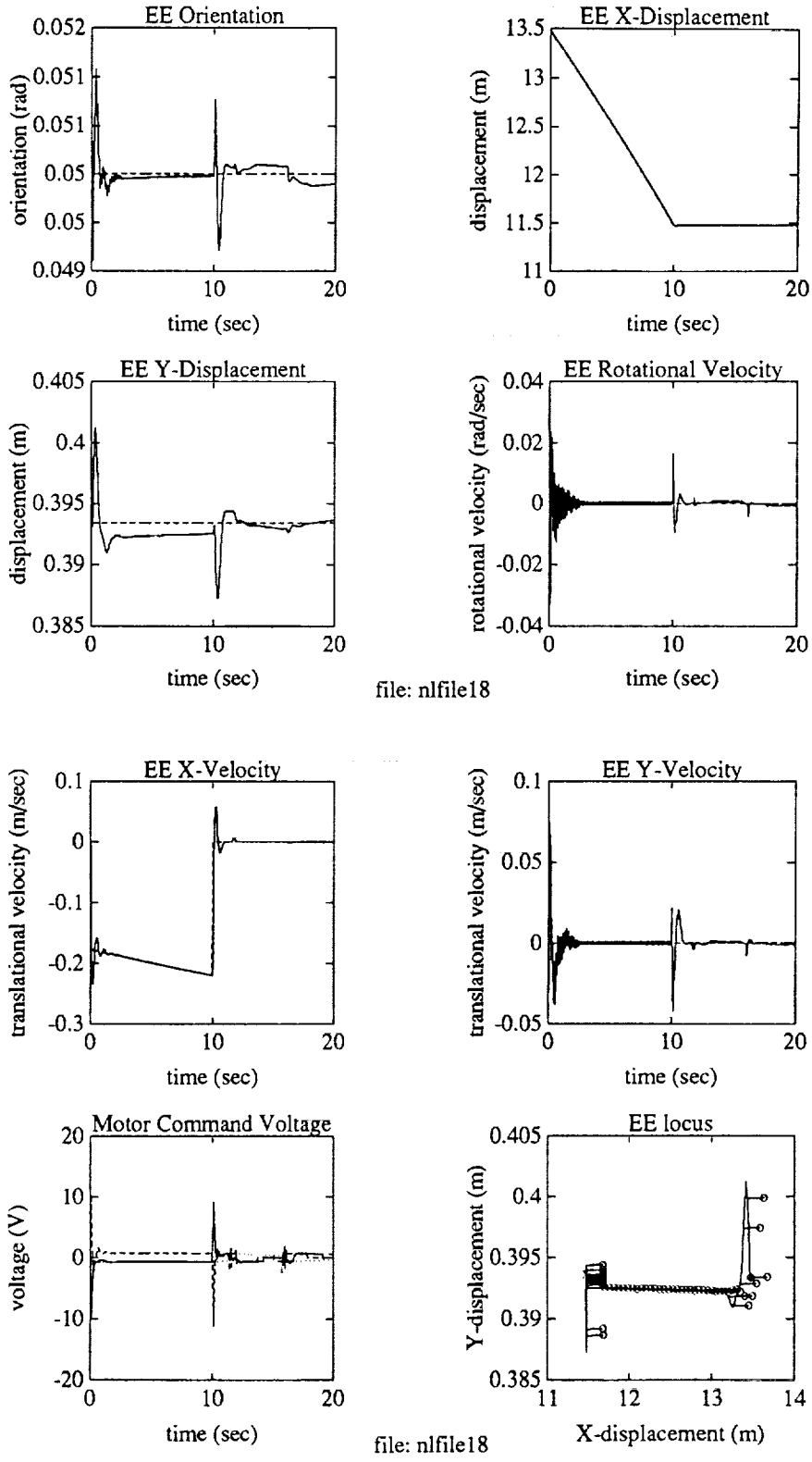

Figure 33: Step x Velocity with Modified Controller (Gain 2) and with Input Saturation

6 Future Work

The research results presented in this report shows the efficacy of the passivity approach in the control of flexible joint robots with massive links, such as the shuttle RMS arm and the anticipated space station arm. As stated in the introduction section, several assumptions have been made in the model to simplify the analysis. These assumptions need to be placed on a rigorous theoretical footing. In addition, performance optimization criteria should be included in the feedback gain selection, and the improved performance should be demonstrated experimentally in some form. Based on these considerations, we propose the following agenda for the future tasks:

1. Observer for link variables: Existing RMS controller only uses motor angular velocity feedback (motor angles are derived from motor velocities). The most effective form of the modified controllers requires link angle and angular velocity feedback. We will derive nonlinear observers (most likely only including nonlinearities such as mass matrix and Coulomb frictions, while ignoring Coriolis and centrifugal terms) to estimate the link variables based on the motor variable measurements.

2. Saturation Avoidance: When the velocity or the command torque are too high, they become saturated. In the existing RMS controller, there is already a commanded Cartesian velocity modification algorithm if the joint velocity becomes saturated. We will also apply the trajectory modification technique for the torque saturation, such as the method proposed in [22] (slowing down the commanded trajectory until the arm is out of the saturation condition).

3. Robustness Analysis: The feedforward that has been proposed involves some assumptions to simplify its expression (c.f. section 4). A rigorous stability analysis (most likely a local analysis) needs to be performed to justify this simplification. Even after simplification, the feedforward still requires considerable amount of model information, including mass matrix, link and motor frictions, and joint spring characteristics. Errors in this information needs to be evaluated in terms of stability and performance.

4. Optimal Feedback Tuning: We have seen that there is considerable leeway in choosing the motor rate feedback and this choice can significantly affect the transient performance. A systematic method of designing this feedback based on performance considerations need to be developed. A possibility is to apply a parameter optimization approach based on, for example, settling time, overshoot, etc.

5. Experimental Validation: To truly validate the effectiveness of the proposed approach, implementation and demonstration on a physical arm should be performed. As a first step in that direction, we propose to implement the proposed control algorithms on the simulated RMS arm at JSC.

7 Conclusion

In this report, we have presented a general theory for the stabilization (vibration suppression and disturbance rejection) and output tracking of flexible robots. This theory includes

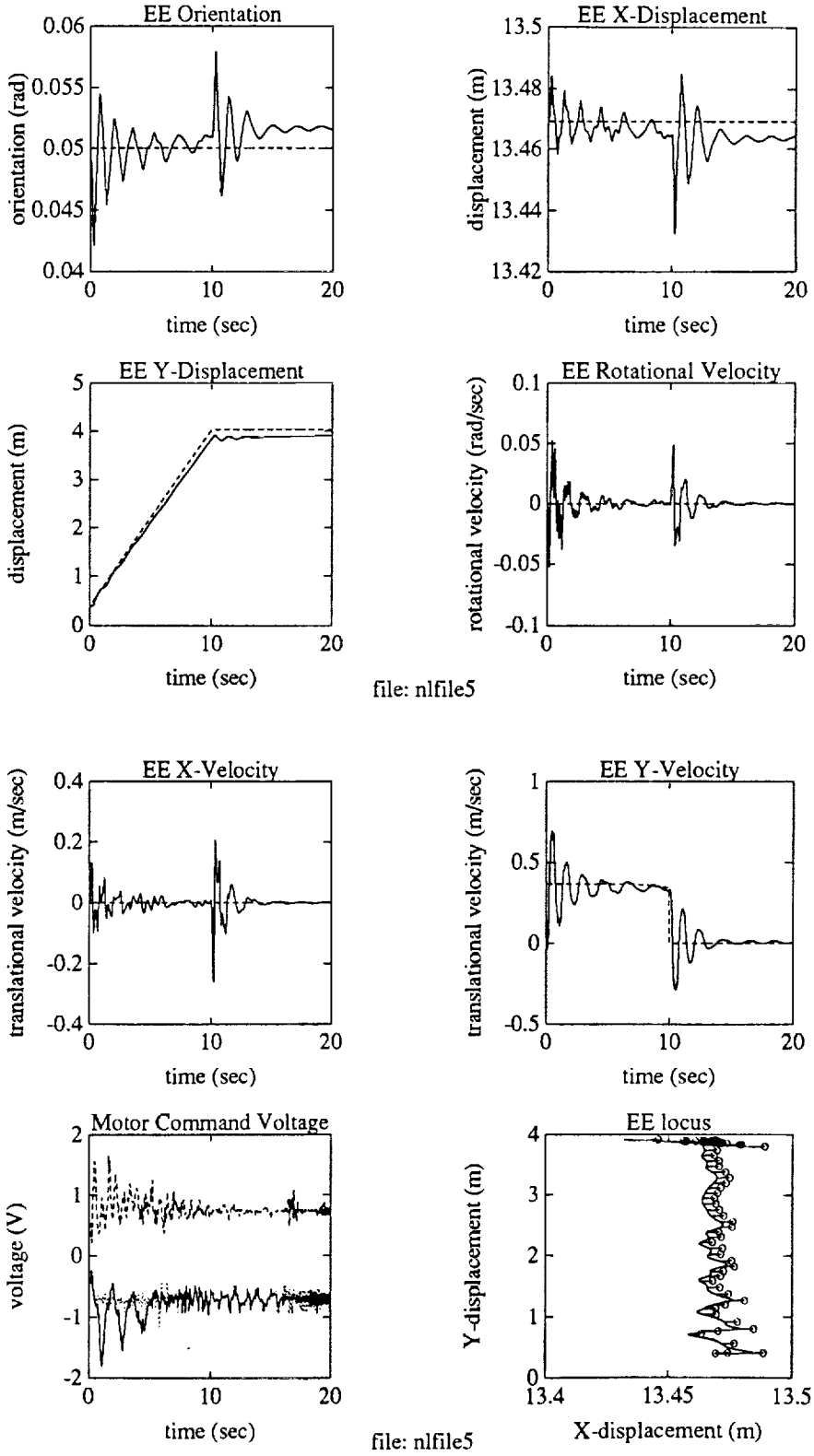

Figure 34: Step y Velocity with RMS Controller

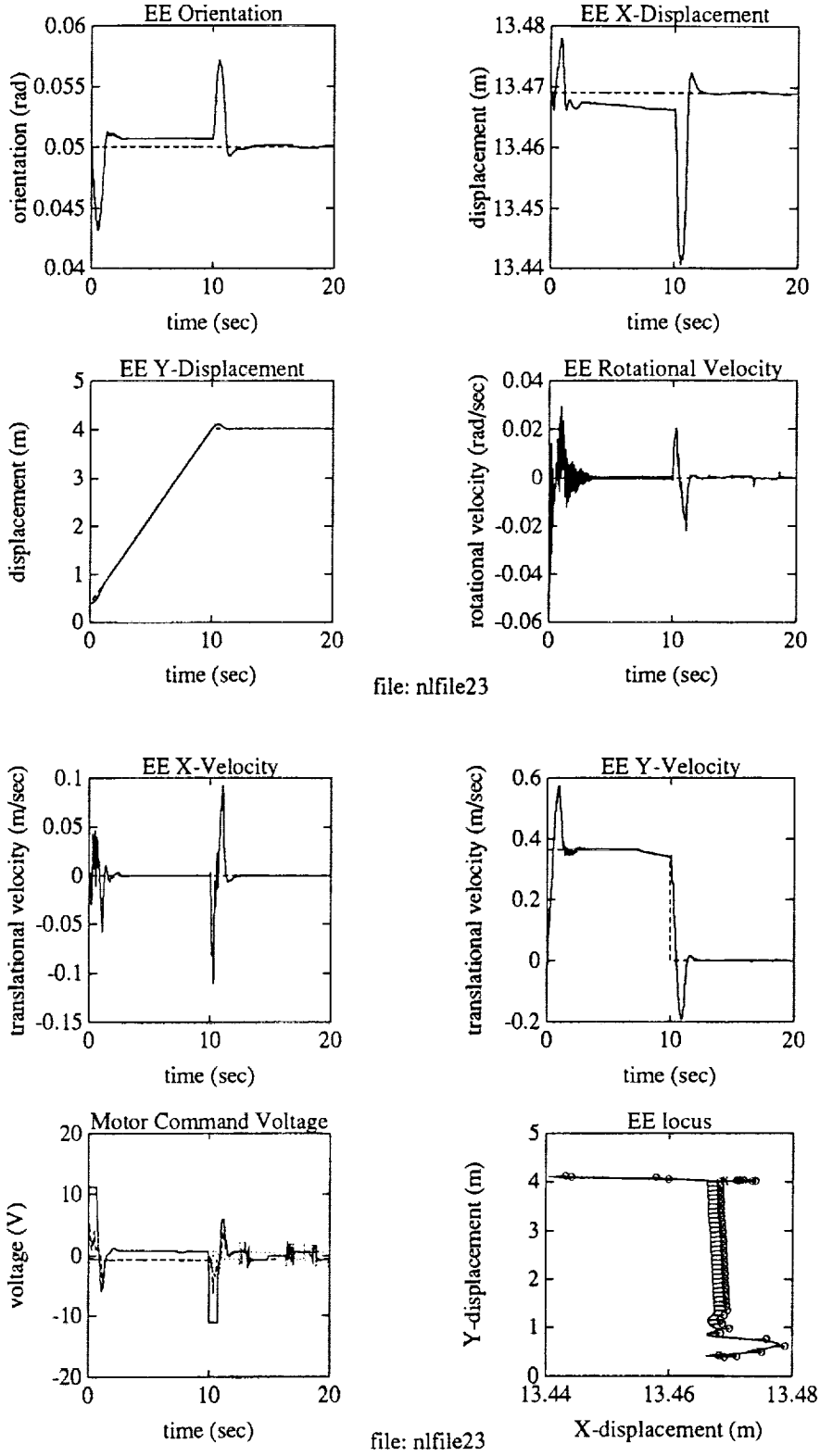

Figure 35: Step y Velocity with Modified Controller (Gain 2) and with Input Saturation

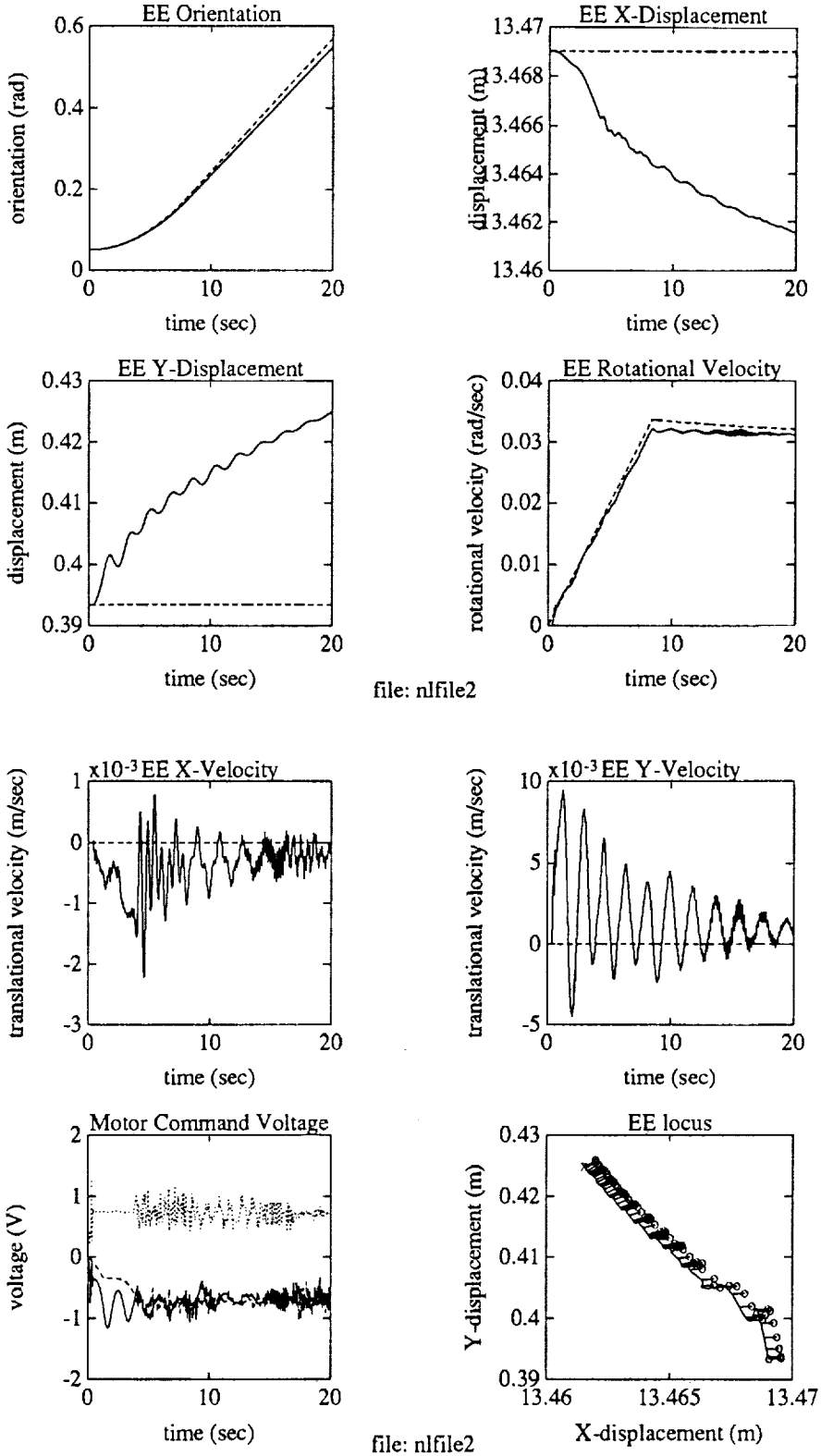

Figure 36: Ramp θ Velocity with RMS Controller

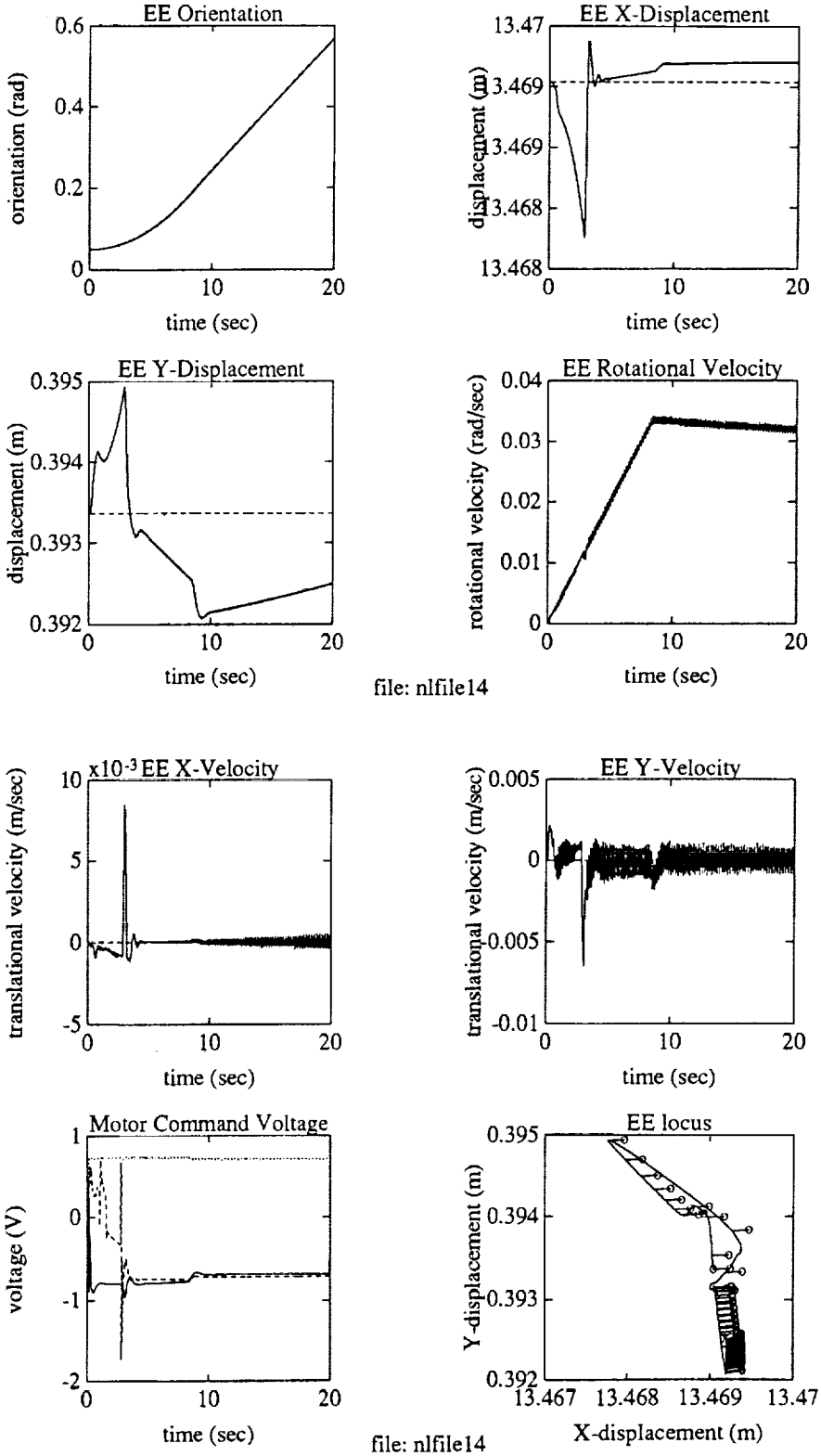

Figure 37: Ramp θ Velocity with Modified Controller (Gain 2) and with Input Saturation

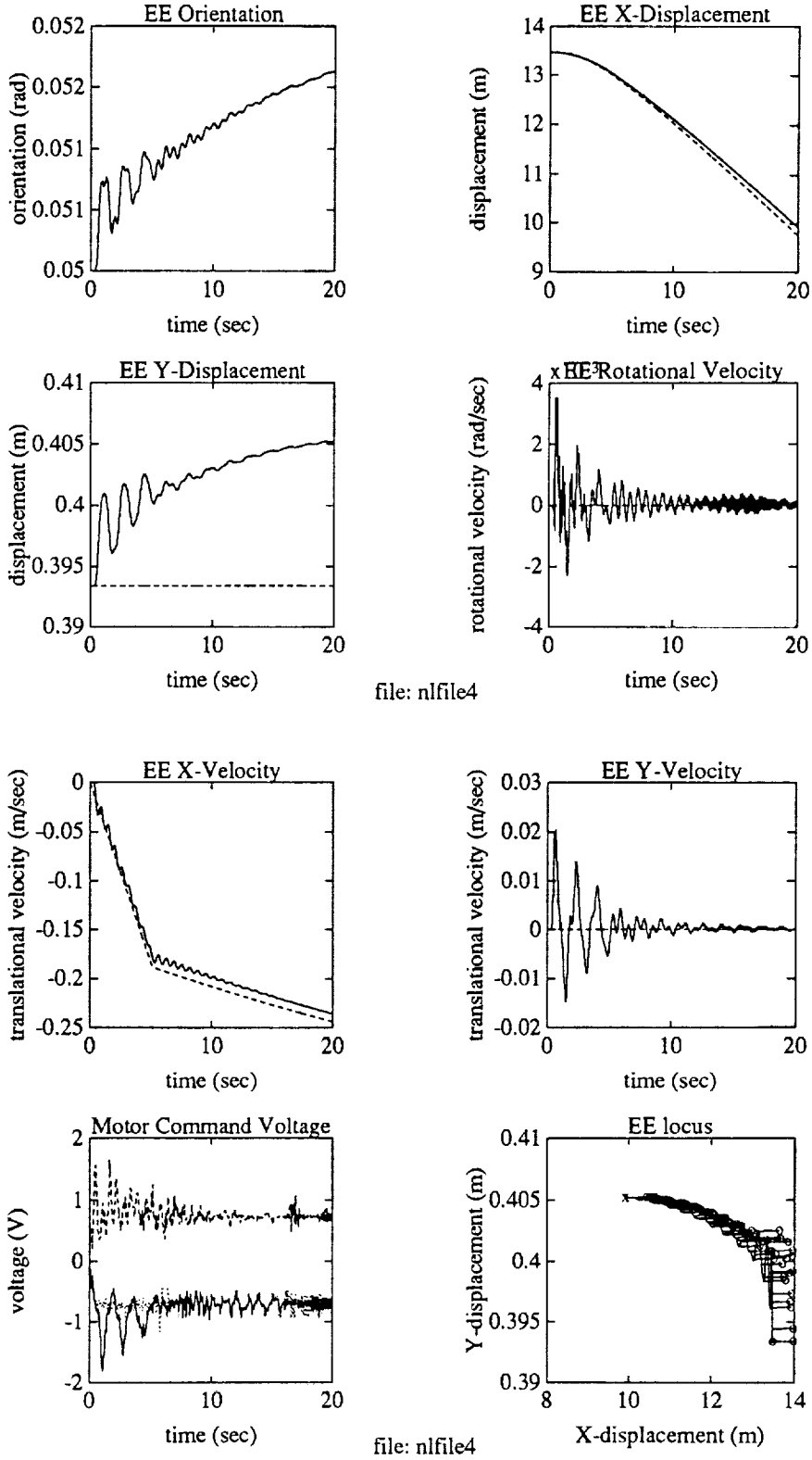

Figure 38: Ramp x Velocity with RMS Controller

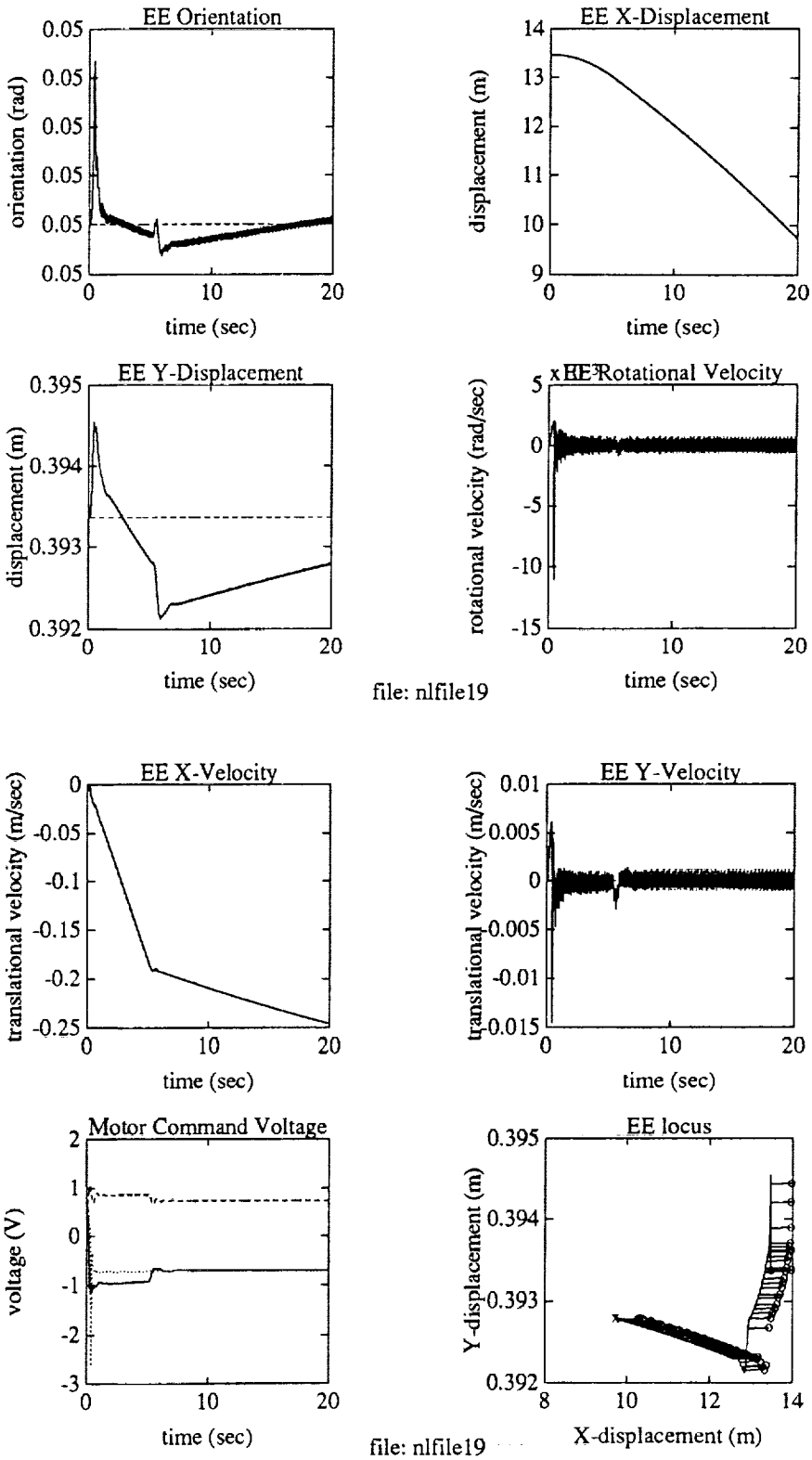

Figure 39: Ramp x Velocity with Modified Controller (Gain 2) and with Input Saturation

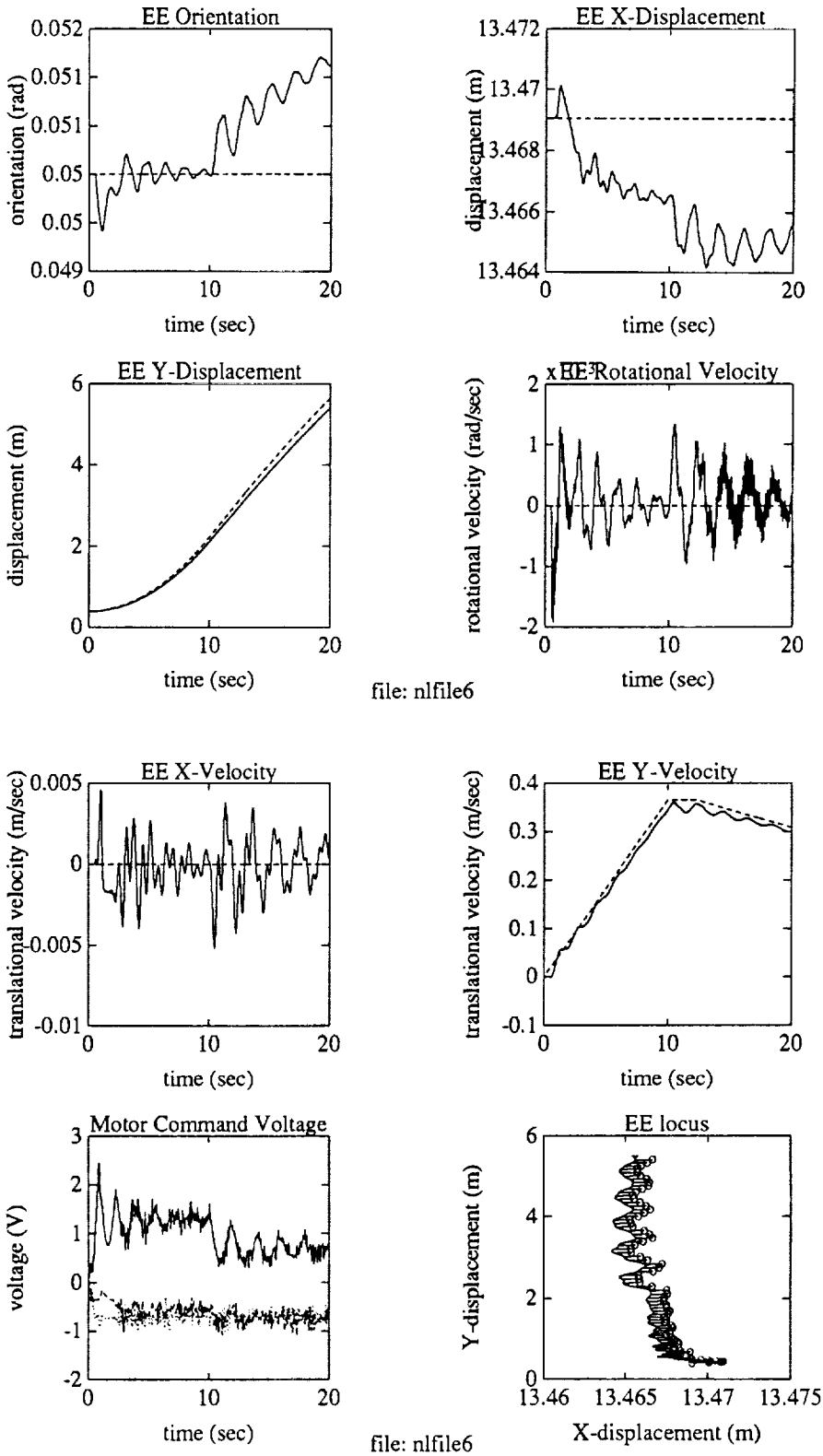

Figure 40: Ramp y Velocity with RMS Controller

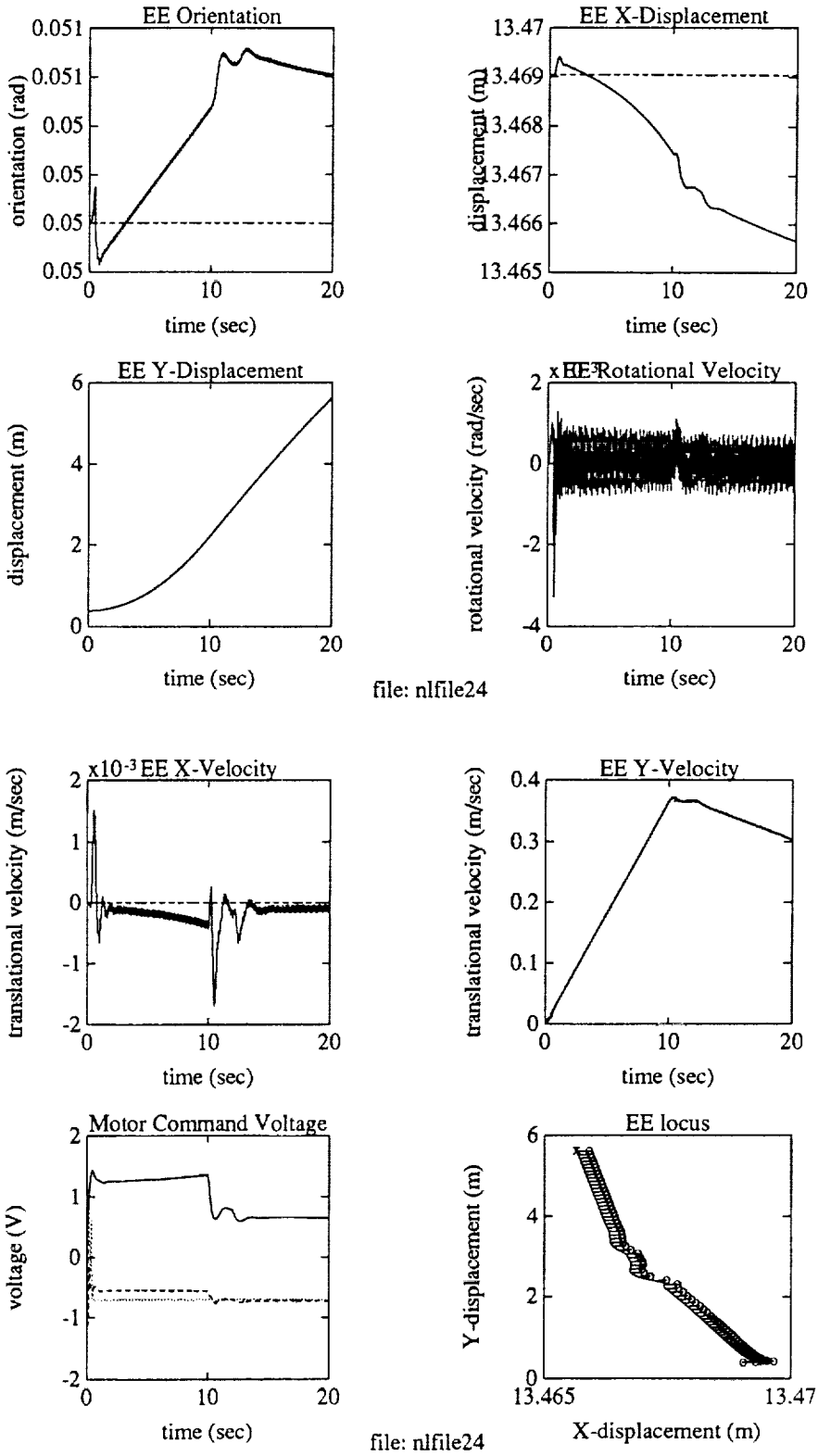

Figure 41: Ramp y Velocity with Modified Controller (Gain 2) and with Input Saturation

flexible joint robots as a special case. The structure of this family of controllers consists of a passivity based feedback and an inverted plant based feedforward. Through extensive simulation on a three–link test arm modeled after RMS shoulder yaw joint, we have demonstrated the efficacy of this approach as compared to the existing RMS controller. Future task includes observer design, saturation avoidance, robustness analysis, optimal feedback tuning, and experimental validation.

Acknowledgment

The authors gratefully acknowledge many helpful discussions with Leonardo Lanari and Steve Murphy. The first author is affiliated with University of Quebec at Trois–Rivieres. The second author has been supported in part by the Center for Intelligent Robotic Systems for Space Explorations (CIRSSE) at the Rensselaer Polytechnic Institute under grant NAGW 1333. Computer simulations related to this report have been conducted on the CIRSSE computer network.

APPENDIX

A General Theory

A.1 Mathematical Background

The time evolution of 'energy' is an important and useful characterization of stability for physical systems, linear and nonlinear alike. Energy based stability analysis has been widely applied to the study of systems such as electrical networks, mechanical structures, thermal systems, etc [23]. The concept of passivity is traditionally defined as an input/output (I/O) condition [24] describing a common class of physical systems which do not generate energy. Relationship between I/O passivity and state space parameters was extensively explored in the 60's [25] in part by using the Lyapunov's method. In this section, we will summarize some basic definition and results that will be useful for the rest of the paper.

Define the input and output signal spaces, $\mathcal{U}_e$, $\mathcal{Y}_e$, respectively, as extended spaces $L_{2e}(\mathbf{R}_+, \mathbf{R}^m)$. Let P_T denote the operator which truncates a signal at time T. Define the truncated inner product by

$$\langle u(\cdot), v(\cdot)\rangle_T \triangleq \langle P_T u(.), P_T v(.)\rangle_2 = \int_0^\infty (P_T u(t))^T P_T v(t)\, dt.$$

By a dynamical system, we mean an I/O mapping $H : \mathcal{U}_e \to \mathcal{Y}_e$. The input–output stability considered here is the finite-gain I/O stability. A system H is said to be finite-gain I/O stable if there exists a constant k such that

$$\|P_T y\| \leq k \|P_T u\| \quad \text{for all } T \geq 0.$$

H is passive if

$$\langle y, u\rangle_T \geq 0 \quad \text{for all } T \geq 0.$$

The concept of passivity can be generalized to dissipativity [26]. A system H is dissipative with respect to the triple (Q, S, R) if

$$\langle y, Qy \rangle_T + 2 \langle y, Su \rangle_T + \langle u, Ru \rangle_T \geq 0$$

for all $T \geq 0$ and $u \in \mathcal{U}_e$, where Q, S and R are memoryless bounded operators with Q and R self-adjoint. Clearly, a finite-gain stable system is dissipative with respect to $(-I, 0, k^2 I)$, while a passive system is dissipative with respect to $(0, \frac{1}{2}I, 0)$.

An important theorem which can be used to determine the I/O stability of the interconnection of passive systems is the Passivity Theorem. In its simplest form, it states that if the open–loop system is passive and the feedback system is strictly passive, then the closed–loop system is L_2-stable i.e. finite-gain I/O stable.

I/O stability infers internal state space asymptotic stability if the closed–loop system is stabilizable and zero–state detectable (if these properties hold globally, the internal stability is also global). A system H is said to be zero–state detectable if $u(t) \equiv 0$ and $y(t) \equiv 0$ imply that the state $x(t) \equiv 0$. For linear systems, this corresponds to observability. Under the stabilizability and detectability conditions, a dissipative system with $Q < 0$, i.e. a finite gain I/O stable system, has an asymptotically stable equilibrium at zero. Sometimes, it is possible to show via a Lyapunov type argument $y(t) \to 0$ if $u(t) \equiv 0$. Then the zero–state detectability alone guarantees internal asymptotic stability.

A.2 Main procedure

The general class of systems considered in this report is described by the following dynamical equation of motion:

$$M(\theta)\ddot{\theta} + D(\dot{\theta}) + C(\theta, \dot{\theta})\dot{\theta} + f(\theta) = Bu \tag{59}$$

where $\theta \in \mathbf{R}^n$ is the displacement vector, $u \in \mathbf{R}^m$ is the input force vector, M is the mass–inertia matrix, D is the damping, C corresponds to the centrifugal and coriolis forces, and f contains the gravity force, spring coupling force, friction, etc.

Most mechanical systems belong to this class; additional assumptions will be imposed later as required. Particular systems of interest that can be considered include fully actuated robots, flexibly jointed robot, robots with flexible links, and satellites with flexible appendages. For the general discussion, we assume zero damping, i.e., $D(\dot{\theta}) = 0$. All the results are of course valid for the damped case also.

We will first consider the output set point control problem.

Assume the measured outputs are $B^T\theta$ and $B^T\dot{\theta}$, i.e., the generalized coordinate and velocity that are directly actuated. Suppose the output of interest is

$$y = C\theta. \tag{60}$$

Choose a feedback control law u based on the measured output, so that $y(t)$ asymptotically converges to the desired output set point y_{des}.

Based on the inherent passivity property of this class of systems, the general procedure described below can be used to construct a solution to the output set point control problem. Extension to output tracking will be addressed in Section A.6.

1. **Steady State Analysis.** The first step is to find a desired state θ_{des} and a feedforward u_{ff} such that

$$C\theta_{des} = y_{des} \quad (61)$$
$$Bu_{ff} = f(\theta_{des}). \quad (62)$$

   If these equations are solvable, then the feedforward control can be used to form the error system:

$$M(\theta)\ddot{\theta} + D(\dot{\theta}) + C(\theta,\dot{\theta})\dot{\theta} + f(\theta) - f(\theta_{des}) = Bu_o$$

   where $u = u_o + u_{ff}$.

2. **Error system Stabilization.** Assume that with a static feedback $u_o = g(B^T\theta)$, the map from u_o to $B^T\dot{\theta}$ is passive (this assumption will be justified for a number of applications). Then any strictly passive map from $B^T\dot{\theta}$ to u_o can be used to feedback I/O stabilize the error system. If the closed loop system is further stabilizable and zero–state detectable with respect to u_o and $B^T\dot{\theta}$, respectively, then the zero error state is asymptotically stable.

We will focus on three examples, flexibly jointed robots, flexible beams, and fully actuated robots, to demonstrate the application of the above simple approach.

Remarks:

1. If the system is linear, then the passivity of the original system (between u and $B^T\dot{\theta}$) implies the passivity of the error system (between u_o and $B^T\dot{\theta}$). For nonlinear systems, additional assumption on f needs to be placed, for example, the joint flexibility is sufficiently strong relative to the gravity load for flexibly jointed robots.

2. It is well known that passive linear systems are necessarily minimum phase and, conversely, a minimum phase plant can be rendered passive through a static state feedback. A similar relationship for nonlinear systems has also been recently published [27]. It is shown that a nonlinear system can be rendered passive by static feedback (i.e., it is feedback equivalent to a passive system) if and only if the zero–dynamics are weakly-minimum phase and the relative degree is one. It is known that flexibly jointed robots and flexible beams have stable zero–dynamics with respect to the motor velocity and hub velocity, respectively. We will show that the static position feedback renders these systems passive.

3. The classical proportional–derivative (PD) control law (for the actuated variable) is a special case of the family of control laws developed here. However, the velocity feedback can be augmented by any passive system in parallel. Through an example, we will see that the dynamic nature of the passive system can be exploited to enhance the closed–loop performance.

4. As it will be shown in the application examples in sections to follow, the above analysis does not require any structural damping in the model. Damping, however, will be useful in the output tracking problem.

A.3 Application to Flexibly Jointed Robots

Consider the general model for an n–link flexibly jointed robot ($2n$ degrees of freedom) [28]. This model contains the gyroscopic forces that are commonly assumed approximately zero [29, 30, 31]. Denote the link angle vector by θ_ℓ and motor angle vector by θ_m. Define $\theta = \left[\begin{array}{cc} \theta_\ell{}^T & \theta_m{}^T \end{array} \right]^T$. The dynamic equation of motion is given by

$$M(\theta)\ddot{\theta} + C(\theta,\dot{\theta})\dot{\theta} + g(\theta) + k(\theta) = Bu \tag{63}$$

where B is of the form $\left[\begin{array}{cc} 0 & I \end{array} \right]^T$ due to the assumption that only motor shafts are actuated, $g(\theta)$ denotes the gravity load, and $k(\theta)$ denotes the spring coupling between motor shafts and the link shafts.

A.3.1 Feedforward Compensation based on Steady State Analysis

The control objective is to steer θ_ℓ to some desired constant $\theta_{\ell_{des}}$ (i.e., in (60), $y = \theta_\ell$). The first step is to form an error system:

$$M(\theta)\ddot{\theta} + C(\theta,\dot{\theta})\dot{\theta} + g(\theta) - g(\theta_{des}) + k(\theta) - k(\theta_{des}) = Bu - g(\theta_{des}) - k(\theta_{des}). \tag{64}$$

In order to cancel the additional terms on the right hand side, we need to find a feedforward torque u_{ff} and a desired set of angles θ_{des} (as in (61)–(62)) that satisfies

$$\begin{aligned} u &= u_o + u_{ff} && (65)\\ Bu_{ff} &= g(\theta_{des}) + k(\theta_{des}). && (66) \end{aligned}$$

Equation (66) can be restated as follows: for a given $\theta_{\ell_{des}}$, find $\theta_{m_{des}}$ and u_{ff} such that

$$\begin{aligned} 0 &= \tilde{B}(g(\theta_{des}) + k(\theta_{des})) && (67)\\ u_{ff} &= (B^TB)^{-1}B^T(g(\theta_{des}) + k(\theta_{des})) = B^T(g(\theta_{des}) + k(\theta_{des})) && (68) \end{aligned}$$

where $\tilde{B}$ is the annihilator matrix for B, i.e., $B\tilde{B} = 0$ or $\tilde{B} = \left[\begin{array}{cc} I & 0 \end{array} \right]$. The terms $g(\theta_{des})$ and $k(\theta_{des})$ are usually in the form

$$\begin{aligned} g(\theta_{des}) &= \left[\begin{array}{c} g_1(\theta_{\ell_{des}}) \\ 0 \end{array} \right] && (69)\\ k(\theta_{des}) &= \left[\begin{array}{c} k_1(\theta_{\ell_{des}}, \theta_{m_{des}}) \\ -k_1(\theta_{\ell_{des}}, \theta_{m_{des}}) \end{array} \right]. && (70) \end{aligned}$$

This implies that u_{ff} and $\theta_{m_{des}}$ should satisfy

$$\begin{aligned} u_{ff} &= g_1(\theta_{\ell_{des}}) && (71)\\ k_1(\theta_{\ell_{des}}, \theta_{m_{des}}) &= -g_1(\theta_{\ell_{des}}). && (72) \end{aligned}$$

To solve (72), we assume that for a given $\theta_{\ell_{des}}$, $\nabla_{\theta_m} k_1(\theta_{\ell_{des}}, \theta_m)$ is invertible in some open set in θ_m. Then by the Implicit Function Theorem [32], there exists a locally unique solution $\theta_{m_{des}}$ to the equation (72). A common form of k_1 is

$$(k_1)_i(\theta_\ell, \theta_m) = f(N_i\theta_{\ell i} - \theta_{mi})$$

where N_i is the gear ratio of the ith joint and f is monotonically increasing, continuously differentiable, and the range of f is $\mathbf{R}$. In that case, since f is globally invertible, a unique solution, $\theta_{m_{des}}$, to (72) can be found for any $\theta_{\ell_{des}}$.

A.3.2 Passivity

With the desired motor angle and feedforward torque chosen as in (71) and (72), the equation of motion becomes

$$M(\theta)\ddot{\theta} + C(\theta,\dot{\theta})\dot{\theta} + g(\theta) - g(\theta_{des}) + k(\theta) - k(\theta_{des}) = Bu_o. \tag{73}$$

If the sum of the gravitational potential energy and spring potential energy is positive semidefinite in $\Delta\theta$, $\Delta\theta = \theta - \theta_{des}$, then one can show that the map from u_o to $\dot{\theta}$ is passive. This is not true in general since $\theta_{\ell_{des}}$ can be arbitrarily chosen. Therefore, we introduce an artificial potential energy by using a proportional feedback in u_o; more specifically, choose u_o to be

$$u_o = u_1 - K_p B^T \Delta\theta. \tag{74}$$

Assume that it is possible to choose K_p so that for some $\delta > 0$

$$\nabla_\theta g(\theta_{des}) + \nabla_\theta k(\theta_{des}) + BK_pB^T \geq \delta I > 0. \tag{75}$$

Consider $g(\theta)$ and $k(\theta)$ as modeled by (69) and (70), respectively, where k_1 is

$$k_1(\theta_\ell, \theta_m) = f(N\theta_\ell - \theta_m) \tag{76}$$

f is a monotonically increasing function and N is a diagonal matrix containing the gear ratios. Then condition (75) becomes

$$\begin{bmatrix} \nabla_{\theta_\ell} g_1(\theta_{\ell_{des}}) & 0 \\ 0 & 0 \end{bmatrix} + \begin{bmatrix} N\nabla f(N\theta_{\ell_{des}} - \theta_{m_{des}}) & -\nabla f(N\theta_{\ell_{des}} - \theta_{m_{des}}) \\ -N\nabla f(N\theta_{\ell_{des}} - \theta_{m_{des}}) & \nabla f(N\theta_{\ell_{des}} - \theta_{m_{des}}) \end{bmatrix} + \begin{bmatrix} 0 & 0 \\ 0 & K_p \end{bmatrix} > 0 \tag{77}$$

If the spring at the joint is sufficiently stiff in the sense that

$$N\nabla f(N\theta_{\ell_{des}} - \theta_{m_{des}}) > -\nabla_{\theta_\ell} g_1(\theta_{\ell_{des}}) \tag{78}$$

then condition (77) is satisfied for a sufficiently large K_p.

Now consider the following scalar function

$$V(\Delta\theta, \dot{\theta}) = \frac{1}{2}\dot{\theta}^T M(\theta)\dot{\theta} + U(\Delta\theta)$$

where the first term on the right hand side is the kinetic energy and the second term is the sum of the potential energies:

$$\begin{aligned} U(\Delta\theta) \;=\; & G(\Delta\theta + \theta_{des}) - G(\theta_{des}) - g(\theta_{des})^T\Delta\theta + K(\Delta\theta + \theta_{des}) - K(\theta_{des}) \\ & -k(\theta_{des})^T\Delta\theta + \frac{1}{2}\Delta\theta^T BK_pB^T\Delta\theta \end{aligned} \tag{79}$$

where G and K are the gravitational and spring potential energies, respectively. Under the assumption that (75) is satisfied, $U(\Delta\theta)$ is positive definite. The derivative of V along the solution of the equation of motion, denoted by $\dot{V}$, is

$$\dot{V} = \dot{\theta}^T B u_1 \tag{80}$$

where we have used the fact that $C(\theta, \dot{\theta})$ can be chosen (only $C(\theta, \dot{\theta})\dot{\theta}$ is unique, but $C(\theta, \dot{\theta})$ is not) so that $\frac{1}{2}\dot{M} - C(\theta, \dot{\theta})$ is skew symmetric (a fact that was used in [2, 33, 4, 5, 21] and many others). Integrating both sides of (80) and using the fact that V is positive definite, it follows that the map from u_1 to $B^T\dot{\theta} = \dot{\theta}_m$ is passive.

A.3.3 Stabilization

Once the passivity from u_1 to $B^T\dot{\theta}$ is established, a large family of feedback control law can be used to achieve I/O stability:

$$u_1 = u_2 - \mathcal{C}_v(B^T\dot{\theta}) \tag{81}$$

where $\mathcal{C}_v$ is any strictly passive system. Since the closed-loop system is the feedback connection of a passive system and a strictly passive system, by the Passivity Theorem, the map from u_2 to $B^T\dot{\theta}$ is L_2-stable. Furthermore, if $u_2 = 0$, we can conclude from (80) and the Invariance Principle that $(\theta, \dot{\theta})$ converges to the largest invariant set in $\{(\theta, \dot{\theta}) : B^T\dot{\theta} = 0\}$. To see this, recall that the strict passivity of $\mathcal{C}_v$ means

$$\int_0^T w^T \mathcal{C}_v(w)\, dt \geq -\gamma^2 + \eta \int_0^T \|w\|^2\, dt. \tag{82}$$

for any $w \in L_{2_e}$. Substituting $B^T\dot{\theta}$ into w, and noting that the left hand side of (82) asymptotically vanishes due to (80), it follows that $B^T\dot{\theta} \in L_2$. Now by applying the standard argument that $\ddot{\theta}$ are uniformly bounded, we can conclude $B^T\dot{\theta} \to 0$ asymptotically. Furthermore, since all higher derivatives of $\dot{\theta}$ are uniformly bounded, all higher derivatives of $B^T\dot{\theta}$ also tend to zero asymptotically. If the closed loop system is zero state detectable from $B^T\dot{\theta}$, then the zero error state is asymptotically stable. If the detectability is global, then so is the asymptotic stability.

Under the following assumptions (slight generalization of the conditions in [10] and including the approximate model in [29] as a special case), the zero state detectability can be shown:

1. The mass matrix M is of the special form

$$M(\theta) = \begin{bmatrix} M_{11}(\theta_\ell) & M_{12}(\theta_\ell) \\ M_{12}{}^T(\theta_\ell) & M_{22} \end{bmatrix}.$$

   This assumption is valid when the motor is symmetric about its axis of rotation; otherwise, all four blocks would depend on both θ_ℓ and θ_m [34].

2. The gravity load g and elastic coupling k are given by (69) and (70).

3. k is diagonal (i.e., k_i only depends on $\theta_{\ell i}$ and $\theta_{m i}$).

4. $\nabla_{\theta_\ell} k(\theta_\ell, \theta_m)$ is positive semi-definite for all θ_ℓ and θ_m, and (θ_ℓ, θ_m) for which $\nabla_{\theta_\ell} k(\theta_\ell, \theta_m)$ loses rank are discrete.

To see how this set of assumptions lead to detectability, substitute $\ddot{\theta}_m = 0$ into the dynamical equation (59), then we have

$$M_{11}(\theta_\ell)\ddot{\theta}_\ell = -C_1(\theta_\ell, \dot{\theta}_\ell)\dot{\theta}_\ell - g_1(\theta_\ell) + g_1(\theta_{\ell_{des}}) - k_1(\theta_\ell, \theta_m) + k_1(\theta_{\ell_{des}}, \theta_{m_{des}}) \quad (83)$$

$$M_{12}{}^T(\theta_\ell)\ddot{\theta}_\ell = k_1(\theta_\ell, \theta_m) - k_1(\theta_{\ell_{des}}, \theta_{m_{des}}) - K_p \Delta\theta_m. \quad (84)$$

Differentiate (84) once more, we have

$$M_{12}{}^T(\theta_\ell)\dddot{\theta}_\ell = \nabla_{\theta_\ell} k_1(\theta_\ell, \theta_m)\dot{\theta}_\ell.$$

It has been independently pointed out in [34] and [10] (the former is for the exact case) that M_{12} is strictly upper triangular. By assumptions 3 and 4, $\dot{\theta}_\ell = 0$. Substituting back into (73), we obtain

$$g(\theta) - g(\theta_{des}) + k(\theta) - k(\theta_{des}) - K_p B^T \Delta\theta = 0. \quad (85)$$

From the assumption that K_p has been chosen sufficiently large as in (75), (85) implies local asymptotic stability. If (75) holds uniformly for all θ_{des}, then the asymptotic stability is in fact global.

For the general model, the observability condition can be checked for the linearized system. First set $u_2(t) = 0$ and $B^T\dot{\theta}(t) = B^T\ddot{\theta}(t) = 0$. From linearized closed-loop equation of motion, we have

$$B^T M(\theta_{des})^{-1}(\nabla_\theta g(\theta_{des}) + \nabla_\theta k(\theta_{des}) + BK_pB^T)\Delta\theta = B^T M(\theta_{des})^{-1}\hat{K}\Delta\theta = 0.$$

Differentiating this equation twice more and use the equation of motion again, we have

$$B^T M(\theta_{des})^{-1}\hat{K}\dot{\theta} = 0$$

$$B^T M(\theta_{des})^{-1}\hat{K}M(\theta_{des})^{-1}\hat{K}\Delta\theta = 0.$$

These equations together imply the full state is identically zero if and only if $M(\theta_{des}) - \hat{K}$ is nonsingular, where $\hat{K} \triangleq \nabla_\theta g(\theta_{des}) + \nabla_\theta k(\theta_{des}) + BK_pB^T$.

From the above analysis, it is clear that under fairly mild conditions, the zero error state of the closed-loop system is globally asymptotic stable. But which $\mathcal{C}_v$ should one choose among the many possibilities in order to enhance a specified performance measure? This appears to be a hard question in general. We shall again encounter the same question in the next section. At the present, we do have some intuitive rules of thumb for the selection of $\mathcal{C}_v$. The simplest choice of $\mathcal{C}_v$ would be just a constant gain. Then the closed-loop control law is of the PD type (but only the motor variables are fed back). As demonstrated in simulation in [1], in contrast to the fully actuated robots, large PD gains degrade the closed-loop performance in terms of the settling time and amplitude of oscillation. This is due to the fact that the zeros in the u_1 to $\dot{\theta}_m$ system are on the $j\omega$-axis, high gains would then drive some of the poles toward these zeros and the response would become increasingly oscillatory. It is intuitively plausible to choose $\mathcal{C}_v$ to be an SPR (i.e., linear time invariant and strictly passive) compensator where the gain is concentrated at the open-loop resonant frequencies

(so that a small oscillation in $\dot{\theta}_m$ will cause large a corrective action) and at the disturbance frequencies (as in notch filters). In simulation [1], much improvement is obtained by using this approach. This idea is similar to a common practice in servo control where a band pass or high pass filter is used in the motor velocity loop (usually analog), in addition to the usual PID loop, to improve performance in the higher frequency range (for example, see the servo controller for space shuttle remote manipulator system in [17]). For the type of systems considered here, we can be more specific about the class of filters that can be tuned for increased performance with affecting the stability.

In the feedforward, the only model-dependent information that is required is the gravity load and spring coupling. If this information is inexact, then u_2 in (81) is a nonzero constant. Since local internal asymptotic stability implies bounded-input/bounded-output (BIBO) stability for sufficiently small initial error, the output error $\theta_\ell - \theta_{\ell_{des}}$ is also proportionally bounded, and the internal states would remain bounded. In Section A.7, we will adaptively update this constant; not surprisingly, the resulting control law is of the standard proportional-integral-derivative (PID) structure.

In the case that the full state is available, an interesting question arises: How can θ_ℓ and $\dot{\theta}_\ell$ be included in this passive control framework? A reasonable approach would be to find another output which is independent from $\dot{\theta}_m$ and passive with respect to u_2 (i.e., after the $\Delta\theta_m$ and $\dot{\theta}_m$ loops have been closed as described above). Then an additional strictly passive feedback can be applied to enhance transient performance. Finding an additional passive output for a linear system of the form $\dot{x} = Ax + Bu$ is straightforward: solve the Lyapunov Equation $A^TP + PA + Q$ for some $Q > 0$, then choose the output map to be $C = B^TP$. A general procedure for nonlinear systems such as the flexible joint robots is unknown at the present.

A.3.4 A Simplified Dynamical Model

The exact model for flexibly jointed robots is not exact linearizable [35]. In [29], a simplified model for flexibly jointed robots was proposed. This model ignores the gyroscopic forces due the motion of rotating motors in the inertial space. Based on this model, an exact linearizing control law was obtained. The simplified and full models have been compared in [28] based on the parameters of a PUMA 560 robot and it is concluded that the approximate model is a very good one for earth bound applications (when the arm is mounted on a mobile base, the effect is far more drastic). The space shuttle remote manipulator system is also modeled under this assumption [17]. In this subsection, we consider the stability analysis and control design discussed above as applied to this simplified model.

The simplified model is of the form

$$M_1(\theta_\ell)\ddot{\theta}_\ell + C_1(\theta_\ell, \dot{\theta}_\ell)\dot{\theta}_\ell + g_1(\theta_\ell) + k_1(N\theta_\ell - \theta_m) = 0 \quad (86)$$

$$I_m\ddot{\theta}_m - k_1(N\theta_\ell - \theta_m) = u. \quad (87)$$

Given the desired link angle vector $\theta_{\ell_{des}}$, the steps in section A.3.1 can be followed to obtain the feedforward control u_{ff} and desired motor angle vector $\theta_{m_{des}}$ for the error system:

$$u_{ff} = g_1(\theta_{\ell_{des}}) \quad (88)$$

$$\theta_{m_{des}} = N\theta_{\ell_{des}} - k_1^{-1}(-g_1(\theta_{\ell_{des}})) \quad (89)$$

where k_1 is assumed to be globally invertible. The spring model for k_1 is usually assumed to be diagonal (i.e., the ith component of $k_1(x)$ only depends on x_i) and each component is monotonically increasing. Hence, the invertibility assumption on k_1 is a very reasonable one.

The error system is described by

$$M_1(\theta_\ell)\ddot{\theta}_\ell + C_1(\theta_\ell,\dot{\theta}_\ell)\dot{\theta}_\ell + g_1(\theta_\ell) - g_1(\theta_{\ell_{des}}) + k_1(N\theta_\ell - \theta_m) - k_1(N\theta_{\ell_{des}} - \theta_{m_{des}}) = 0 \quad (90)$$

$$I_m\ddot{\theta}_m - k_1(N\theta_\ell - \theta_m) + k_1(N\theta_{\ell_{des}} - \theta_{m_{des}}) = u_o \quad (91)$$

where $u = u_o + u_{ff}$ has been used. As in section A.3.2, in order to show passivity, we introduce a proportional feedback to create a positive definite potential energy at the desired set point:

$$u_o = u_1 - K_p\Delta\theta_m.$$

Now, assume

$$\begin{bmatrix} \nabla_\theta g_1(\theta_{\ell_{des}}) + N\nabla_\theta k_1(N\theta_{\ell_{des}} - \theta_{m_{des}}) & -\nabla_\theta k_1(N\theta_{\ell_{des}} - \theta_{m_{des}}) \\ -N\nabla_\theta k_1(N\theta_{\ell_{des}} - \theta_{m_{des}}) & K_p + \nabla_\theta k_1(N\theta_{\ell_{des}} - \theta_{m_{des}}) \end{bmatrix} > 0. \quad (92)$$

This condition is satisfied if the spring is sufficiently stiff compared to the gravity load (typically a reasonable assumption especially for geared robots) and K_p is sufficiently large in the following sense:

$$N\nabla_\theta k_1(N\theta_{\ell_{des}} - \theta_{m_{des}}) > -\nabla_\theta g_1(\theta_{\ell_{des}}) \quad (93)$$

$$\sigma_{\min}(K_p) > \frac{N\,\|\nabla_\theta k_1(N\theta_{\ell_{des}} - \theta_{m_{des}})\|^2}{\sigma_{\min}\left(N\nabla_\theta k_1(N\theta_{\ell_{des}} - \theta_{m_{des}}) + \nabla_\theta g_1(\theta_{\ell_{des}})\right)} - \sigma_{\min}\left(\nabla_\theta k_1(N\theta_{\ell_{des}} - \theta_{m_{des}})\right). \quad (94)$$

With the storage function

$$V = \frac{1}{2}\dot{\theta}_\ell{}^T M_1(\theta_\ell)\dot{\theta}_\ell + \frac{1}{2}\dot{\theta}_m{}^T I_m\dot{\theta}_m + U(\Delta\theta_\ell, \Delta\theta_m) \quad (95)$$

where

$$\begin{aligned} U(\Delta\theta_\ell, \Delta\theta_m) \;=\; & G_1(\Delta\theta_\ell + \theta_{\ell_{des}}) - G_1(\theta_{\ell_{des}}) - g_1(\theta_{\ell_{des}})^T\Delta\theta_\ell \\ & + K_1(N\Delta\theta_\ell - \Delta\theta_m + N\theta_{\ell_{des}} - \theta_{m_{des}}) - K_1(N\theta_{\ell_{des}} - \theta_{m_{des}}) \\ & - k_1(N\theta_{\ell_{des}} - \theta_{m_{des}})^T(N\Delta\theta_\ell - \Delta\theta_m) + \frac{1}{2}\Delta\theta_m{}^T K_p\Delta\theta_m. \end{aligned} \quad (96)$$

The scalar functions K_1 and G_1 are the spring potential energy and gravity potential energy, respectively. Again use the skew symmetric property of $\frac{1}{2}\dot{M}_1 - C_1$; it follows that the derivative of V along the solution trajectory of (86)-(87) is

$$\dot{V} = \dot{\theta}_m{}^T u_1$$

which implies that the map from u_1 to $\dot{\theta}_m$ is passive.

The final step is to choose a motor velocity feedback for stabilization. Again by the Passivity Theorem, u_1 can be chosen as

$$u_1 = u_2 - C_v(\Delta\theta_m)$$

where C_v is strictly passive, the closed-loop system is L_2 I/O stable from u_2 to $\Delta\theta_m$.

Since the simplified model in this section satisfies all the assumptions stated in the last section, global asymptotic stability of the zero error equilibrium follows from the I/O stability.

A.4 Application to a Single Flexible Link

Consider the linearized model for a single link flexible link [36, 13] discretized in terms of the natural modes:

$$\ddot{q} + \Omega^2 q = bu \tag{97}$$

where q is the modal amplitude, u is the hub torque, and

$$\Omega^2 = \begin{bmatrix} 0_{1\times 1} & 0_{1\times n} \\ 0_{n\times 1} & \mathrm{diag}_{n\times n}\{\omega_i^2\} \end{bmatrix}, \qquad b^T = \frac{1}{\rho}\begin{bmatrix} \psi_0'(0) & \psi_1'(0) & \dots & \psi_n'(0) \end{bmatrix}$$

where ρ is the link density (over unit length), ω_i's are the natural modal frequencies and ψ_i's are the corresponding mode shapes. Spatial derivatives are denoted by $'$. Here we consider only an $(n+1)$-mode approximation to avoid the technicality associated with infinite dimensional systems. For a discussion in the infinite dimensional context, see [13]. Note also that the nonlinear model in [13] is of the same form as (64) in the flexibly jointed robot case. The same analysis as in the previous section can be applied. Here we will concentrate on the linearized model.

Let $x = [q, \dot{q}]^T$. The state space equation is

$$\dot{x} = \begin{bmatrix} 0 & I \\ -\Omega^2 & 0 \end{bmatrix} x + \begin{bmatrix} 0 \\ b \end{bmatrix} u. \tag{98}$$

Assume that the hub angle and angular velocity can be measured. The corresponding output equations are

$$y_p = [b^T \quad 0]x \tag{99}$$

$$y_v = [0 \quad b^T]x \tag{100}$$

where y_p and y_v are proportional to the hub angular position and velocity, respectively.

A.4.1 Feedforward Compensation based on Steady State Analysis

Suppose the output of interest is the scalar variable

$$y = Cq.$$

Consider the set point control problem of steering an arbitrary initial state $(q(0), \dot{q}(0))$ to a steady state which corresponds to a specified desired output y_{des}. As in (61)–(62), we are interested in finding a full state set point q_{des} which maps to the desired output y_{des}, and a feedforward u_{ff} that cancels the extra terms in the error dynamical equation for $\Delta q = q - q_{des}$. This means q_{des} and u_{ff} must satisfy the following equations:

$$\Omega^2 q_{des} - b u_{ff} = 0 \tag{101}$$

$$C q_{des} = y_{des}. \tag{102}$$

Assume the leading components in b and c, b_0 and c_0, respectively, are nonzero. Then the model matching equations (101)–(102) imply

$$u_{ff} = 0 \tag{103}$$

$$q_{des0} = \frac{y_{des}}{c_0} \tag{104}$$

$$q_{desi} = 0 \qquad \text{for } i \geq 1. \tag{105}$$

The error equation is then governed by

$$\ddot{q} + \Omega^2 \Delta q = bu \tag{106}$$

$$\Delta y_p = b^T \Delta q \tag{107}$$

where $\Delta q = q - q_{des}$.

A.4.2 Passivity

In the error dynamical equation, Ω^2 is only positive semidefinite. For internal stability, cf. section A.4.3 below, it is important that the stiffness matrix is positive definite. To achieve this, a proportional feedback loop is first closed:

$$u = u_1 - k_p b^T q. \tag{108}$$

The effective closed–loop stiffness matrix is then

$$\tilde{\Omega}^2 = \Omega^2 + k_p b b^T.$$

Since it is assumed that $b_0 \neq 0$, $\tilde{\Omega}^2$ is positive definite for any $k_p > 0$.

To show the mapping u_1 to $b^T \dot{q}$ is passive, consider the storage function

$$V(x) = \frac{1}{2} \|\dot{q}\|^2 + \frac{1}{2} q^T \tilde{\Omega}^2 q.$$

It is easily verified that the derivative of V along the solution is $\dot{V} = (b^T \dot{q})^T u_1$. The passivity from u_1 to $b^T \dot{q}$ follows from the fact that V is a positive function.

A.4.3 Stabilization

For the open–loop error system (106), the controllability matrix, after reordering the columns, is

$$\mathcal{C} = \begin{bmatrix} 0 & \mathcal{C}_0 \\ \mathcal{C}_0 & 0 \end{bmatrix}$$

with

$$\mathcal{C}_0 = \begin{bmatrix} b & -\Omega^2 b & \Omega^4 b & \dots & (-\Omega^2)^n b \end{bmatrix}.$$

Assume the modal frequencies are all distinct and every component of b is nonzero, then $\mathcal{C}_0$ is invertible which means that the system is controllable.

The observability matrix with respect to y_v for the open-loop error system is

$$\mathcal{O} = \begin{bmatrix} 0 & -\Omega^2 C_0 \\ C_0 & 0 \end{bmatrix}.$$

Since Ω^2 is singular, $\mathcal{O}$ is singular which means that the system is not observable from y_v. However, with the proportional feedback of the motor position as in (108), Ω^2 in the observability matrix is replaced

$$\tilde{\Omega}^2 = \Omega^2 + k_p b b^T$$

Since $\tilde{\Omega}^2$ is nonsingular, the observability matrix is also nonsingular and the system is observable.

By the Passivity Theorem, the hub velocity loop can be closed with any strictly passive feedback $\mathcal{C}_v$, i.e.,

$$u_1 = u_2 - \mathcal{C}_v(b^T \dot{q}),$$

and the resulting closed-loop system is L_2-stable from u_2 to $b^T \dot{q}$. For the internal asymptotic stability, we need detectability. From the analysis above, it is evident that if the poles of $\mathcal{C}_v$ do not cancel with the zeros of the system with proportional feedback, then the overall closed-loop system is controllable and observable, and, therefore, internally asymptotically stable.

It is tempting to choose $\mathcal{C}_v$ to be an SPR filter which, over certain bandwidth, approximates the plant inverse (this is possible since the plant is passive, therefore, minimum phase). Then the I/O map from u_2 to $b^T \dot{q}$ is approximately constant in that frequency range. This would result in an excellent I/O response; however, the internal state becomes almost unobservable which means a very poor internal state response. This has indeed been observed experimentally, where excellent step response is obtained at the hub but the beam oscillates at a frequency corresponding to the pair of zeros with the lowest frequency.

A.5 Application to Fully Actuated Robots

The passivity property of fully actuated robots has been much exploited in recent years, starting from the path breaking work in [2] to many later extensions in, for example, [33, 4, 5, 37] and many others. This section briefly reviews some of these results and shows how they fit into the framework outlined in Section A.2.

The equation of motion for a fully actuated arm is the same as that for the flexibly jointed robot (63) except for $B = I$ and $k = 0$:

$$M(\theta)\ddot{\theta} + C(\theta, \dot{\theta})\dot{\theta} + g(\theta) = u. \tag{109}$$

Consider the set point control problem, i.e., the control objective is to steer an arbitrary initial condition $(\theta(0), \dot{\theta}(0))$ to a specified set point $(\theta_{des}, 0)$.

The first step is to choose a feedforward control to form the error system

$$u = u_o + u_{ff}$$

where u_{ff} may either be the gravity load cancellation or the gravity load at the desired set point:

$$u_{ff} = g(\theta_{des}) \qquad \text{or} \tag{110}$$

$$u_{ff} = g(\theta). \tag{111}$$

In both cases, a position feedback loop needs to be closed to ensure a positive definite stiffness:

$$u_o = u_1 - K_p \Delta\theta$$

where K_p is positive definite. In the first case, K_p should be chosen large enough so that the combination with the gravity potential energy is positive definite. To show the passivity from u_1 to $\dot{\theta}$, the following storage function can be used:

$$V(\theta, \dot{\theta}) = \frac{1}{2}\dot{\theta}^T M(\theta)\dot{\theta} + U(\Delta\theta) \tag{112}$$

where U is the total potential energy (including the position feedback loop)

$$U(\Delta\theta) = \frac{1}{2}\Delta\theta^T K_p \Delta\theta + G(\Delta\theta + \theta_{des}) - G(\theta_{des}) - g(\theta_{des})^T \Delta\theta \quad \text{for (110)}$$

$$U(\Delta\theta) = \frac{1}{2}\Delta\theta^T K_p \Delta\theta. \quad \text{for (111)}$$

Now, any strictly passive feedback from $\dot{\theta}$ to u_1 can be used:

$$u_1 = u_2 - C_v(\dot{\theta}).$$

By the Passivity Theorem, the closed–loop is L_2–stable from u_2 to $\dot{\theta}$. Since the stiffness term is globally positive definite, $\dot{\theta}$ is globally zero state detectable. Hence, the zero equilibrium of the error system is globally asymptotically stable.

A.6 Tracking Control Problem

So far we have considered only the set point control problem. A good set point controller is an important facet of the control design as it implies good transient behavior in disturbance rejection (the initial error state can be considered as the result of the past disturbance). Another important aspect of the control design is the trajectory tracking problem. An intuitive approach is to simply replace $\dot{\theta}$ by $\Delta\theta$ in the set point controller with the hope that a well tuned set point controller would also imply good tracking. In this section, we will both justify and modify this intuitive approach.

Given the general dynamical equation (59), consider the problem of finding a feedback control u so that the output $y = C\theta$ tracks an arbitrary trajectory y_{des} asymptotically. A natural extension of the set point control approach presented before is to express the system dynamics in the error coordinate and choose a feedforward control u_{ff} to cancel the extra terms in the dynamics, assuming that this is possible:

$$M(\theta)\Delta\ddot{\theta} + C(\theta, \dot{\theta})\Delta\dot{\theta} + f(\theta) - f(\theta_{des}) = Bu_o \tag{113}$$

where $u = u_o + u_{ff}$ has been used and

$$Bu_{ff} = M(\theta)\ddot{\theta}_{des} + C(\theta,\dot{\theta})\dot{\theta}_{des} + f(\theta_{des}) \tag{114}$$

is assumed to have a solution, given $y_{des}(t) = C\theta_{des}(t)$, $t \geq 0$ (this issue is discussed in greater detail in Section A.6.4). Note that in contrast to the set point control case, not only is the model information required in the feedforward but, in general, the full state measurements as well.

An important extension of (114) is to add to $\ddot{\theta}_{des}$ with an error feedback, $\ell(\Delta\theta, \Delta\dot{\theta})$ (assume the equation is solvable). Then the feedforward to be solved is

$$Bu_{ff} = M(\theta)(\ddot{\theta}_{des} - \ell(\Delta\theta, \Delta\dot{\theta})) + C(\theta,\dot{\theta})\dot{\theta}_{des} + f(\theta_{des}). \tag{115}$$

The solvability of this equation in the flexible joint robot case is discussed in section A.6.4. The error equation with this feedforward becomes

$$M(\theta)\Delta\ddot{\theta} + M(\theta)\ell(\Delta\theta, \Delta\dot{\theta}) + C(\theta,\dot{\theta})\Delta\dot{\theta} + f(\theta) - f(\theta_{des}) = Bu_o. \tag{116}$$

The additional term ℓ can now be chosen to augment performance (this is especially effective if M strongly couples different degrees of freedom).

Next close a position loop:

$$u_o = u_1 - K_p B^T \Delta\theta$$

where it is assumed that K_p can be chosen sufficiently large so that $BK_pB^T + \nabla_\theta f(\theta_{des}) > 0$ (same as the set point case). The problem is that $f(\theta_{des})$ is now time varying and, consequently, the passivity property from u_1 to $\Delta\dot{\theta}$ cannot be easily shown as before (an exception is when f is linear, a fact we shall use in section A.6.2). There are three approaches to approach this issue:

1. The only time varying term in the error system is due to θ_{des}. For each fixed time, the same passivity analysis as before can be applied to show local asymptotic stability. By applying a well known theorem for time varying systems [38], closed loop asymptotic stability is preserved if θ_{des} is sufficiently slow time varying.

2. If the feedforward torque, u_{ff}, is chosen to compensate for $g(\theta)$ rather than for $g(\theta_{des})$, provided that it is solvable, then the passivity analysis can again be applied.

3. Define a new output $z = B^T\dot{\theta} + \mu B^T\theta$ where μ is a small positive parameter. If $B = I$ (full actuation case) or there is inherent structural damping D such that $D + BK_vB^T$ is positive definite for some $K_v > 0$, then the map from u_1 to z is passive for μ sufficiently small, and the same passivity analysis can be applied.

In the remainder of this section, we will elaborate on each of these approaches, and also discuss in detail the solution of the feedforward torque.

A.6.1 Tracking for Slowly Varying Trajectories

To apply the stability result for slowly time varying systems, the feedforward in (114) needs to be slightly modified to

$$Bu_{ff} = M(\theta)\ddot{\theta}_{des} + C(\theta,\dot{\theta})\dot{\theta}_{des} + C(\theta,\dot{\theta}_{des})\Delta\dot{\theta} + f(\theta_{des}). \tag{117}$$

Then the error equation becomes

$$M(\theta)\Delta\ddot{\theta} + C(\theta,\Delta\dot{\theta})\Delta\dot{\theta} + f(\theta) - f(\theta_{des}) = Bu_o. \tag{118}$$

In (118), the only time varying quantities are θ_{des} and $\dot{\theta}_{des}$. If they are "frozen" at a particular constant value $(\theta_{des},\dot{\theta}_{des}) = (\theta_{des}(T),\dot{\theta}_{des}(T))$ where $T \geq 0$ is a constant, then the derivative of the following scalar function

$$V(\Delta\theta,\Delta\dot{\theta}) = \frac{1}{2}\Delta\dot{\theta}^T M(\Delta\theta+\theta_{des})\Delta\dot{\theta} + U(\Delta\theta+\theta_{des}) - \Delta\theta^T f(\theta_{des}) - U(\theta_{des}) + \frac{1}{2}\Delta\theta^T BK_pB^T\Delta\theta$$

is $\dot{V} = \Delta\dot{\theta}^T Bu_1$, where U is the potential energy corresponding to f and $BK_pB^T + \nabla_\theta f(\theta_{des})$ is assumed to be positive definite uniformly in θ_{des}. Hence, the stabilizing control law design based on the passivity approach as described in the previous sections (with $\dot{\theta}$ replaced by $\Delta\dot{\theta}$) stabilizes all frozen systems. Under the additional assumption that the frozen systems are locally uniformly (with respect to T) exponentially stable, the slowly time varying theorem as stated in [38, Theorem 5.6.6] can be applied to show local exponential stability of the closed loop system provided $\sup_t \max\left\{\dot{\theta}_{des}(t),\ddot{\theta}_{des}(t)\right\}$ is sufficiently small. Simulations in [1] confirm this result, where a slowly time varying sinusoid can be closely tracked, but not a fast time varying sinusoid.

A.6.2 Tracking by Direct Compensation

Another possibility is to directly compensate for part of $f(\theta)$ in (113). The feedforward torque that needs to be solved is now

$$Bu_{ff} = M(\theta)\ddot{\theta}_{des} + C(\theta,\dot{\theta})\dot{\theta}_{des} + f_1(\theta) + F\theta_{des} \tag{119}$$

where we have decomposed $f(\theta)$ according to $f(\theta) = f_1(\theta) + F\theta$ where F is a square matrix. The reason that we decompose f in this fashion is related to the solvability of (119) (see section A.6.4 for detail).

Assume that a solution exists, then the error equation is of the form

$$M(\theta)\Delta\ddot{\theta} + C(\theta,\dot{\theta})\Delta\dot{\theta} + F\Delta\theta = Bu_o. \tag{120}$$

Now the same passivity analysis as before can be applied for the control law

$$u_o = -K_pB^T\Delta\theta - \mathcal{C}_v(\Delta\dot{\theta}) \tag{121}$$

for any strictly passive $\mathcal{C}_v$.

A.6.3 Tracking by Output Modification

Even in the local version of (113), with $f(\theta)-f(\theta_{des})$ replaced by $\nabla_\theta f(\theta_{des})\Delta\theta$, $\nabla_\theta f(\theta_{des}) > 0$, the map from u_o to $B^T\Delta\dot{\theta}$ is still not passive in general. This can be seen by evaluating the L_2 innerproduct between this input/output pair:

$$\begin{aligned}\int_0^T (B^T\Delta\dot{\theta})^T u_o\, dt &= \int_0^T \Delta\dot{\theta}^T(M(\theta)\Delta\ddot{\theta} + C(\theta,\dot{\theta})\Delta\dot{\theta} + \nabla_\theta f(\theta_{des})\Delta\theta)\, dt \\ &= \frac{1}{2}\Delta\dot{\theta}^T M(\theta)\Delta\dot{\theta}\Big|_0^T + \frac{1}{2}\Delta\theta^T\nabla_\theta f(\theta_{des})\Delta\theta\Big|_0^T \\ &\quad -\frac{1}{2}\int_0^T \Delta\theta^T\frac{d}{dt}(\nabla_\theta f(\theta_{des}))\Delta\theta\, dt. \end{aligned} \tag{122}$$

Since $\frac{d}{dt}(\nabla_\theta f(\theta_{des})$ may be sign indefinite, the integral cannot be bounded below by a constant. To counter the effect of this last term, we consider adding a proportional feedback, $B^T\Delta\theta$. The contribution to the input/output innerproduct due to this addition is

$$\begin{aligned}\int_0^T (B^T\Delta\theta)^T u_o\, dt &= \int_0^T \Delta\theta^T(M(\theta)\Delta\ddot{\theta} + C(\theta,\dot{\theta})\Delta\dot{\theta} + \nabla_\theta f(\theta_{des})\Delta\theta)\, dt \\ &= \Delta\dot{\theta}^T M(\theta)\Delta\theta\Big|_0^T - \int_0^T (\Delta\dot{\theta}^T M(\theta)\Delta\dot{\theta} + \Delta\theta^T(\dot{M}(\theta,\dot{\theta}) - C(\theta,\dot{\theta}))\Delta\dot{\theta})\, dt \\ &\quad + \int_0^T \Delta\theta^T\nabla_\theta f(\theta_{des})\Delta\theta\, dt. \end{aligned} \tag{123}$$

For the local analysis, we shall ignore the higher order term $(\dot{M}(\theta,\dot{\theta}) - C(\theta,\dot{\theta}))$. Now, consider adding a static PD loop:

$$u_o = -K_p B^T\Delta\theta - K_v B^T\Delta\dot{\theta} + u_1. \tag{124}$$

Then the innerproduct between u_1 and $B^T\Delta\dot{\theta}$ is the same as (122) except $\nabla_\theta f(\theta_{des})$ is replaced by $\nabla_\theta f(\theta_{des}) + BK_pB^T$ and there is an additional term:

$$\int_0^T \Delta\dot{\theta}^T BK_v B^T\Delta\dot{\theta}\, dt.$$

The innerproduct between u_1 and $B^T\Delta\theta$ are the same as (123) except $\nabla_\theta f(\theta_{des})$ is replaced by $\nabla_\theta f(\theta_{des}) + BK_pB^T$ and there is an additional term:

$$\frac{1}{2}\Delta\theta^T BK_v B^T\Delta\theta\Big|_0^T.$$

Now form the augmented output

$$z = B^T\Delta\dot{\theta} + cB^T\Delta\theta.$$

For c sufficiently small and θ_{des} sufficiently slowly time varying, all terms in $\int_0^T z^T(t)u_1(t)\, dt$ can be bounded below by a constant except for the integral involving the quadratic term in $\Delta\dot{\theta}$ which is $\int_0^T \Delta\dot{\theta}^T(-cM(\theta) + BK_vB^T)\Delta\dot{\theta}\, dt$. There are two situations in which this term is also bounded below by a constant:

1. The arm is fully actuated, i.e., $B = I$. This approach is the same as in [39].

2. There is an inherent damping, $D\dot{\theta}$, which gives rise to the term $D\Delta\dot{\theta}$ in the error equation (the feedforward u_{ff} needs to be modified accordingly). If $D + BK_vB^T$ is positive definite, then for c sufficiently small, the integral is bounded below by a constant.

If either of the above situation holds, then the map from u_1 to z is passive and the same analysis can be carried as before to generate stabilizing control laws based on passive map from z to u_1. In the example in [1], it has been shown that link damping in the flexibly jointed robot allows tracking of a fast trajectory that could not be tracked when the damping is absent.

A.6.4 Derivation of the Feedforward Compensation

Flexible Joint Robot Case
To form the tracking error dynamic equation, we need to solve for u_{ff} in either (114) or (119). In this section, we will consider this problem for the special cases of flexible jointed robot and a single flexible link.

We will consider only the simplified flexible joint model given in (86)-(87); the general case is considerably more complicated. Suppose $y = \theta_\ell$. Then (114) involves solving for $(u_{ff}(t), \theta_{m_{des}}(t), \dot{\theta}_{m_{des}}(t))$, given $\theta_{\ell_{des}}(t)$ and its higher time derivatives (as many as required) and $(\theta_m(t), \dot{\theta}_m(t), \theta_\ell(t), \dot{\theta}_\ell(t))$, from the following set of equations:

$$M_1(\theta_\ell)\ddot{\theta}_{\ell_{des}} + C_1(\theta_\ell, \dot{\theta}_\ell)\dot{\theta}_{\ell_{des}} + g_1(\theta_{\ell_{des}}) + k_1(N\theta_{\ell_{des}} - \theta_{m_{des}}) = 0 \quad (125)$$

$$I_m\ddot{\theta}_{m_{des}} - k_1(N\theta_{\ell_{des}} - \theta_{m_{des}}) = u_{ff}. \quad (126)$$

Assuming k_1 is monotonically increasing so an inverse function k^{-1} exists. Assume k_1 is twice differentiable. Then $\theta_{m_{des}}$ can be solved from (125):

$$\theta_{m_{des}} = N\theta_{\ell_{des}} - k_1{}^{-1}\Big(-[M_1(\theta_\ell)\ddot{\theta}_{\ell_{des}} + C_1(\theta_\ell, \dot{\theta}_\ell)\dot{\theta}_{\ell_{des}} + g_1(\theta_{\ell_{des}})]\Big). \quad (127)$$

To solve u_{ff} from (126), $\ddot{\theta}_{m_{des}}$ must first be computed. This can be done by differentiating (127) twice:

$$\ddot{\theta}_{m_{des}} = N\ddot{\theta}_{\ell_{des}} - \frac{d^2}{dt^2}\Big[k_1{}^{-1}\Big(-[M_1(\theta_\ell)\ddot{\theta}_{\ell_{des}} + C_1(\theta_\ell, \dot{\theta}_\ell)\dot{\theta}_{\ell_{des}} + g_1(\theta_{\ell_{des}})]\Big)\Big]. \quad (128)$$

Note that the second term involves $\ddot{\theta}_\ell$ and $\dddot{\theta}_\ell$, which can in turn be resolved using the dynamic equation (86) and its derivative. Finally, u_{ff} can be computed from (126).

For the direct compensation case, cf. (119), the feedforward compensation equation based on the simplified flexible joint model is

$$M_1(\theta_\ell)\ddot{\theta}_{\ell_{des}} + C_1(\theta_\ell, \dot{\theta}_\ell)\dot{\theta}_{\ell_{des}} + g_1(\theta_\ell) + k_2(N\theta_\ell - \theta_m) + K(N\theta_{\ell_{des}} - \theta_{m_{des}}) = 0 \quad (129)$$

$$I_m\ddot{\theta}_{m_{des}} - k_2(N\theta_\ell - \theta_m) - K(N\theta_{\ell_{des}} - \theta_{m_{des}}) = u_{ff} \quad (130)$$

where K is any square invertible matrix and k_2 is chosen from $k_2(x) = k_1(x) - Kx$. Following similar steps as before, (129) can be used to solve for $\theta_{m_{des}}$:

$$\theta_{m_{des}} = K^{-1}(-M_1(\theta_\ell)\ddot{\theta}_{\ell_{des}} - C_1(\theta_\ell, \dot{\theta}_\ell)\dot{\theta}_{\ell_{des}} - g_1(\theta_\ell) - k_2(N\theta_\ell - \theta_m)) + N\theta_{\ell_{des}}. \tag{131}$$

To solve for u_{ff} from (130), again $\ddot{\theta}_{m_{des}}$ needs to be computed by directly twice differentiating both sides of (131). However, $\ddot{\theta}_{m_{des}}$ now not only contains $\ddot{\theta}_\ell$ and $\dddot{\theta}_\ell$ which can be resolved using the dynamical equation and its derivative as before, but also $\ddot{\theta}_m$ (through the derivative of k_2) which in turn depends on u_{ff}. Therefore, to solve u_{ff}, we need the invertibility of $I - I_m K^{-1} \nabla_x k_2(x)\big|_{N\theta_\ell - \theta_m} I_m{}^{-1}$ for all θ_ℓ and θ_m, which does not appear to be a severe limitation. Note that if the spring is assumed to be linear as common practiced in the literature, this additional assumption would not be needed.

For flexible joint robots, Eq. (115) can be solved in exactly the same fashion as above. A simple but useful choice of the function ℓ is simply

$$\ell(\Delta\theta, \Delta\dot{\theta}) = K_{p_\ell}\Delta\theta + K_{v_\ell}\Delta\dot{\theta}. \tag{132}$$

The closed loop equation is now of the following form

$$\begin{aligned} &M_1(\theta_\ell)\Delta\ddot{\theta}_\ell + C_1(\theta_\ell, \dot{\theta}_\ell)\Delta\dot{\theta}_\ell + g_1(\theta_\ell) - g_1(\theta_{\ell_{des}}) \\ &\quad + k_1(N\theta_\ell - \theta_m) - k_1(N\theta_{\ell_{des}} - \theta_{m_{des}}) + K_{v_\ell}\Delta\dot{\theta}_\ell + K_{p_\ell}\Delta\theta_\ell = 0 \qquad (133) \\ &I_m\Delta\ddot{\theta}_m - k_1(N\theta_\ell - \theta_m) + k_1(N\theta_{\ell_{des}} - \theta_{m_{des}}) + k_p\Delta\theta_m = u_1 \qquad (134) \end{aligned}$$

The system linearized about $(\Delta\theta, \Delta\dot{\theta}) = (0, 0)$ is passive between u_1 and $\Delta\dot{\theta}_m$ since the stiffness matrix

$$\begin{bmatrix} N^2\nabla k(N\theta_{\ell_{des}} - \theta_{m_{des}}) + M(\theta_{\ell_{des}})K_{p\ell} & -N\nabla k(N\theta_{\ell_{des}} - \theta_{m_{des}}) \\ -N\nabla k(N\theta_{\ell_{des}} - \theta_{m_{des}}) & \nabla k(N\theta_{\ell_{des}} - \theta_{m_{des}}) + k_p \end{bmatrix}$$

is positive definite. Hence, any strictly passive loop between $\Delta\theta_m$ and u_1 can be closed to ensure closed loop asymptotic stability of the error system.

The purpose of the feedforward control can be thought of as winding up the spring torque so that the link dynamics is governed by

$$\Delta\ddot{\theta}_\ell + K_{v_\ell}\Delta\dot{\theta}_\ell + K_{p_\ell}\Delta\theta_\ell = 0.$$

The role of the feedback control is to produce the motor trajectory that is required for this feedforward.

Flexible Link Case

For the flexible link case, the situation is quite different since the acceleration of the actuated degrees of freedom are not decoupled from the acceleration of the unactuated degrees of freedom as in the simplified model of a flexibly jointed robot. We now need to solve for (u_{ff}, q_{des}) given a desired output trajectory y_{des}:

$$\ddot{q}_{des} + \Omega^2 q_{des} = Bu_{ff} \tag{135}$$

$$Cq_{des} = y_{des} \tag{136}$$

with the additional constraint that u_{ff} needs to be uniformly bounded for implementability. This problem is almost identical to the inverse plant problem considered by [40], but here we solve for the *desired* plant trajectory rather than the actual plant trajectory. Consequently, while the control law obtained in [40] is entirely open-loop, here we have a feedback control structure.

To analyze the solution of (135)-(136), first express q_{des} is of the following form:

$$q_{des} = C^+ y_{des} + \tilde{C}\xi \tag{137}$$

where $C^+ = C^T(CC^T)^{-1}$ is the pseudo-inverse of C and $\tilde{C}$ is the $n \times (n-m)$ full rank matrix that is annihilated by C ($C\tilde{C} = 0$). Note that $\tilde{C}$ can be formed by the linearly independent columns of $(I - C^+C)$, but $\tilde{C} \neq (I - C^+C)$ since $\tilde{C}$ is full rank.

Differentiating the equation twice, we have

$$\ddot{q}_{des} = C^+ \ddot{y}_{des} + \tilde{C}\ddot{\xi}.$$

Substitute back into (135) and assume B is full rank, we can solve for u_{ff}:

$$u_{ff} = (B^TB)^{-1}\Big(B^TC^+\ddot{y}_{des} + B^T\tilde{C}\ddot{\xi} + B^T\Omega^2(C^+y_{des} + \tilde{C}\xi)\Big). \tag{138}$$

Now, u_{ff} can be eliminated from (135), and after rearranging terms, we obtain

$$(I - B(B^TB)^{-1}B^T)(\tilde{C}\ddot{\xi} + \Omega^2\tilde{C}\xi) = -(I - B(B^TB)^{-1}B^T)(C^+\ddot{y}_{des} + \Omega^2C^+y_{des}). \tag{139}$$

Since $\mathcal{R}(\tilde{C}) \subset \mathbf{R}^n$ and $\mathbf{R}^n = \mathcal{R}(B) \overset{\perp}{\oplus} \mathcal{N}(B^T)$, $\tilde{C}$ can be decomposed as

$$\tilde{C} = BK_1 + \widetilde{B^T}K_2 \quad \text{i.e.} \quad \begin{bmatrix} K_1 \\ K_2 \end{bmatrix} = \begin{bmatrix} B & \widetilde{B^T} \end{bmatrix}^{-1}\tilde{C}$$

where $\widetilde{B^T} \in \mathbf{R}^{n\times(n-m)}$ is full rank and annihilated by B, i.e., $B^T\widetilde{B^T} = 0$, and $K_2 \in \mathbf{R}^{(n-m)\times(n-m)c}$ is square invertible. Then (139) becomes

$$\widetilde{B^T}K_2\ddot{\xi} + (I - B(B^TB)^{-1}B^T)\Omega^2\tilde{C}\xi = -(I - B(B^TB)^{-1}B^T)(C^+\ddot{y}_{des} + \Omega^2C^+y_{des}).$$

After multiplying through ${K_2}^T\widetilde{B^T}^T$, and noting $\widetilde{B^T}^T$ is the annihilator of B, we obtain

$$\begin{aligned}\ddot{\xi} &+ ({K_2}^T\widetilde{B^T}^T\widetilde{B^T}K_2)^{-1}{K_2}^T\widetilde{B^T}^T\Omega^2\tilde{C}\xi \\ &= -({K_2}^T\widetilde{B^T}^T\widetilde{B^T}K_2)^{-1}{K_2}^T\widetilde{B^T}^T(C^+\ddot{y}_{des} + \Omega^2C^+y_{des}).\end{aligned} \tag{140}$$

Writing the above equation in a more compact form, we have

$$\ddot{\xi} + \Lambda\xi = L\rho \tag{141}$$

where $\rho = \begin{bmatrix} y_{des} & \ddot{y}_{des} \end{bmatrix}^T$. For implementability, the initial condition, $(\xi(0), \dot{\xi}(0))$, needs to be chosen so that $\xi(t)$ is uniformly bounded for all t. There are two equivalent approaches to find the initial condition. A Laplace transform approach was stated in [40] and a time domain approach in [41]. We will discuss both approaches here.

In the first approach, the Laplace transform of (141) is taken:

$$\hat{\xi}(s) = (s^2 I + \Lambda)^{-1}(L\hat{\rho}(s) + s\xi(0) + \dot{\xi}(0)).$$

Suppose $\hat{\rho}(s)$ is analytic in the open right half plane and has only simple poles on the imaginary axis (i.e., $\ddot{y}_{des}(t)$ is uniformly bounded), then the terms in $\hat{\xi}(s)$ that can lead to unbounded time response are only those associated with the unstable roots of $\det(s^2 I + \Lambda)$. Since Λ is $n-m \times n-m$, there can be at most $n-m$ unstable roots. Correspondingly, there are $n-m$ $\mathbf{R}^m$ residue vectors which, when the contributions in u_{ff} are all set to zero, lead to $m(n-m)$ equations. There are $2(n-m)$ constants that we can choose in $(\xi(0), \dot{\xi}(0))$. Hence, if $m = 2$, an initial condition can be chosen in general to nullify the residues associated with the unstable poles. If $m = 1$, all residues can be nullified, implying the time response of $\xi(t)$ is zero after some finite t. The requirement that $m \leq 2$ appears to be unnecessarily strong as will be evident from the time domain analysis below.

An equivalent time domain approach can also be taken. First write (141) in the first order form:

$$\begin{bmatrix} \dot{\xi} \\ \ddot{\xi} \end{bmatrix} = \begin{bmatrix} 0 & I \\ -\Lambda & 0 \end{bmatrix} \begin{bmatrix} \xi \\ \dot{\xi} \end{bmatrix} + \begin{bmatrix} 0 \\ L \end{bmatrix} \rho.$$

After transforming the coordinate according to the stable (including eigenvalues on the imaginary axis) and unstable eigenspace, the system is partitioned as

$$\begin{bmatrix} \dot{\gamma}_+ \\ \dot{\gamma}_- \end{bmatrix} = \begin{bmatrix} \Lambda_+ & 0 \\ 0 & -\Lambda_- \end{bmatrix} \begin{bmatrix} \gamma_+ \\ \gamma_- \end{bmatrix} + \begin{bmatrix} L_+ \\ L_- \end{bmatrix} \rho$$

where Λ_+ and Λ_- are both strictly unstable. The unstable response is given by

$$\begin{aligned} \gamma_+(t) &= e^{\Lambda_+ t}\gamma_+(0) + \int_0^t e^{\Lambda_+(t-\tau)} L_+ \rho(\tau)\, d\tau \\ &= e^{\Lambda_+ t}(\gamma_+(0) + \int_0^t e^{-\Lambda_+ \tau} L_+ \rho(\tau)\, d\tau) \end{aligned} \tag{142}$$

Choose

$$\gamma_+(0) = -\int_0^\infty e^{-\Lambda_+ \tau} L_+ \rho(\tau)\, d\tau \tag{143}$$

assuming the integral exists (which is true if $\ddot{y}_{des}$ is uniformly bounded). If

$$(\gamma_+(0) + \int_0^t e^{-\Lambda_+ \tau} L_+ \rho(\tau)\, d\tau) \leq M e^{-\sigma_+ t}$$

where σ_+ is the eigenvalue of Λ_+ with the largest real part, then $\gamma_+(t)$ would be uniformly bounded as required. Again, a sufficient condition for this is that $\ddot{y}_{des}$ is uniformly bounded. Note that the condition on the number of input/output pairs is no longer required in this analysis. This discrepancy appears to be due to some relationship in the residues that we are not taking advantage of.

As in the Laplace transform approach, $\gamma_-(0)$ can be chosen to achieve the zero steady state for γ_+ and γ_- if $\int_0^\infty e^{\Lambda_- \tau} L_- \rho(\tau)\, d\tau < \infty$.

In [40], it was pointed out that the procedure of choosing the initial condition to guarantee the boundedness of u_{ff} is highly sensitive numerically since any slight numerical error could

lead to divergence. To show that $\gamma_+(t)$ in (143) can be computed in a numerically stable way, we substitute (143) into (142). Then

$$\begin{aligned}\gamma_+(t) &= -e^{\Lambda_+ t}\int_t^\infty (e^{-\Lambda_+\tau}L_+\rho(\tau))\,d\tau \\ &= -\int_t^\infty e^{\Lambda_+(t-\tau)}L_+\rho(\tau)\,d\tau \\ &= -\int_0^\infty e^{-\Lambda_+\tau}L_+\rho(t+\tau)\,d\tau \end{aligned} \tag{144}$$

where the last expression can be stably calculated since $-\Lambda_+$ is stable.

To illustrate the procedure described above, consider a simple example presented in [40]:

$$\begin{aligned}\ddot{q}+\begin{bmatrix}1 & -1\\ -1 & 1\end{bmatrix}q &= \begin{bmatrix}\frac{2}{3}\\ -\frac{1}{3}\end{bmatrix}u \\ y &= \begin{bmatrix}0 & 1\end{bmatrix}q.\end{aligned}$$

After some algebra, we obtain

$$\ddot{\xi}-\xi = y_{des}-2\ddot{y}_{des} \tag{145}$$

where

$$\ddot{y}_{des} = \begin{cases}1 & 0\le t<1\\ -1 & 1\le t<2\\ 0 & t\ge 2.\end{cases} \tag{146}$$

and $y_{des}(0)=\dot{y}_{des}(0)=0$. For simplicity, make a change of variable $\eta=\xi-y$, then

$$\ddot{\eta}-\eta = -3\ddot{y}_{des}.$$

The Laplace transform of $\ddot{y}_{des}$ is

$$\widehat{\ddot{y}_{des}}(s) = \frac{(1-e^{-s})^2}{s}.$$

Therefore,

$$\hat{\eta}(s)(s) = \frac{(-3s^{-1}(1-e^{-s})^2+s\eta(0)+\dot{\eta}(0))}{s^2-1}.$$

If only the unstable residue is to be canceled as suggested in [40], one choice for the initial condition is

$$\eta(0)=\dot{\eta}(0)=\frac{3}{2}(1-e^{-1})^2. \tag{147}$$

In this case, since $m=1$, residues associated with both poles can in fact be canceled by choosing

$$\begin{bmatrix}\eta(0)\\ \dot{\eta}(0)\end{bmatrix} = \begin{bmatrix}\frac{3}{2}((1-e^{-1})^2+(1-e)^2)\\ -\frac{3}{2}(-(1-e^{-1})^2+(1-e)^2)\end{bmatrix}. \tag{148}$$

An equivalent time domain approach can also be taken. The solution of (145) is

$$\eta(t) = \begin{bmatrix}\cosh t & \sinh t\\ \sinh t & \cosh t\end{bmatrix}\Big(\begin{bmatrix}\eta(0)\\ \dot{\eta}(0)\end{bmatrix} - 3\int_0^t \begin{bmatrix}\cosh\tau & -\sinh\tau\\ -\sinh\tau & \cosh\tau\end{bmatrix}\begin{bmatrix}0\\ 1\end{bmatrix}\ddot{y}_{des}(\tau)\,d\tau\Big).$$

After using (146), the integral, for $t \geq 2$, is a constant:

$$\int_0^t \begin{bmatrix} \cosh\tau & -\sinh\tau \\ -\sinh\tau & \cosh\tau \end{bmatrix} \begin{bmatrix} 0 \\ 1 \end{bmatrix} \ddot{y}_{des}(\tau)\, d\tau = \begin{bmatrix} 1 - 2\cosh 1 + \cosh 2 \\ 2\sinh 1 - \sinh 2 \end{bmatrix}.$$

Since the stable eigenspace is spanned by $\begin{bmatrix} 1 \\ -1 \end{bmatrix}$ and the unstable eigenspace is spanned by $\begin{bmatrix} 1 \\ 1 \end{bmatrix}$, choosing the initial condition according to (147) leads to

$$\eta(t) = e^{-t}(1 + e^2 - 2e)$$

for $t \geq 2$ and choosing the initial condition according to (148) leads to $\eta(t) = 0$ for $t \geq 2$.

When the desired output is assumed generated from a reference model and the model and plant parameters satisfy a model matching condition, a solution of (135)-(136) can be more easily solved. This is called the regulator approach, a version of which, called the command generator tracker theory, was proposed in [12]. The nonlinear version can be found in [42]. Application to the flexible arm control can be found in [43]. We present this approach for a general linear time invariant system. Consider

$$\begin{aligned} \dot{x}_{des} &= Ax_{des} + Bu_{ff} \\ y_{des} &= Cx_{des}. \end{aligned}$$

The desired output y_{des} is generated from a linear time invariant reference model:

$$\begin{aligned} \dot{w} &= Sw \\ y_{des} &= Qw \end{aligned}$$

where $w \in \mathbf{R}^k$. We seek a solution of the form

$$u_{ff} = Fw \tag{149}$$

where F and a matrix P together should satisfy

$$PS - AP = BF \tag{150}$$

$$CP = Q \tag{151}$$

which are called the model matching conditions. The initial condition $x_{des}(0)$ should be chosen as

$$x_{des}(0) = Pw(0). \tag{152}$$

Clearly, if the exosystem is stable, the feedforward signal will be uniformly bounded.

The model matching condition (150) can be written as a generalized Lyapunov equation:

$$\begin{bmatrix} -A & -B \\ C & -S \end{bmatrix} \begin{bmatrix} P \\ F \end{bmatrix} + \begin{bmatrix} P \\ F \end{bmatrix} S = \begin{bmatrix} 0 \\ Q \end{bmatrix} \tag{153}$$

where the unknown matrix $\begin{bmatrix} P \\ F \end{bmatrix}$ is of dimension $(n+m) \times k$. By using the Kronecker product, this linear matrix equation can be written as a vector equation:

$$(\overline{A} \otimes I_k + I_{n+m} \otimes S)\chi = \gamma \tag{154}$$

where

$$\overline{A} \triangleq \begin{bmatrix} -A & -B \\ C & -S \end{bmatrix}$$

and χ and γ are the columnwise stacked vector from $\begin{bmatrix} P \\ F \end{bmatrix}$ and $\begin{bmatrix} 0 \\ Q \end{bmatrix}$, respectively. For a given plant and exosystem, the solvability of (154) can be readily checked, and if solvable, χ can also be easily found. A sufficient condition (for the invertibility of the matrix in (154)) is that the spectrum of $-\overline{A}$ and S do not intersect.

The feedforward u_{ff} given by the linear regulator approach is a particular solution of (138) from the plant inversion. It would be interesting to query if the initial condition chosen as in (152) is related to the initial condition chosen based on the plant inversion approach described earlier (either through the Laplace transformation or time domain solution). In Appendix A, it was shown for a single flexible link tracking a sinusoid, that the initial condition from the regulator approach is the same as the one chosen to cancel all of the residues. We are currently seeking the generalization of this result.

A.7 Adaptive Control

The feedforward control in either set point or tracking case requires a great deal of model information. It is highly desirable to adaptively update this signal without requiring explicit knowledge of the plant parameters. To this end, consider the closed loop system as an internally asymptotically stable system driven by the input u_{ff}. Based on our passivity approach, the closed loop system is passive but in general not strictly passive. Our basic idea is to choose a new output such that the I/O pair with respect to this output is strictly passive. Then any passive adaptation for u_{ff} can be used to preserve the state asymptotic stability.

We will only consider the linearized closed loop plant here, the full nonlinear version is under development. Suppose that the linearized closed loop plant is of the form

$$\dot{x} = Ax + B(u - u_{ff})$$

where A is exponentially stable, u_{ff} is the unknown desired feedforward, and u is the adaptive feedforward. By the Lyapunov's theorem [44], for any $Q > 0$, there exists $P > 0$ such that

$$A^T P + PA = -Q.$$

Now define $C = B^T P$ as the new output map. Then the triplet (A, B, C) is strictly positive real [45]. The adaptation for u_{ff} is now straightforward. Using the standard linear-in-parameter formulation [46], suppose u_{ff} can be parameterized as

$$u_{ff} = H\lambda$$

where H in the known regressor matrix and λ is the unknown parameters. For the set point control case, $H = I$ and λ is a constant vector. For the regulator approach, H contains w (state of the exosystem) and λ consists of columns of F (cf. (149)). For the tracking of a general desired output, H depends on θ, $\dot{\theta}$, y_{des} and its higher derivatives. In this case, finding the structure of H itself may be difficult. A viable approach may be to approximate H by some expansion and slowly adapt the approximation. The neural net approach in [47] is a possibility that we shall explore.

To derive the adaptation rule, consider the Lyapunov function candidate

$$V = x^T P x + \Delta\lambda^T \Gamma^{-1} \Delta\lambda \tag{155}$$

where $\Delta\lambda = \lambda - \hat{\lambda}$, $\hat{\lambda}$ is the estimate of the unknown vector λ. Since the output is chosen so the system is strictly positive real, the derivative along the solution becomes

$$\dot{V} = -x^T Q x + 2(u - u_{ff})^T y + 2\Delta\lambda^T \Gamma^{-1} \Delta\dot{\hat{\lambda}}.$$

Choose the adaptive feedforward based on the estimated parameter:

$$\hat{u}_{ff} = H\hat{\lambda}. \tag{156}$$

Then

$$\dot{V} = -x^T Q x + 2\Delta\lambda^T (H^T y + \Gamma^{-1} \Delta\dot{\hat{\lambda}}).$$

Hence, with the following gradient update rule for $\hat{\lambda}$:

$$\dot{\hat{\lambda}} = -\Gamma H^T y \tag{157}$$

$\dot{V}$ is negative semidefinite. This implies that all states and parameter estimate error are bounded, and furthermore, by Barbalat's Lemma [48], x converges to zero asymptotically. For the set point control case, the adaptive parameter update simply reduces to the integral control law.

We are currently extending this argument to the nonlinear systems by using the nonlinear Lyapunov equation.

References

[1] L. Lanari and J.T. Wen. A family of asymptotic stable control laws for flexible robots based on a passivity approach. CIRSSE Report 85, Rensselaer Polytechnic Institute, February 1991.

[2] M. Takegaki and S. Arimoto. A new feedback method for dynamic control of manipulators. *ASME J. Dynamic Systems, Measurement and Control*, 102, June 1981.

[3] D.E. Koditschek. Natural motion for robot arms. In *Proc. IEEE Conf. Decision and Control*, pages 733–735, Las Vegas, NV, 1984.

[4] J.-J. E. Slotine and W. Li. On the adaptive control of robot manipulators. In *ASME Winter Meeting*, pages 43–50, Anaheim, CA, 1986.

[5] J.T. Wen and D.S. Bayard. Simple robust control laws for robotic manipulators, part I: Non-adaptive case. In *JPL/NASA Telerobotics Workshop*, January 1987.

[6] P.E. Crouch and B. Bonnard. An appraisal of linear analytic systems theory with applications to attitude control. ESTEC Contract 3771/78/NL/AK(SC), European Space Agency Contract Report, May 1980.

[7] B. Wie, H. Weiss, and A. Arapostathis. Quaternion feedback regulator for spacecraft eigenaxis rotations. *J. Guidance & Control*, 12(3):375-380, 1989.

[8] J.T. Wen and K.Kreutz. Globally stable control laws for the attitude control problem: Tracking control and adaptive control. In *Proc. 27th IEEE Conf. Decision and Control*, Austin, TX, 1988.

[9] S. Arimoto and F. Miyazaki. Stability and robustness of pd feedback control with gravity compensation for robot manipulator. In *ASME Winter Meeting*, pages 67-72, Anaheim, CA, December 1986.

[10] P. Tomei. Point-to-point control of elastic joint robots. In *Proc. Int. Symp. on Intelligent Robotics*, Bangalore, India, January 1991.

[11] H.G. Lee, H. Kanoh, S. Kawamura, F. Miyazaki, and S. Arimoto. Stability analysis of a one-link flexible arm control by a linear feedback law. In S.G. Tzafestas T. Futagami and Y. Sunahara, editors, *Distributed Parameter Systems: Modelling and Simulation*, pages 345-352. Elsevier Science Publishers B.V. (North-Holland), 1989.

[12] R.J. Benhabib, R.P. Iwens, and R.L. Jackson. Stability of distributed control for large flexible structures using positivity concepts. In *AIAA Guidance and Control Conference, Paper No. 79-1780*, Boulder, Co., August 1979.

[13] F. Wang and J.T. Wen. Nonlinear dynamical model and control for a flexible beam. CIRSSE Report 75, Rensselaer Polytechnic Institute, November 1990.

[14] B. Paden, B. Riedle, and E. Bayo. Exponentially stable tracking control for multi-joint flexible-link manipulators. In *Proc. 1990 American Control Conference*, pages 680-684, San Diego, CA, June 1990.

[15] B. Paden and B. Riedle. A positive-real modification of a class of nonlinear controllers for robot manipulators. In *Proc. 1988 American Control Conference*, Atlanta, GA, June 1988.

[16] M.W. Spong. Control of flexible joint robots: A survey. UILU-ENG-90-2203 DC-116, University of Illinois at Urbana-Champagne, February 1990.

[17] C. Trudel. SRMS joint servo and gearbox math model. Technical Report SPAR-TM. 1213, SPAR Aerospace, May 1977.

[18] R. Theobald. Data package for manipulator flexible joint control system feasibility study, May 1990. Lockheed Co., Houston, TX.

[19] Spar-rms.r.073, issue b. SPAR RMS Document.

[20] Srms parameter sets and their applications, 1987. SPAR RMS Document.

[21] R. Ortega and M.W. Spong. Adaptive motion control of rigid robots: A tutorial. In *Proc. 27th IEEE Conf. Decision and Control*, pages 1575–1584, Austin, TX, December 1988.

[22] O Dahl and L. Nielsen. Torque-limited path following by on-line trajectory time scaling. *IEEE Transaction of Robotics and Automation*, 6(5):554–561, 1990.

[23] J.C. Willems. Dissipative dynamical systems, part I: General theory, part II: Linear systems with quadratic supply rate. *Arch. Rational Mech. Anal.*, 45:321–393, 1972.

[24] P.J. Moylan. Implication of passivity in a class of nonlinear systems. *IEEE Transaction on Automatic Control*, 19:373–381, 1974.

[25] G. Zames. On the input/output stability of time-varying nonlinear feedback systems, part I: Conditions derived using concepts of loop gain, conicity, and positivity, part II: Conditions involving circles in the frequency plane and sector nonlinearities. *IEEE Transaction on Automatic Control*, 11(3):465–476, 1966.

[26] D.J. Hill and P.J. Moylan. Dissipative dynamical systems: Basic input-output and state properties. *J. Franklin Institute*, 309(5):327–357, 1980.

[27] C.I. Byrnes, A. Isidori, and J.C. Willems. Stabilization and output regulation of nonlinear systems in the large. In *Proc. 29th IEEE Conf. Decision and Control*, Honolulu, HI, December 1990.

[28] S.H. Murphy. *Modeling and Simulation of Multiple Cooperating Manipulators on a Mobile Platform.* PhD thesis, Rensselaer Polytechnic Institute, Troy, NY., Nov 1990.

[29] M.W. Spong. Modeling and control of elastic joint robots. *ASME J. Dynamic Systems, Measurement and Control*, 109:310–319, Dec. 1987.

[30] A. De Luca. Dynamic control of robots with joint elasticity. In *Proc. 1988 IEEE Robotics and Automation Conference*, pages 152–158, Philadelphia, PA, 1988.

[31] S. Nicosia, F. Nicolò, and D. Lentini. Dynamical control of industrial robots with elastic and dissipative joints. In *Proc. 8th IFAC World Congress*, pages 1933–1939, Kyoto, 1981.

[32] T.M. Apostol. *Mathematical Analysis.* Addison-Wesley, 2 edition, 1975.

[33] D.E. Koditschek. Adaptive techniques for mechanical systems. In *Proc. 5th Yale Workshop on Applications of Adaptive Systems Theory*, pages 259–265, New Haven, CT, May 1987.

[34] S.H. Murphy, J.T. Wen, and G.N. Saridis. Efficient dynamic simulation of flexibly jointed manipulators. In *Proc. 29th IEEE Conf. Decision and Control*, pages 545–550, Honolulu, HI, December 1990.

[35] C. DeSimone and Nicolo F. On the control of elastic robots by feedback decoupling. *IEEE Joural of Robotics and Automation*, 1(2):64–69, 1986.

[36] F. Bellezza, L. Lanari, and G. Ulivi. Exact modeling of the flexible slewing link. In *Proc. 1990 IEEE Robotics and Automation Conference*, pages 734–739, Cincinnati, OH, 1990.

[37] N. Sadegh and R. Horowitz. Stability and robustness analysis of a class of adaptive controllers for robotic manipulators. *Int. J. Robotics Research*, 1988.

[38] M. Vidyasagar. *Nonlinear Systems Analysis.* Prentice–Hall, NJ, 1978.

[39] J.T. Wen and D.S. Bayard. A new class of control laws for robotic manipulators, Part I: Non–adaptive case. *Int. J. Control*, 47(5):1361–1385, 1988.

[40] E. Bayo and H. Moulin. An efficient computation of the inverse dynamics of flexible manipulators in the time domain. In *Proc. 1989 IEEE Robotics and Automation Conference*, Scottsdale, AZ, 1989.

[41] D.S. Kwon and W.J. Book. An inverse dynamic method yielding flexible manipulator state trajectories. In *Proc. 1990 American Control Conference*, pages 186–193, San Diego, CA, May 1990.

[42] A. Isidori. *Nonlinear Control Systems.* Springer–Verlag, second edition, 1989.

[43] A. De Luca, L. Lanari, and G. Ulivi. Output regulation of a flexible robot arms. In *9th INRIA Int. Conf. on Analysis and Optimization*, pages 833–842, Antibes, France, June 1990.

[44] W.M. Wonham. *Linear Multivariable Control: A Geometric Approach.* Springer–Verlag, New York, 1979.

[45] J.T. Wen. Time domain and frequency domain conditions for strict positive realness. *IEEE Trans. on Automatic Control*, 33(10), Oct 1988.

[46] P. Khosla and T. Kanade. Parameter identification of robot dynamics. In *Proc. 25th IEEE Conf. Decision and Control*, Fort Lauderdale, FL, December 1985.

[47] W. Cheng and J. Wen. A two–time–scale neural tracking controller for a class of nonlinear systems. Ral report, Rensselaer Polytechnic Institute, May 1991.

[48] V.M. Popov. *Hyperstability of Control Systems.* Springer–Verlag, New York, 1973.